ABSTRACT

Title of Document: TEMPERATURE CYCLING RELIABILITY OF REBALLED AND REWORKED BALL GRID ARRAY PACKAGES IN SNPB AND SAC ASSEMBLY

Lei Nie, Doctor of Philosophy (Ph.D.), 2010

Directed By: Professor Michael G. Pecht
Department of Mechanical Engineering

In recent years, many countries banned the use of lead in select high volume electronic equipment. However, exemptions from lead-free legislation have been granted for certain products, especially those intended for high-reliability applications. Manufacturers with exemption are facing dwindling supply of lead-based components for their products. This change has left many high-reliability electronic equipment manufacturers with the choices of, mixing lead-free components in tin-lead assembly process, converting products to lead-free, or reprocessing lead-free components to comply with the tin-lead assembly process.

Reballing has been used for component reclamation, but right now it offers a way to reprocess the ball grid array packages. The reliability of reballed BGA assembly needs to be determined before the implementation. Mixing lead-free ball grid array packages with eutectic tin-lead solder paste bring new challenges to the

current electronic industry. The mixed assemblies with long-term reliability need to be investigated. Although rework has been implemented for decades, the impact of multiple rework process on the reliability of lead-free and mixed assemblies is still unknown.

Lead-free ball grid array packages with Sn3.0Ag0.5Cu solder balls were subjected to the reballing process. Ball shear test and cold bump pull test were used to investigate the solder ball attachment strength of the reballed BGAs. Temperature cycling test was used to evaluate the temperature cycling reliability of reballed tin-lead, lead-free and mixed assemblies. The solder ball strength and the temperature cycling reliability of reballed components were independent of the reballing method. The temperature cycling reliability of mixed assemblies was equivalent to that of lead-free assemblies. Microstructure differences in lead-free, mixed and reballed tin-lead assemblies were investigated to explain the temperature cycling reliability results.

Lead-free and mixed assemblies were subjected to the rework process. Temperature cycling test was used to evaluate the temperature cycling reliability of reworked assemblies. Cu over-consumption, Cu pad dissolution and thick interfacial intermetallic layer were found in the reworked assemblies. Microstructural investigation and geometry analysis were used to analyze the temperature cycling reliability degradation in the reworked assemblies after multiples rework processes.

TEMPERATURE CYCLING RELIABILITY OF REBALLED AND REWORKED BALL GRID ARRAY PACKAGES IN SNPB AND SAC ASSEMBLY

By

Lei Nie

Dissertation submitted to the Faculty of the Graduate School of the
University of Maryland, College Park, in partial fulfillment
of the requirements for the degree of
Doctor of Philosophy
2010

Advisory Committee:
Professor Michael G. Pecht, Chair
Professor Abhijit Dasgupta
Professor Lourdes Salamanca-Riba
Associate Professor Patrick McCluskey
Assistant Professor Teng Li
Senior Research Scientist Dr. Michael Osterman

© Copyright by
Lei Nie
2010

Dedication

This dissertation is dedicated to my husband and my parents, who support me all the time.

Acknowledgment

First, I would like to express my gratitude and respect to Prof. Michael Pecht for having granted me this opportunity to work on this dissertation topic and challenging me to set a higher standard. I appreciate him for his continuous support towards the progress of this work and taking the time to review and guide me throughout the course of this study.

I would like to especially thank Dr. Michael Osterman for his excellent guidance, and support for this study. I am also thankful to Prof. Abhijit Dasgupta, Prof. Lourdes Salamanca-Riba, Prof. Patrick McCluskey, and Prof. Teng Li for their continued interest and efforts involved in reviewing my work. I further extend my thanks to Dr. Azarian for his insightful advice to this work.

I further thank the Electronic Products and System (EPS) Consortium in Center for Advanced Life Cycle Engineering (CALCE) for its support. I would like to thank Dr. Diganta Das, Bhanu Sood, Anshul Shrivastava and Ahmed Amin for their guidance and support during conducting the experiments in the laboratories for this thesis.

I would like to thank all my friends and colleagues for their support and encouragement. I am thankful to Maik Mueller for his advice and encouragement to this work. I would like to thank Lyudmyla Panashchenko and Vidyu Challa for their help in my experimental and thesis work. I further extend my thank to Dr. Rui Wu, Dr. Jie Gu, Dr. Yuxun Zhou, Weiqiang Wang, Shunfeng Cheng, Xiaofei He, Jun Dai,

Preeti Chauhan, Vikram Srinivas, Elviz George, Samir Agrawal, Nicholas Williard, Ravikumar Sanapala, Lili Ma, Vasilis Sotiris and Daeil Kwon for their help through the course of completing this thesis.

Finally, I would like to extend very special thanks to my husband Chunsheng Ji for his constant support and encouragement towards my work. I would like to thank my parents for standing by all my decision and constantly encouraging me towards my endeavors.

Table of Contents

List of Publications

- L. Nie, M. Osterman, and M. Pecht, "Microstructure Analysis of Reworked Ball Grid Array Assemblies under Thermomechanical Loading Conditions", Submitted to IEEE Transactions on Device and Materials Reliability.

- L. Nie, M. Mueller, M. Osterman, M. Pecht, "Microstructural Analysis of Reballed Tin-Lead, Lead-Free, and Mixed Ball Grid Array Assemblies under Temperature Cycling Test", Accepted by Journal of Electronic Materials.

- L. Nie, M. Osterman, M. Pecht, F. Song, J. Lo and S.K. Lee, "Solder Ball Attachment Assessment of Reballed Plastic Ball Grid Array Packages", IEEE Transactions on Components and Packaging Technologies, Volume 32, Issue 4, 2009, pp. 901-908.

- L. Nie, M. Osterman, and M. Pecht, "Assessing Reliability of Reballed Ball Grid Array Assemblies under Temperature Cycling Test", Proceedings of the 25th SMTA International Conference, San Diego, CA, October 4-8, 2009.

- L. Nie, M. Dong, J. Cai, M. Osterman, and M. Pecht, "Interfacial Reaction of Reballed BGAs Experienced Isothermal Aging", Proceedings of the 10th International Conference on Electronics Packaging Technology, Beijing, China, August 10-13, 2009.

- L. Nie, M. Osterman, M. Pecht, "Copper Pad Dissolution and Microstructure Analysis of Reworked Plastic Grid Array Packages in Lead-free and Mixed Assemblies", L. Nie, M. Osterman, and M. Pecht, Journal of Surface Mount Technology, April-June 2009, Volume 22, Issue 2, pp. 13-20.

- L. Nie, M. Osterman, and M. Pecht, "Copper Pad Dissolution and Microstructure Analysis of Reworked Plastic Grid Array Assemblies", Proceedings of IPC APEX 2009, Las Vegas, NV, March 31-April 2, 2009, S08-01.

- L. Nie, M. Osterman, M. Pecht, F. Song, J. Lo and S.K. Lee, "Solder Ball Attachment Assessment of Reballed Plastic Ball Grid Array Packages", Proceeding of IPC APEX 2008, Las Vegas, NV, March 30-April 3, 2008.

- L. Nie, M. Azarian, M. Keimasi, and M. Pecht, "Prognostics of Ceramic Capacitor Temperature-Humidity-Bias Reliability Using Mahalanobis Distance Analysis," Circuit World, Vol. 33, No. 3, 2007, pp. 21-28.

- L. Nie and M. Pecht, "Regulations and Market Trends in Lead-free and Halogen-free Electronics", Circuit World, Vol. 33, No. 2, 2007, pp. 4-9.

List of Tables

List of Figures

Chapter 1: INTRODUCTION

1.1. Brief Overview

The Directive on the Restriction of the Use of Certain Hazardous Substances in Electrical and Electronic Equipment (RoHS), which became effective on July 1, 2006, mandates that electronics industries replace tin-lead solder with lead-free solder. China, Japan and other countries have also published environmental regulations to restrict tin-lead solder [1]-[5]. However, exemptions from lead-free legislation have been granted for certain products, especially those intended for high-reliability applications [1]-[5]. Manufacturers with exemption are facing dwindling supply of lead -based components for their products. This change has left many high-reliability electronic equipment manufacturers with the choices of, mixing lead-free components in tin-lead assembly process, or converting products to lead-free, or reprocessing lead-free components to comply with the tin-lead assembly process.

1.2. Reballing of Ball Grid Array Packages

Reballing is a technology for repairing the Ball Grid Array (BGA) package. Reballing has been used to reclaim components from defective or discarded assemblies, but today it offers a way to convert lead-free solder into tin-lead solder. In the reballing process, the original solder balls are removed and new solder balls are attached on the component pads.

The reballing process has two major procedures: solder ball removal and solder ball re-attachment. The solder ball removal process removes the original solder

from the component. The solder ball re-attachment process attaches new solder balls on the component pads. Since each procedure in the process has different methods, there are multiple combinations in the reballing process. There are several thermal procedures in the reballing process, which leads to the microstructure changes in reballed BGAs. The temperature cycling reliability of reballed BGA assemblies needs to be determined before the implementation.

1.3. Mixed Ball Grid Array Assembly

In the transition from tin-lead to lead-free, it may necessary to use lead-free terminated component with tin-lead solder paste. The mixing of different solder materials can induce new reliability concerns, because the reliability of a solder joint depends on loading conditions, materials properties, and the microstructure of the solder joint. The implementation of mixed assemblies has been limited due to concerns about the long-term reliability of mixed solder joints. For leaded components, the reliability of mixed assemblies is not a major concern, because the amount of solder in component finish is small when compared to solder paste volume. However, for array area packages, the amount of solder in the solder ball is comparable to the amount of solder paste, which leads to reliability concerns when mixing metallurgies in array-area assemblies.

1.4. Rework of Ball Grid Array Assembly

Rework is defined as the correction of a defect before the printed board assembly leaves the plan and repair as the correction of a defect found in the field [6]. Global transition from lead-base solder to lead-free solder makes rework processes

facing new challenges, such as higher operating temperature and materials selection. With the uncertainty associated with lead-free reliability and issues associated with mixing lead-free solder with tin-lead solder, it is important to understand the impact of the rework process and on the reliability of reworked assemblies.

1.5. Problem Statement

Reballing technology, which substitutes new solder balls for the original ones, provides a solution for ball grid array (BGA) packages for the shortage of tin-lead array components. There is little literature address on the temperature cycling reliability of reballed BGAs. The impact of different reballing methods on the temperature cycling reliability of reballed BGA assemblies has not been studied yet. A lot of issues are involved in reballing technology. 1) When changing the solder ball materials (lead-free to tin-lead or tin-lead to lead-free), different reballing methods may lead to different intermetallic compounds (IMCs). 2) High temperature exposure in the reballing processes leads to thicker IMC layer thickness in reballed components than that in the non-reballed ones. 3) Whether the selection of different reballing method leads to changes in the bulk solder microstructure of reballed BGAs.

In the transition from tin-lead to lead-free, it may necessary to use lead-free terminated component with tin-lead solder paste. There are many challenges existed when using lead-free BGA mixed with tin-lead solder paste in the current. 1) The impact of Pb distribution in the mixed assembly on the temperature cycling reliability of assembly is still unknown. 2) There is still no clear conclusion whether the

temperature cycling reliability of mixed assembly is comparable to that of lead-free assembly.

Global transition to lead-free solder has raised several concerns for rework such as higher operating temperature and materials selection. In particular, the rework of mixed assemblies (lead-free components with tin-lead paste) requires restrict thermal profile setup to get a uniform mixing structure to ensure the reliability [7]-[9]. Sometimes, the same site on the PCB needs to be reworked multiple times. The reliability of the BGA assemblies after multiple rework processes needs to be determined.

1.6. Overview of Thesis

The structure of this dissertation is as follows; chapter 2 provides the literature review on reballed BGA components and assemblies, lead-free BGA assemblies, mixed BGA assemblies, as well as the reworked BGA assemblies. Chapter 3 provides the microstructural analysis of reballed BGA components and the solder ball strength assessment of reballed BGA components. Chapter 4 provides the temperature cycling test results and failure microstructural analysis of reballed tin-lead, lead-free, and mixed assemblies. Chapter 5 discusses the impact of multiple rework processes on the microstructure and the temperature cycling reliability of lead-free and mixed assemblies.

Chapter 2: LITERATURE REVIEW

There are numbers of studies have been conducted on evaluating reballed BGAs, and reworked BGA assemblies, including evaluating the solder ball attachment strength of the reballed BGA components, Cu dissolution in the reworked BGA assemblies and intermetallic compound analysis. However, little literature addresses on the temperature cycling reliability of reballed BGA assemblies, and temperature cycling reliability of reworked BGA assemblies after multiple rework processes. This chapter summarizes the studies related to reballed BGA components, reballed BGA assemblies, and reworked BGA assemblies. Table 1 provides summary and key findings from various studies on the reworked assemblies. Table 2 summarizes all the key finding of mixed assemblies from various studies.

2.1. Studies on Reballed BGA Components and Reballed BGA Assemblies

There is a concern whether the components after reballing act as the same as the non-reballed (virgin) BGA components. Thus, the same evaluation approaches are carried out on both non-reballed BGAs and reballed BGAs in order to compare the test results. Ball shear test and cold bump pull test are the common methods to evaluate the solder ball strength. Several studies have focused on assessing the solder ball attachment strength of reballed BGAs [10]-[12]. However, there is no literature mentioned that reballing lead-free BGA with tin-lead solder, and evaluating the reballed BGAs using different reballing methods.

Solder ball strength is considered as one type of quality evaluation methods of reballed BGAs. In order to understand temperature cycling reliability of reballed BGAs, it requires the reballed BGAs assembled on printed circuit boards (PCBs) and then subjected to the reliability testing. Unfortunately, there is little literature addressed on the reliability testing of reballed BGAs. Beair and Vuono [12] used the temperature cycling test to evaluate the temperature cycling reliability of reballed SnPb BGAs, but there was no test result reported. Chatterji [13] reported fatigue crack propagation at the board side in the reballed SnPb assemblies after they were subjected to the temperature cycling test, but large voids were observed in the reballed BGAs due to an improper reballing process and reflow profile setup.

While reballing has been considered as an alternative assembly method, there are several issues yet to be answered for the industry, such as the effect of different reballing methods on the temperature cycling reliability of reballed BGAs and the failure modes of the reballed BGAs.

2.2. Studies on Reworked BGA Assemblies

Since the electronics industry is now using lead-free solder predominately, it is important to understand the impact of the rework process on the temperature cycling reliability of the reworked assemblies. Some literature addresses Cu dissolution in plated through-hole (PTH) barrels in the rework process [14]-[17]. This creates a concern because it is possible for a hidden defect to be present after reworking PTH assemblies. S. Chada et.al, found out that the amount of Cu dissolution increased as the soldering temperature and time increasing [18]. Thus, the

rework process parameters, such as the peak temperature and the time above liquidus, are important to the Cu dissolution in the reworked assemblies. Currently, no literature has focused on the Cu dissolution of reworked ball grid array (BGA) assemblies, which is another possible hidden defect.

Only several studies focused on the temperature cycling reliability of reworked assemblies [19]-[24]. Russell, et al [19] has reported the temperature cycling reliability of mixed and tin-lead reworked BGA assemblies under accelerated thermal cycling (ATC) test with the temperature range of -55°C to 125°C in accordance with the IPC-9701 specification. The temperature cycling reliability showed that reworked assemblies have equivalent characteristic lives with the as-assembled assemblies. Kelly, et al [20] conducted ATC test to lead-free reworked BGA assemblies. The BGA assemblies were qualified to a 2X rework process, and the as-assembled lead-free assemblies were taken as a reference. Both the as-assembled assemblies and reworked assemblies were subjected to ATC test with the temperature range of 0-100 °C (one hour per cycle). All the test samples passed the ATC test of 1000 cycles and 3000 cycles.

There are a lot of issues not been addressed on the temperature cycling reliability of reworked assemblies in the current literature, such as the impact of multiple rework processes on the temperature cycling reliability of reworked assemblies, the microstructure differences between non-reworked and reworked assemblies. Table 1 provides summary and key findings from various studies on the reworked assemblies. It offered the assembly and rework methods, the temperature cycling reliability test condition and the findings.

Table 1: Literature summary of reworked BGA assemblies

Ref	Package / PCB finish	Assembly Method	Rework Method	TC Reliability Test	Findings
Russell, et al [19]	PBGA225, Sn3.9Ag0.6Cu & 63Sn37Pb balls, SnPb HASL finish	Lead-free and tin-lead BGAs were assembled with eutectic SnPb paste	The mixed assemblies (SAC balls with SnPb paste) were reworked with Sn3.9Ag0.6Cu paste, the tin-lead assemblies were reworked with SnPb paste	ATC: -55°C~125°C, 30 min at high temp. extreme, 10 min at low temp. extreme, ramp rate: 10°C/min.	Reworked assemblies had equivalent characteristic life to the as-assembled assemblies.
Kelly, et al [20]	FCPBGA, PBGA, CSP, SAC305/SAC405 balls, OSP finish	All BGAs were assembled with SAC405 paste	All BGAs were qualified to 2X rework processes with SAC 405 paste	ATC: 0~100 °C, one hour per cycle, 1000 cycles & 3000 cycles	Reworked assemblies and as-assembled assemblies passed both ATC tests.
Sy, et al [21]	PBGA81 SAC405 balls, NiAu & OSP finish	All BGAs were assembled with Sn3.5Ag0.7Cu solder paste	All BGAs were reworked with Sn3.5Ag0.7Cu paste	ATC: -40°C~125°C, 2500 cycles	Reworked assemblies passed 2500 cycles ATC.

Table 1: Literature summary of reworked BGA assemblies

Ref	Package / PCB finish	Assembly Method	Rework Method	TC Reliability Test	Findings
Butel [22]	CBGA1837, SnAC305 & high Pb balls with eutectic SnPb, OSP finish	Lead-free CBGAs were assembled with SAC paste, and the high Pb CBGAs were assembled with eutectic SnPb paste	Lead-free CBGA assemblies were reworked with SAC paste; High Pb CBGA assemblies were reworked with SnPb paste	ATC: 0~100 °C, IPC 9701	Reworked SAC assemblies had equivalent characteristic life to the SAC assemblies; Reworked high Pb BGAs failed fast due to insufficient paste deposited during rework process
Manjunath, et al [23]	FBGA60 SAC305 balls, OSP finish	All the BGAs were assembled with Sn3.8Ag0.7Cu paste	All BGAs were reworked with Sn3.8Ag0.7Cu paste	ATC, 0~125 °C, dwell time at extreme: 12 min, ramp rate:10°C/min, 1000 cycles	Reworked assemblies passed ATC tests.
Gowda, et al [24]	CSP, Sn3.2Ag0.5Cu, Sn3.5Ag and Sn37Pb balls, NiAu finish	Lead-free CSPs were assembled with S3.5Ag paste, and the tin-lead CSPs were assembled with eutectic SnPb paste	Lead-free CSPs were reworked with S3.5Ag paste, and CSPs were reworked with eutectic SnPb paste	ATC, 0 ~100 °C, 20 min per cycle, ramp and soak time was 5 min.	Reworked CSP passed 920 cycles.

2.3. Studies on Reliability of Mixed Assembly

In cases where conventional tin-lead ball grid array (BGA) components are not available, it may be necessary to use Pb-free version of that component with an existing SnPb assembly process. A solder joint formed due to the mixing of SnPb and Pb-free materials is termed a "mixed solder joint" [25]. The mixing of different solder materials can induce new reliability concerns, because the reliability of solder joint depends on loading conditions, materials properties, and microstructure of the solder joint. The implementation of mixed assemblies has been limited due to concerns about the long-term reliability of the mixed solder joints. For leaded components, the reliability of mixed assemblies is not a big concern, because the amount of solder in component finish is too small as compared to solder paste volume. However, for array area packages, the amount of solder in solder ball is comparable to the amount of solder paste, which leads to reliability concerns of mixing metallurgies in array area assemblies.

From 2005 until 2009, a significant number of studies addressed the reliability of mixed assemblies. People care about the long-term reliability of mixed assemblies. The pure SnPb and Pure SAC assemblies are usually taken as controls. Majority of current studies focused on thermo-mechanical fatigue life of mixed assemblies under accelerated temperature cycling (ATC) test [26]-[34] [38]-[56]. Mechanical bending test, drop test, and mechanical shock test were used to evaluate the mechanical reliability of mixed assemblies [29] [32] [35] [50].

Snugovsky reported that mixed solder fatigue life was component dependent and could be better, equal, or worse than the fatigue life of SnPb [26]. About 12 of 27 studies showed that the temperature cycling reliability of mixed assemblies is equal to or better than pure SnPb assemblies. Based on the statement above, it is possible to achieve some mixed assemblies with acceptable temperature cycling reliability. Table 2 summarizes all the ATC tests of mixed assemblies.

Majority of studies believed that full mixing metallurgy structure in solder joints is directly related to the temperature cycling and mechanical reliability of mixed assemblies. A typical study [53] claimed that partial mixing led to early failure in ATC test. Field programmable gate array (FPGA) with SAC405 solder alloys were assembled with eutectic SnPb solder. The first BGA failed at 137 cycles of the ATC test with temperature range of -55°C to 125°C. Crack initiated at the board side instead of the typical failure site, component side. D. Hillman et al, claimed that Pb redistributed or Pb segregation at interfaces reduced the temperature cycling reliability of mixed assemblies. Full mixing is very important for ceramic ball grid array (CBGA) mixed assemblies. Studies focused on CBGA assemblies showed that partial mixed CBGAs had much worse performance than SnPb assemblies and full mixed assemblies [26] [42] [49] [56].

Table 2: Summary of ATC test results of mixed assemblies

Ref.	BGA Type/ Solder Ball Composition	TC Reliability Test Condition	Temperature Cycling Reliability Test Findings
[26]	CBGA937/SAC405, PBGA256/SAC405, PBGA196/SAC405, CSP46/SAC305	0 ~ 100°C, dwell: 10 min, 6000 cycles	PBGA196: TC reliability of mixed assemblies is similar to Pb-free assemblies, better than SnPb assemblies; PBGA256: TC reliability of mixed assemblies is equal to or better than SnPb assemblies; CBGA937: TC reliability of full mixed similar to SnPb assemblies, TC reliability of partial mixed assemblies is much worse than SnPb assemblies.
[27]	DDR2 BGA memory component/SAC305 & SAC405	0 ~ 100°C, dwell: 10 min, 2000 cycles	solder joint cracking length was lesser for the full mixed assemblies compared to SnPb assemblies
[28]	BGAs/SAC305	-40°C~125°C, 4300 cycles; 0 ~ 100°C, 13000 cycles	No more than 15% variation was observed in the thermal fatigue of mixed assemblies reflowed below and above the Pb-free ball melting temperature; TC Reliability of mixed assemblies is better than that of SnPb assemblies.
[29]	PBGA676/SAC405	0 ~ 100°C, dwell: 10 min or 60 min at high extreme	TC reliability of mixed assemblies is worse than that of Pb-free assemblies; Partial mixed assemblies and full mixed assemblies have similar TC reliability.
[30]	CBGA575/SAC387 SBGA560/SAC405 PBGA1156/SAC405 µBGA288/SAC405 CSP132/SAC405	-55°C ~125°C 60 min/cycle > 4000 cycles	Larger BGAs with full mixing has better TC reliability than SnPb assemblies; Larger BGAs with partial mixing has acceptable TC reliability; Small BGAs with full mixing has acceptable TC reliability or better TC reliability than SnPb assemblies.

Table 2: Summary of ATC test results of mixed assemblies

Ref.	BGA Type/ Solder Ball Composition	TC Reliability Test Condition	Temperature Cycling Reliability Test Findings
[31]	PBGA/SAC305 PBGA/SAC405 CSP46/SAC405 CSP46/SAC305	0 ~ 100°C, dwell: 10 min 6000 cycles	TC reliability decreases slightly with increasing peak temperature; Degree of mixing does not appear to have an effect on the TC reliability of partial mixed assemblies.
[32]	PBGA196/SAC305 CSP8/SAC305	-40°C ~ 85°C dwell: 15 min	Pb-free assemblies outperformed mixed assemblies; Mixed assemblies reflowed at a higher temperature outperformed than the mixed assemblies reflowed at a lower temperature
[33]	SBGA600/SAC405 PBGA324/SAC405 CABGA288/SAC405 CTBGA132/SAC405	-40°C~125°C dwell: 10 min 3559 cycles	Smallest BGA (CTBGA132): TC reliability of mixed assemblies is better than SnPb assemblies and equal to SAC assemblies; Larger BGA (CABGA288): TC reliability of mixed assemblies is worse than pure SnPb and SAC assemblies; Largest BGAs (PBGA324 and SBGA600): TC reliability of mixed assemblies is better than pure SnPb and SAC assemblies.
[34]	CBGA937/SAC405 CBGA937/SAC 305 PBGA/SAC405 PBGA/SAC305 CSP64/SAC405 CSP64/SAC305	0 ~ 100°C, 6000 cycles	Mixed assemblies with SAC405 balls outperform that with SAC305 balls; TC reliability of mixed assemblies decreased with increasing reflow peak temperature; Full mixing is not required to create reliable solder joints.
[38]	PBGA256/SAC405, PBGA256/SAC305 PBGA196/SAC405, PBGA196/SAC305, CSP46/SAC405 CSP46/SAC305	0 ~ 100°C, dwell: 10 min 6000 cycles	Early indications are that the TC reliability of components will be acceptable for many applications.

Table 2: Summary of ATC test results of mixed assemblies

Ref.	BGA Type/ Solder Ball Composition	TC Reliability Test Condition	Temperature Cycling Reliability Test Findings
[39]	PBGA376/SAC305	0 ~ 100°C, dwell: 10 min or 30 min	Partial mixed cells is equal or better than fully mixed cells; TC reliability of mixed assemblies reduced in longer dwell time TC test; TC reliability of mixed assemblies is similar to that of Pb-free assemblies.
[40]	BGA/SAC	-55°C~125°C, dwell: 30 min at hot, 10 min at cold	Crack initiated at component side at 1525 cycles for lead-free assemblies; Mixed assemblies did not show any cracking.
[41]	BGA196/SAC305	-55°C~125°C, dwell: 5min, 20 min/cycle	TC reliability summary: mixed assemblies >Pb-free assemblies>SnPb assemblies
[42]	CBGA/SAC305 CABGA/SAC305 PBGA/SAC305, SAC105, Sn3.5Ag, SAC105 FCBGA/SAC305	N/A	TC reliability of mixed assemblies is comparable to SnPb assemblies.
[43]	CBGA575/SAC405 SBGA560/SAC405 PBGA1156/SAC405 μBGA288/SAC405 CSP132/SAC405	-55°C~125°C, dwell: 15min, 60 min/cycle > 4000 cycles	CBGA assemblies have poor TC reliability compared to Sn90Pb CBGA assemblies; Mixed assemblies have acceptable TC reliability or better TC reliability than SnPb assemblies.
[44]	PBGA 256/SAC305 SnPb2Ag paste	-55°C~125°C, 50 min/cycle, 2000 cycles	Mixed and lead-free assemblies outperform SnPb assemblies； Small level of Pb contamination (1%-10%) does not affect TC reliability。

Table 2: Summary of ATC test results of mixed assemblies

Ref.	BGA Type/ Solder Ball Composition	TC Reliability Test Condition	Temperature Cycling Reliability Test Findings
[45]	PBGA 256/SAC305 SnPb2Ag paste	-55°C~125°C, 50 min/cycle 2000 cycles	Mixed and lead-free assemblies outperform SnPb assemblies，Small level of Pb contamination (1%-10%) does not affect thermal cycling reliability
[46]	BGA/SAC305	0 ~ 100°C, dwell: 18 min at hot, 16 min at cold 1500 cycles	Mixed assemblies failed earlier than SnPb assemblies
[47]	BGA/SAC305	0 ~ 100°C, dwell: 18min at hot, 16min at cold，1500 cycles	Mixed assemblies failed earlier than SnPb assemblies
[48]	BGA208/SAC305 BGA416/SAC305	-40°C~125°C, dwell: 15 min, 90 min/cycle，4800 cycles	TC reliability of mixed assemblies is better than that of SnPb assemblies.
[49]	CBGA937/SAC405	0 ~ 100°C, dwell: 10 min, 6010 cycles	TC reliability of full mixed assemblies is better than SnPb assemblies, slightly worse than Pb-free assemblies; TC reliability of partial mixed is much worse than SnPb assemblies.

Table 2: Summary of ATC test results of mixed assemblies

Ref.	BGA Type/ Solder Ball Composition	TC Reliability Test Condition	Temperature Cycling Reliability Test Findings
[50]	PBGA196/SAC305 CSP8/SAC305	-40°C~ 85°C, dwell: 15 min	Pb-free assemblies outperformed mixed assemblies; Mixed assemblies reflowed at a higher temperature performed better than the mixed assemblies reflowed at a lower temperature.
[52]	PBGA/SAC405	0 ~ 100°C, 60 min/cycle 5000 cycles	Both Pb-free and mixed assemblies pass 5000 cycles.
[53]	BGA256/SAC405	-40°C~125°C, dwell: 11 min, 2000 cycles	Assemblies with partial mixing had early failure.
[54]	BGA/SAC305	0 ~ 100°C, dwell: 15 min, test stopped at 70% failure	Low Pb% will be benefit to ATC reliability, if there is no quality problem; TC reliability of partial mixed assemblies outperform full mixed assemblies, because of higher ball height; The mixed assemblies achieved below SAC melting temperature still have an acceptable TC reliability.
[55]	BGA memory module/SAC305	0 ~ 100°C, dwell: 18 min at hot, 16 min at cold, 1500 cycles	TC reliability of full and partial mixed assemblies is worse than that of SnPb assemblies.
[56]	CBGA 937/SAC 405	0 ~ 100°C, dwell: 10 min, 6010 cycles	TC reliability of full mixed assemblies is better than SnPb assemblies, slightly worse than Pb-free assemblies; TC reliability of partial mixed is much worse than SnPb assemblies.

Chapter 3: MICROSTRUCTURAL ANALYSIS AND SOLDER BALL STRENGTH ASSESSMENT OF REBALLED BGA

Reballing is a technology for repairing the ball grid array (BGA) package. It removes the original solder balls and places new solder on the pads of package. In the reballing process, higher temperature exposure in solder ball removal and solder ball re-attachment procedures leads to microstructural changes at the interface. The initial formation of intermetallic compounds (IMC) during soldering ensures a good metallurgical bond, but the growth of these IMCs results in a weak interface that would lead to failure. The growth of intermetallic compound at the interface is directly proportional to time and temperature. Currently, there is no literature talking about interfacial IMCs on reballed BGAs.

Since reballing changes the solder ball, one measure of reballing quality is the attach strength of the reattached solder ball. Two test methods exist to quantify solder ball attach strength: ball shear test and cold ball pull (CBP) test. The ball shear test is a destructive test conducted to determine the ability of BGA solder balls to withstand mechanical shear forces. JEDEC Standard JESD22-B117A offers guidelines to apply the ball shear test to BGA components, to select the shear speed, and to define failure modes [57]. Substantial literature is focused on the ball shear test on BGA components [58]-[61]. The CBP test is a relatively new destructive test method for assessing the solder ball strength. Currently, there is no industry standard for the cold bump pull test. The CBP test uses tensile force rather than shear force.

3.1. Reballing Processes

The reballing process involved two steps: solder ball removal and solder ball re-attachment. Each step could be achieved by multiple methods. Table 3 shows the reballing process used in this study. Here, 676 I/O and 256 I/O BGAs with Sn3.0Ag0.5Cu (SAC 305) were reballed with eutectic tin-lead solder. The ball diameter for 676 I/O BGA was 630 μm with 1.0mm pitch and solder ball pattern was peripheral area array. While the diameter for 256 I/O BGA was 760 μm with 1.27 mm pitch, and solder ball pattern was full area array. The original metallization of the pads on the PBGA was Cu/Ni with immersion Au.

Table 3: Reballing process matrix

Component	Reballing Process No.	Solder Ball Removal Approach	Solder Ball Re-Attachment Approach
676 I/O PBGA	Reballed I LTWS+PF	Low-temperature wave solder	Preform
676 I/O PBGA	Reballed II SW+PF	Solder wick	Preform
256 I/O PBGA	Reballed I LTWS+PF	Low-temperature wave solder	Preform
256 I/O PBGA	Reballed II LTWS+BD	Low-temperature wave solder	Solder ball drop

The solder ball removal process removes the original solder from the component. This procedure is very important since the pad and substrate can be damaged during the process, degrading the quality of the reballed components. In this

experiment, two methods for solder ball removal were used: solder wick and low-temperature wave solder.

In the low-temperature wave solder process, the component was held by a vacuum nozzle and suspended into the solder wave for a sufficient time to remove the solder balls (see Figure 1). The solder in the wave was eutectic SnPb and the wave temperature was 220°C. The low-temperature wave solder ball removal process requires special equipment, but it can be developed as an automated process suitable for high-volume conversion. It also resolves the handling issue due to the ability to automate the process. This method is much more controllable, but also more expensive, in comparison to the solder wick method.

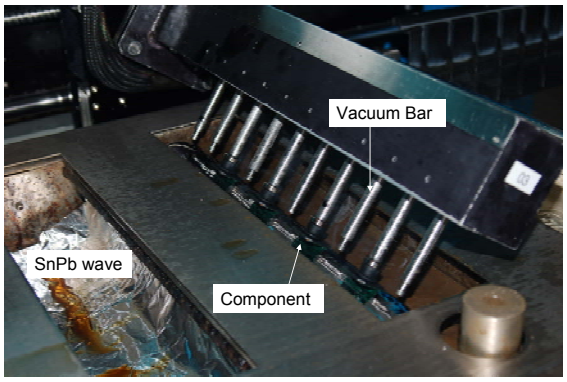

Figure 1: Solder ball removal by low-temperature wave solder

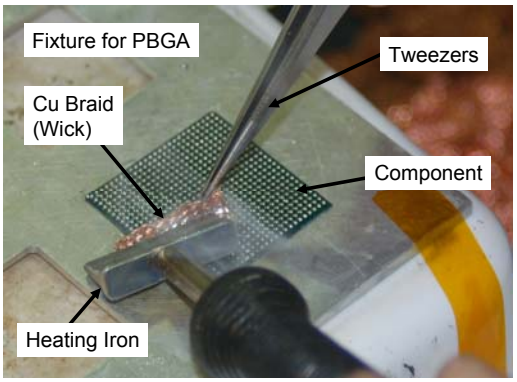

Figure 2: Solder ball removal by solder wick

In the solder wick process, the package is fixed with the solder balls facing upward. A soldering iron is used to heat a Cu braid (wick), which is manually wiped (by tweezers) over the solder ball (see Figure 2). The braid wire melts the solder balls and picks up the molten solder. In this study, the solder iron temperature was set to 250°C. The solder wick method is inexpensive and good for low volume work.

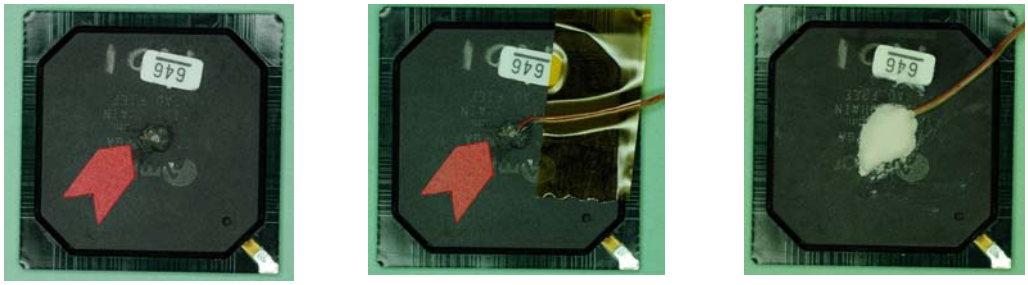

Drill Hole Place Thermocouple Apply Glue

Figure 3: Thermocouple placement

During both solder ball removal processes, the temperature was measured by a K-type thermocouple. A hole was drilled at the plastic mold side to place a thermal couple above the die as shown in Figure 3. Figure 4 and Figure 5 show the thermal profiles measured for low-temperature wave solder and solder wick methods, respectively. The maximum package temperature measured at the die surface was 164.5°C for the low-temperature wave solder method, while the maximum package temperature was 180°C for the solder wick method. The low-temperature wave solder method has a shorter preheat and contact time than the solder wick method, which reduces the thermal shock and damage to the components. The contact time for the low-temperature wave solder procedure was 18 seconds, while the contact time for the solder wick method was 42 seconds.

The solder ball re-attachment procedure in the reballing process places new solder balls on the pads of the package. The preform method was selected in this study. The BGA preform technique, which was originally developed by Raychem, consists of an array of solder balls sandwiched between a lamination of carriers (see Figure 6). Carriers control the pitch, progression, and alignment. Carriers are made of

water-dispersible paper laminates that are easily removed after reflow. In the solder ball re-attachment procedure, the preform and component are matched by the fixture and reflowed together. The solder ball drop method involves applying a layer of flux onto the pad of the package, then attaching the component with the template that is matched with the pattern of the package. The solder balls are poured into the holes of the template as shown in Figure 7. These two methods can use either a hot air tool or oven to reflow.

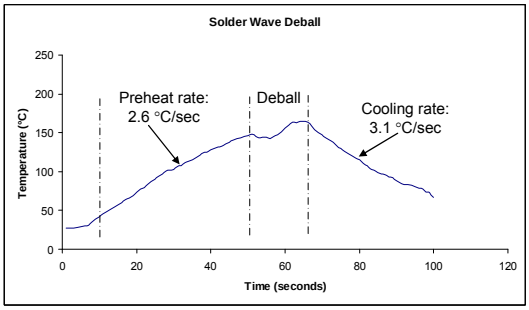

Figure 4: Thermal profile (above die) of low-temperature wave solder method

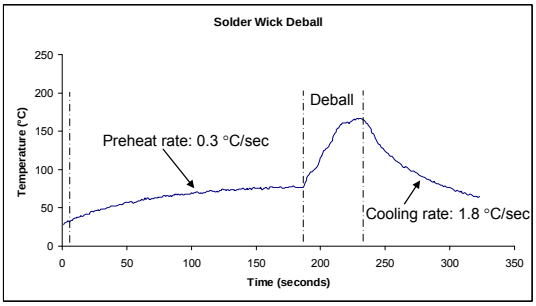

Figure 5: Thermal profile (above die) of solder wick method

The temperature profile above the die is also documented as shown in Figure 8 and Figure 9. In the preform method, the maximum package temperature measured at the die surface was 213°C. The preheat rate and the cooling rate were 1.3°C/s and 1.65°C/s, respectively. In the ball drop method, the maximum package temperature measured at the die surface was 211°C. The preheat rate and the cooling rate were 1°C/s and 1.15°C/s, respectively.

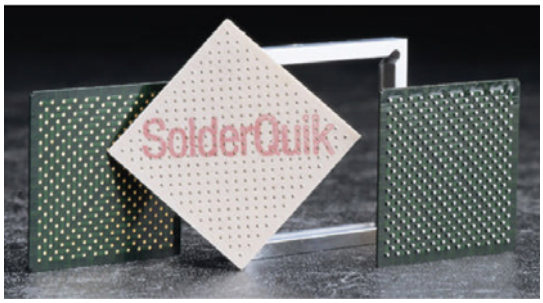

Figure 6: SolderQuik™ BGA preform

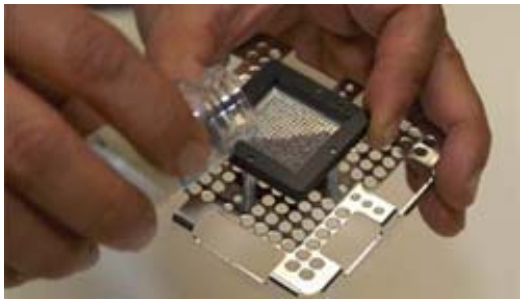

Figure 7: Solder ball drop method

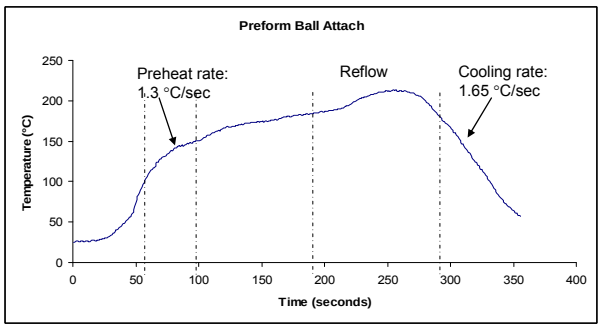

Figure 8: Thermal profile (above die) of preform method

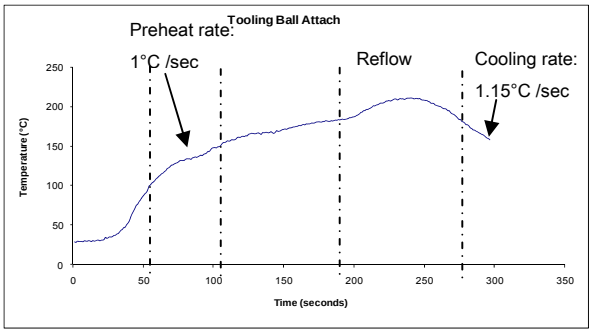

Figure 9: Thermal profile of solder ball drop method

3.2. Solder Ball Attachment Strength of Reballed BGAs

In order to quantify the reliability and quality of reballed BGAs, both the ball shear and cold bump pull (CBP) tests were applied to reballed BGAs. A set of 676 I/O and 256 I/O lead-free (SAC305) BGAs were selected. Two ball removal and two ball re-attachment processes were examined. The ball removal process included solder wick and low-temperature wave solder. Ball re-attachment methods included BGA preform and ball drop. Each of these processes is discussed in this paper. After reballing, the BGA components were subjected to select isothermal aging. For the

ball shear test, one tool speed was used. For the CBP test, two tool speeds were used. The failure modes and failure sites were documented.

3.2.1. Experimental Setup

To assess the quality of the solder ball re-attachment of the reballed components, the ball shear and cold ball pull tests were conducted. As part of the investigation, two isothermal aging conditions, 100°C for 24 hours and 125°C for 350 hours, were also examined.

Table 4: Sample matrix of non-reballed and reballed components

676 (256*) I/O BGA	Non-Reballed			Reballed Type I			Reballed Type II		
	Non-aged	100°C 24 hrs	125°C 350 hrs	Non-aged	100°C 24 hrs	125°C 350 hrs	Non-aged	100°C 24 hrs	125°C 350 hrs
Sample Size	50 balls	50 balls	50 balls	50 balls	50 balls	50 balls	50 balls	50 balls	50 balls

* There are only 6 treatments for 256 I/O BGAs, without non-aged ones.

The equipment used in the ball shear test was DAGE 2400, and the load cell was 2 Kg. The shear speed was 200 μm/sec, and the shear height was 50 μm. JESD 22-B117A recommends that the shear height be no more than 25% of the solder ball height. The equipment used in the cold bump pull test was DAGE 4000, and the load cell was CBP/TP 5 Kg. Two pull speeds were selected: 500 μm/sec and 5000 μm/sec. Fifty balls were tested for each test and each treatment. Table 4 lists the sample matrix and Table 5 lists the test parameters. Figure 10 shows schematic picture of ball shear test and Figure 11 shows cold bump pull test.

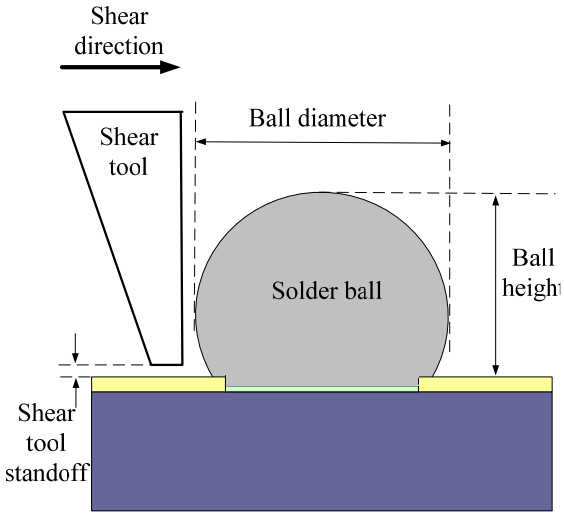

Figure 10: Schematic image of ball shear test

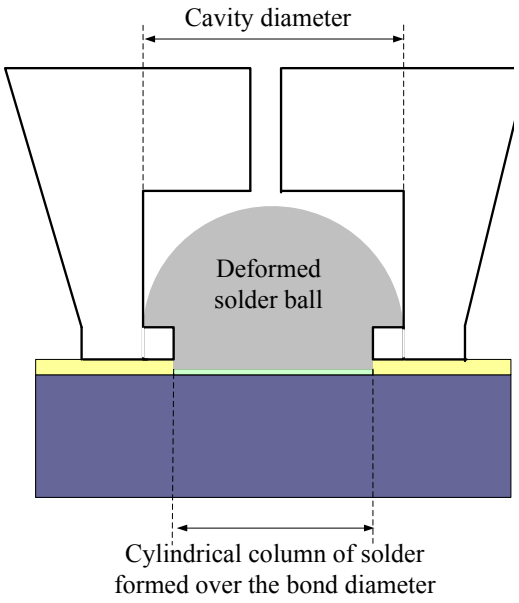

Figure 11: Schematic image of cold bump pull test

Table 5: Test parameter setup for ball shear test and cold bump pull test

Test	Ball shear	Cold bump pull
Speed	200 µm/sec	500 µm/sec 5000 µm/sec
Shear Height	50 µm	N/A
Clamping force	N/A	12 psi

3.2.2. Ball Shear Test Results

Shear strength is defined as the ability of a material to withstand shear stress or the stress at which a material fails in shear. In the ball shear test, the shear strength is measured in gram force (gF). Since the shear strength is not a constant in the test, the peak shear force is documented. The shear force values are plotted in boxplots

using Minitab and presented in Figure 12 and Figure 13. Figure 12 presents the data for the 676 I/O ball grid array packages. Figure 13 presents the shear test data for the 256 I/O ball grid arrays. Both plots contain data sets for the non-reballed (virgin) lead-free BGA and the two types of reballed BGAs under non-aged and isothermal aging conditions. For each data set, the box covers 50% of the data with the line in the box representing the mean. The whisker lines on the top and bottom of the box represent the range of shear strength (see Figure 12 and Figure 13). The stars represent outliers in the data.

For 676 I/O BGAs, the non-reballed (virgin) components with SAC305 exhibited a higher shear strength than the reballed components with Sn37Pb solder. For the lead-free 676 I/O BGAs, the shear strength of non-aged BGAs was lower than that of aged BGAs. This was due to changing grain size in the solder and is typical of short-time thermal aging exposure of as-received solder joints. For the reballed tin-lead 676 I/O BGAs the isothermal aging had no noticeable effect. The reason may be due to the structure and property of different solder materials. Eutectic tin-lead solder has a lamellar eutectic composed of tin and lead phases. Lead-free SAC solder has a tin-rich phase and an Ag_3Sn+Sn phase, and Ag_3Sn shows the fiber shape embedded in Sn phase. The Ag_3Sn particles inside the SAC solder strengthen the solder and vary the grain size of the SAC solder. The changing of grain size is more uniform than lead-free SAC solder under thermal aging conditions. Thus, thermal aging had less effect on tin-lead solder strength than lead-free solder strength. For the reballed 676 I/O BGAs, the shear strength had a smaller distribution. Even though reballed I (LTWS+PF) and reballed II (SW+PF) BGAs have different solder ball removal

methods, the shear strength stays at the same level, which means that the shear strength of reballed BGAs is independent of the solder ball removal methods.

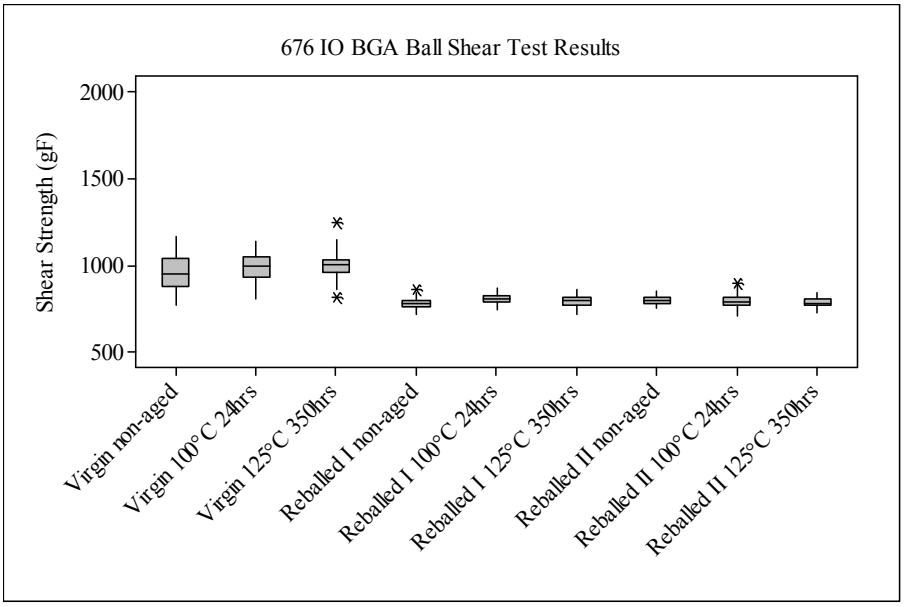

Figure 12: Shear strength of 676 I/O non-reballed and reballed BGAs

For the 256 I/O BGAs, non-aged samples were not included. Like the 676 I/O components, the lead-free 256 I/O components showed a higher shear strength than the tin-lead reballed components. Again, the distribution of shear strength was larger for the lead-free components than the reballed tin-lead components. Unlike the 676 I/O lead-free components, the 256 I/O lead-free components showed a reduction in shear strength with longer isothermal aging. Like the reballed tin-lead 676 I/O components, the reballed tin-lead 256 I/O components showed a lower distribution of shear strength and no noticeable trend related to isothermal aging. Like the 676 I/O reballed components, there does not appear to be a noticeable difference in shear strength even though two types of reballed BGAs have different solder ball attachment methods. From the shear strength measurements, reballed components

exhibited low variation in shear strength, which indicated a consistent and controlled process.

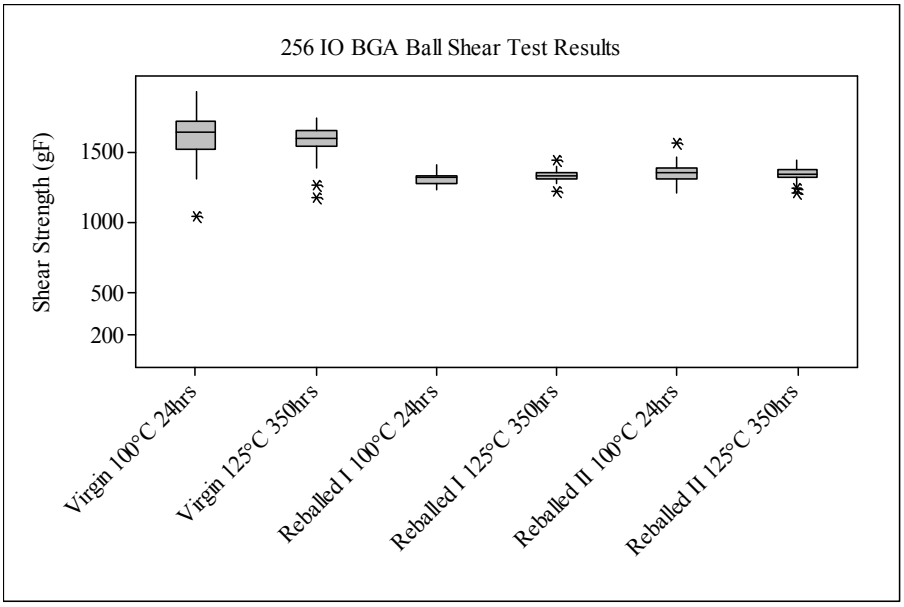

Figure 13: Shear strength of 256 I/O non-reballed and reballed BGAs

The finding that the shear strength of lead-free solder balls was greater than tin-lead solder balls was consistent with prior studies [62] [63]. The reason that SAC solder balls have shear strength is because the SAC solder has higher shear strength. Hernandez et al. used the Cu ring and plug specimens to test the shear strength of Sn3.5Ag alloy [64], which showed that the Sn-3.5Ag (54.95 + 3.65 MPa) has a higher shear strength than eutectic SnPb solder (40.27 + 1.65 MPa). Most of the SAC mechanical properties are 10 MP higher than those of Sn-3.5Ag solder [64]. Thus, the shear strength of SAC solder is about 25 MPa larger than that of SnPb solder, which means that lead-free solder balls have higher strength values in the ball shear test.

3.2.3. Failure Analysis of Ball Shear Test

As per JESD22-B117A [57], the failures under the ball shear test may be divided into four types. The first failure type is ductile, where the solder ball fractures at or above the surface of the solder mask within the bulk solder. The second failure type is pad lift, where the pad lifts together with the solder ball (including the substrate materials, which fracture together with the pad). The third failure type is ball lift, where the fracture happens at the interface of the ball and pad due to weak bonding between the solder ball and pad. The fourth failure type is an interfacial break, where the break is at the solder/intermetallic interface or intermetallic/base metal interface.

In the ball shear tests, ductile failure was observed in all cases. Figure 14 shows the failure site of a non-reballed 676 I/O BGA and Figure 15 shows that of a reballed II (SW+PF) BGA. The fracture sites of non-reballed and reballed components were in the bulk solder. Ductile failure was the expected failure mechanism. Ductile failure occurs when the flow stress of the bulk solder is less than the Cu pad peel strength and the interfacial strength of the joint. As addressed in previous study [61], low shear speeds generated more ductile failure. In this study, the shear speed was 200 μm/sec, which was relatively low. Thus, it was not surprising to find that all the reballed and non-reballed components had ductile failure mechanisms, which also meant that the reballing process was a robust process.

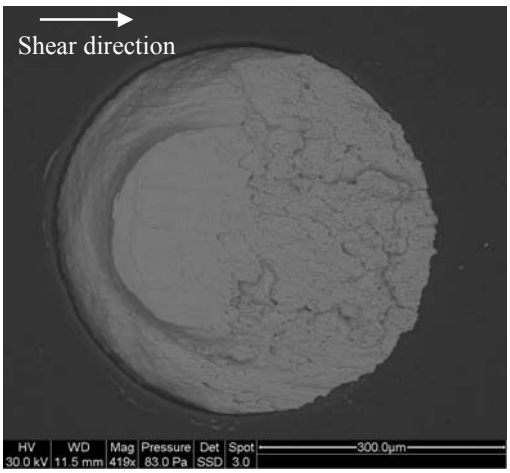

Figure 14: Failure site of a non-reballed 676 I/O BGA with SAC solder balls

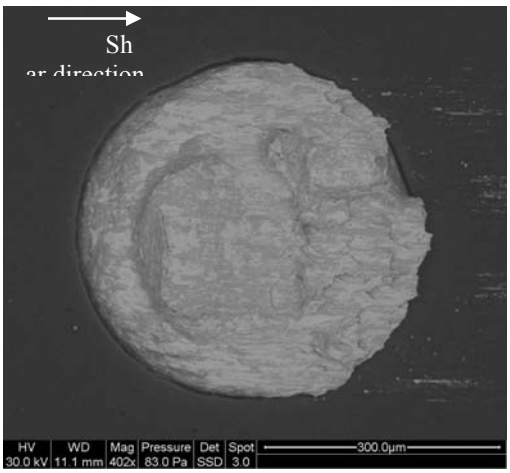

Figure 15: Failure site of a 676 I/O reballed II (SW+PF) BGA with SnPb solder balls

3.2.4. Cold Bump Pull Test Results

As with the ball shear test, the cold bump pull test was conducted on reballed and non-reballed samples. Again, isothermal aging conditions of 100°C for 24 hours and 125°C for 350 hours were examined. For the cold bump pull test, pull speeds of 500 µm/sec and 5000 µm/sec were used. Here, pull strength is defined as the bond strength of an adhesive joint, obtained by pulling in a direction perpendicular to the surface of the layer. As in the ball shear test, the pull strength is measured in gram force and the peak pull strength is documented.

Figure 16 and Figure 17 show the pull strength of 676 I/O BGAs at the two pull speeds. Figure 18 and Figure 19 show the test results for 256 I/O BGAs. For the same I/O BGAs at the same pull speed, the non-reballed components with SAC solder have a higher pull strength than that of the tin-lead reballed components. This result is consistent with the ball shear test results. The reason is also because SAC solder has

higher tensile strength than SnPb solder. The tensile strength of eutectic SnPb is 45.1 MPa, and the tensile strength of SAC solder is about 60 MPa [65].

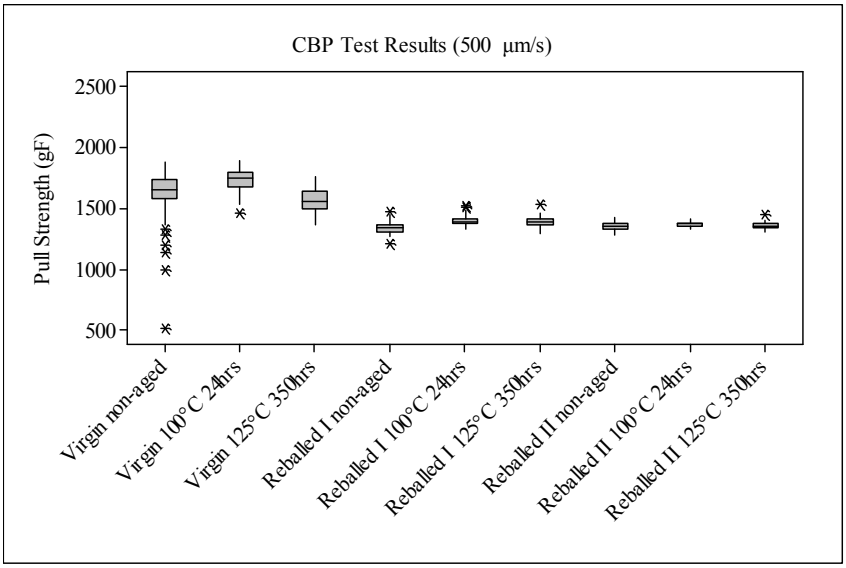

Figure 16: Pull strength of 676 I/O non-reballed and reballed BGAs (500 µm/sec)

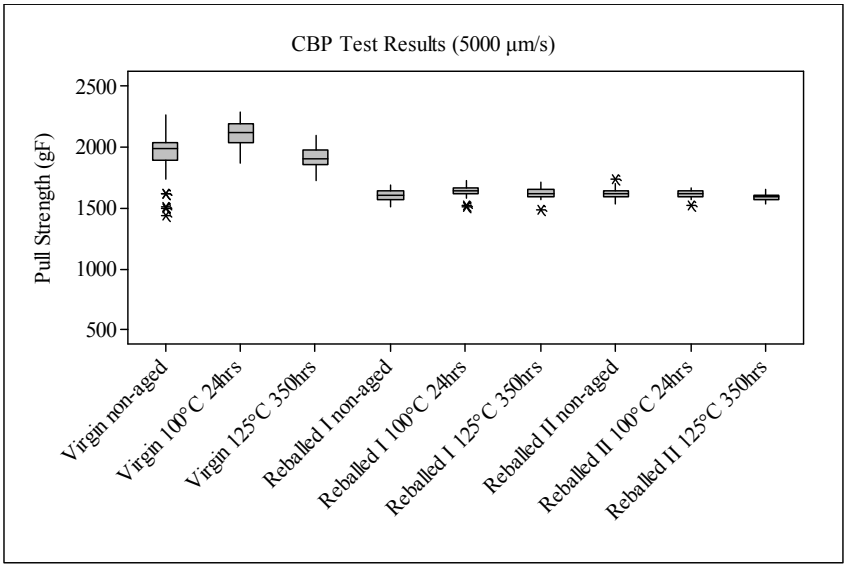

Figure 17: Pull strength of 676 I/O non-reballed and reballed BGAs (5000 µm/sec)

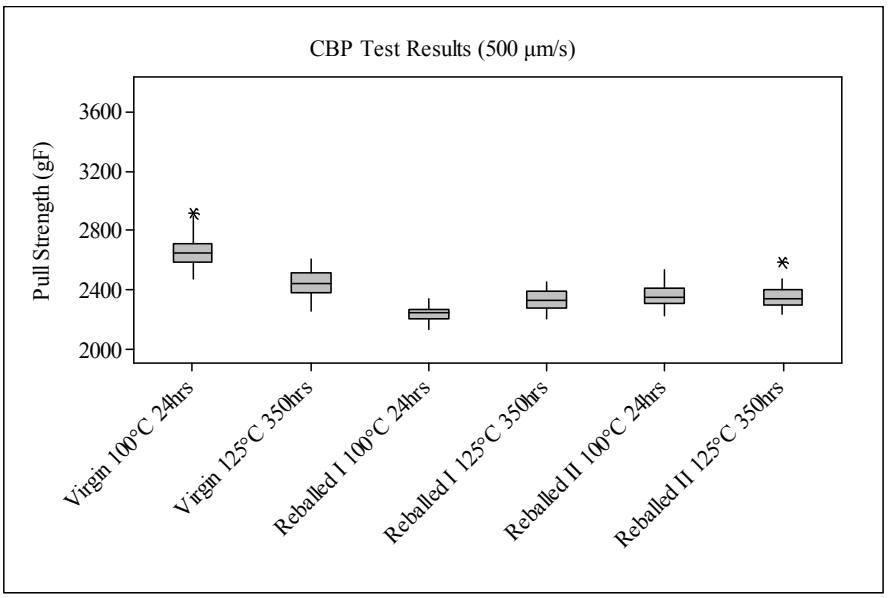

Figure 18: Pull strength of 256 I/O non-reballed and reballed BGAs (500 µm/sec)

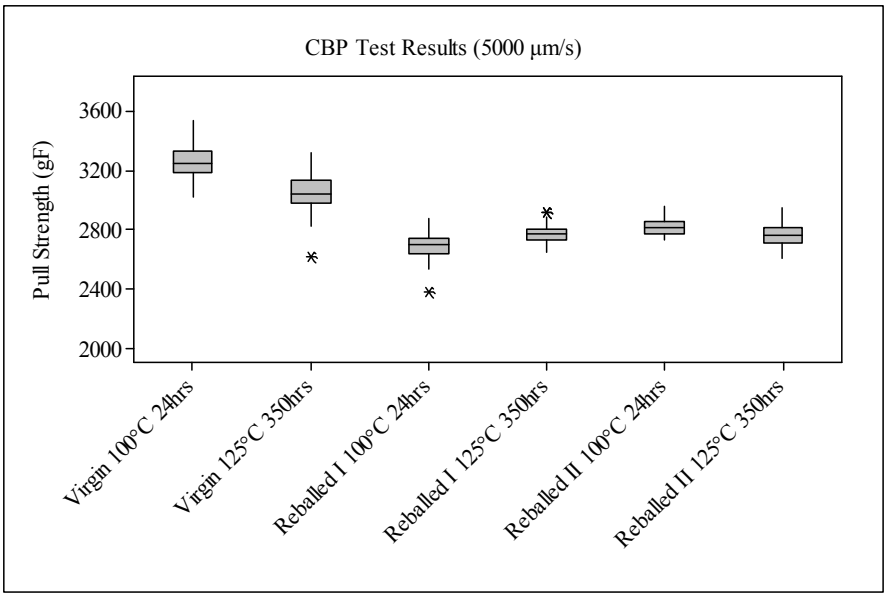

Figure 19: Pull strength of 256 I/O non-reballed and reballed BGAs (5000 µm/sec)

Also, the non-reballed components have a wider strength distribution than the reballed components. The aging condition appeared to have some influence on the lead-free BGA components but a less noticeable effect on the tin-lead reballed components. As the pull speed increased, the shear strength increased, regardless of

solder ball composition. The pull strength showed results consistent with the ball shear test. Therefore, the pull strength is independent of the solder ball removal and solder ball re-attachment methods.

3.2.5. Failure Mode Analysis of Cold Bump Pull Test

In these tests, four failure types were observed. Observed failure types included ball failure, pad failure, bond failure, and ball extrusion. Ball failure occurs when the failure is restricted to the solder. This occurs when the flow stress of the bulk solder is less than the pad peel strength and the interfacial strength of the solder joint. Pad failure occurs when the pad peels off of the substrate or fractures in the substrate materials. Pad failure occurs when the pad material attachment strength is too low or the substrate material fractures easily, which usually indicates a problem in the pad design. Bond failure occurs when the separation is at the interface of the solder and the pad. This occurs when the interfacial strength is less than the flow stress in the bulk solder. Ball extrusion failure occurs when the ball deforms into a cylinder shape due to the jaws pulling away excess solder without producing a bulk solder failure. Ball extrusion occurs when the setup of the pull test has a problem or the solder material is very soft. These four failure modes are depicted for a lead-free SAC BGA in Figure 20.

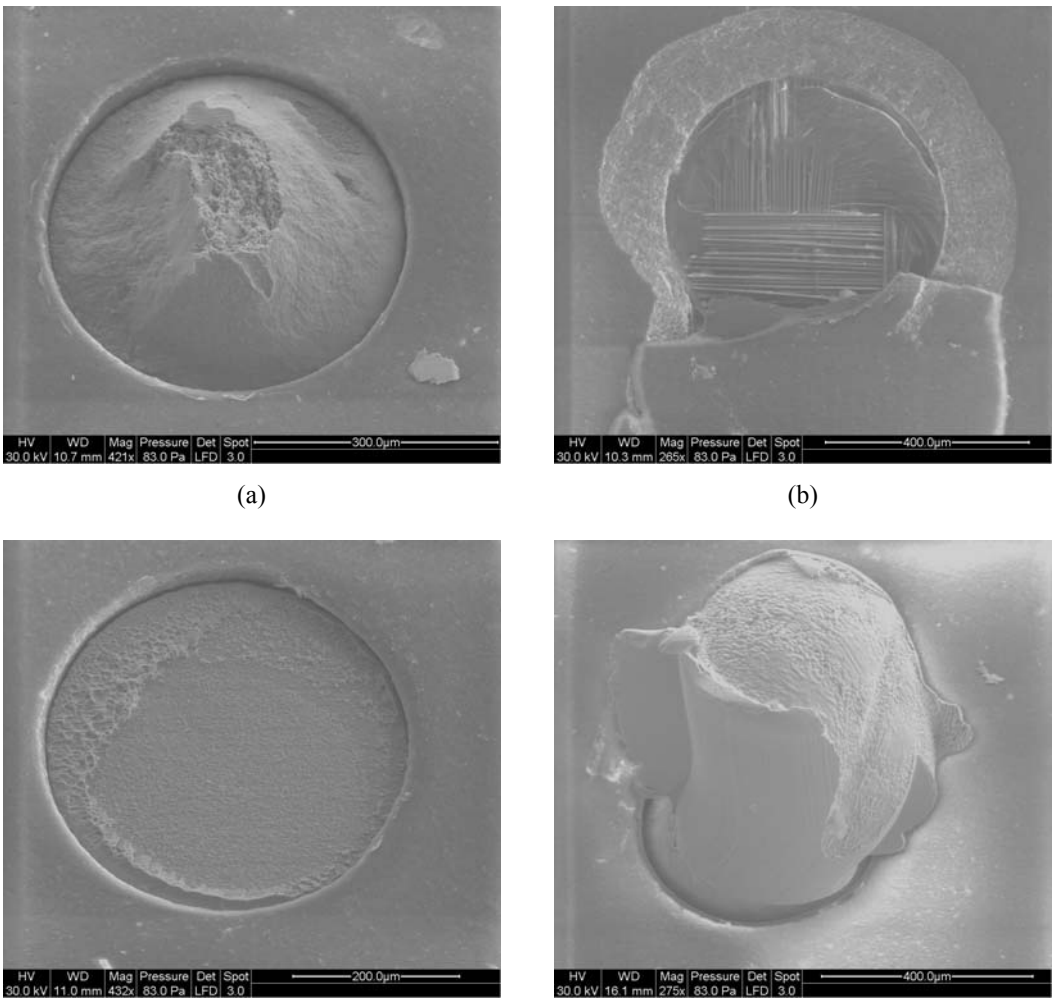

(a) (b)

(c) (d)

Figure 20: Failure modes of non-reballed 676 I/O BGAs

(a) Ball failure; (b) Pad failure; (c) Bond failure; (d) Ball extruded

In this study, all of the tin-lead reballed components exhibit ball failures. For the non-reballed lead-free components, all four types of failures were observed. The results suggested that SAC305 solder had defective interface and bond epoxy, which led to bond failure and pad failure. A breakdown of failure types observed for the lead-free 676 I/O BGAs is presented in Figure 21. From this figure it is observed that the higher pull speed generated a greater number of bond failures. This is because

solder materials are more ductile than interfacial IMC layers. Lower pull speeds allow the solder to deform and fracture. Higher pull speeds harden the solder materials and transfer the load to the solder/pad interface, which generates more pad failure. The ball failure percentage first decreased and then increased with aging. The solder strength first increases and then decreases with aging as addressed in a previous study [61]. As the solder strength increases, the numbers of bulk solder failure decreases, and vice versa.

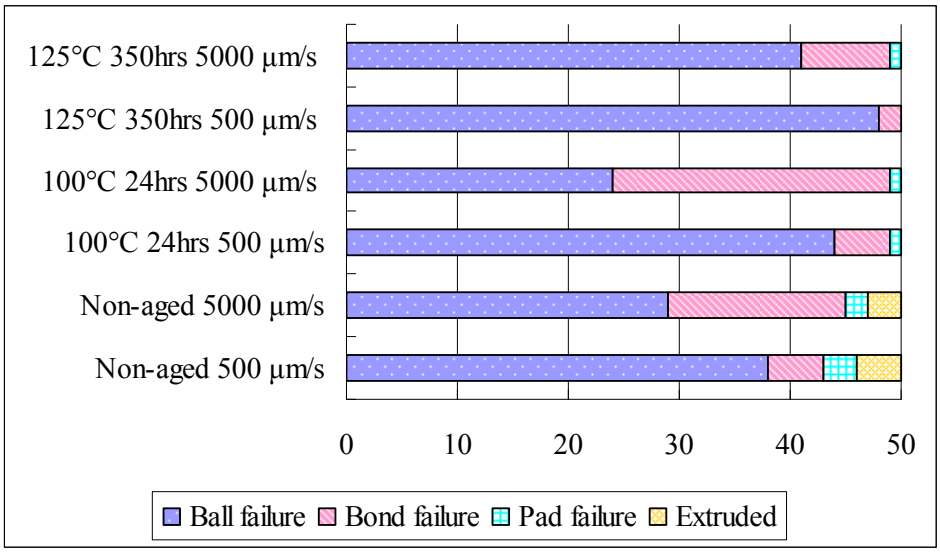

Figure 21: Failure modes breakdown of non-reballed 676 I/O BGAs

3.2.6. Microstructural Analysis of Cold Bump Pull Test

Figure 22 shows the failure surfaces of non-reballed lead-free and reballed tin-lead samples at two speeds: 500 µm/sec and 5000 µm/sec. Examination of the failure surfaces found larger dimples on samples pulled at 500 µm/sec than on samples pulled at 5000 µm/sec. This was because high pull speeds blocked the dimples from coalescing and growing, which led to smaller dimple size. Failure surface

observations also revealed a difference in dimple structure between SAC and SnPb solder. The dimple structure of the non-reballed SAC sample was rougher than that of the reballed SnPb sample. The reason was the different microstructures of SnPb solder and SAC solder. Tin-lead solder has a lamellar eutectic composed of tin and lead phases. But the SAC solder has a tin-rich phase and an Ag_3Sn+Sn phase, and Ag_3Sn shows the fiber shape embedded in the tin phase [60]. During the pull process, the lamellar SnPb structure fractures show a smoother edge than those of SAC solder.

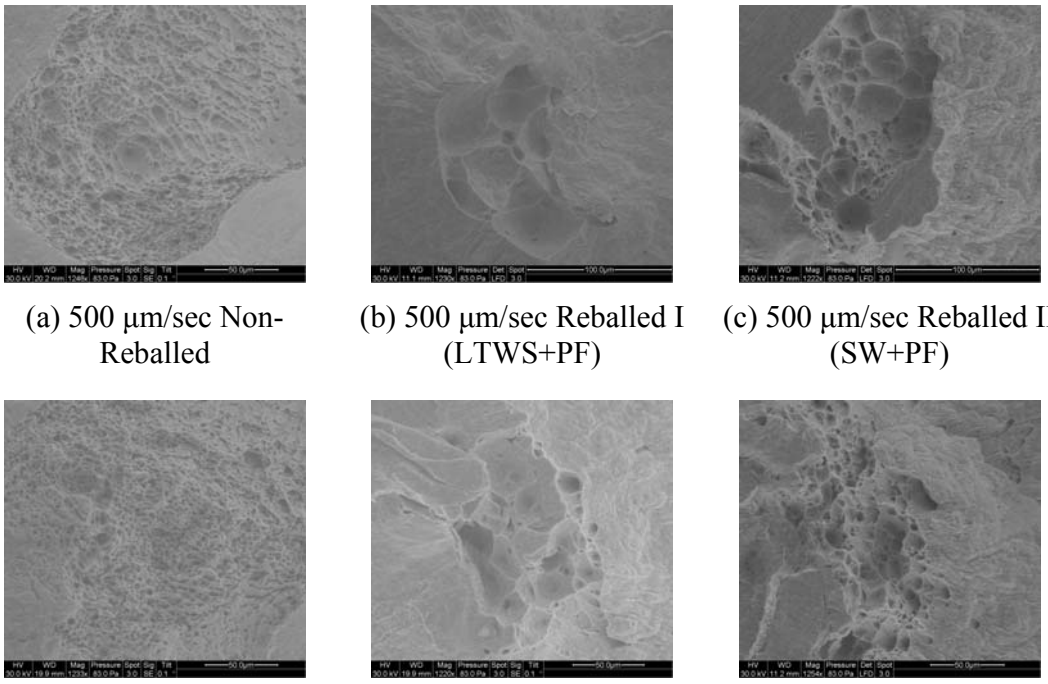

(a) 500 µm/sec Non-Reballed
(b) 500 µm/sec Reballed I (LTWS+PF)
(c) 500 µm/sec Reballed II (SW+PF)
(d) 5000 µm/sec Non-Reballed
(e) 5000 µm/sec Reballed I (LTWS+PF)
(f) 5000 µm/sec Reballed II (SW+PF)

Figure 22: Ball failure fracture surface of non-reballed and reballed components with different speeds (676 I/O BGA)

3.3. Interfacial IMC Analysis of Reballed BGAs

In order to investigate the interfacial IMC composition of reballed BGAs, it is necessary to investigate the interface after the solder ball removal procedure. Also,

the investigation of the interfacial IMC in non-reballed SAC components helps to give a better understanding of the interface after solder ball removal. The interfacial IMC composition and IMC thickness of the reballed components were investigated and discussed in this section as well.

3.3.1. Experiment

The experimental procedure carried out on these components was divided into two parts. Part I investigated interfacial changes due to two different solder ball removal procedures. In Part II the microstructural development of the interfacial IMCs of reballed components due to isothermal aging was examined. Figure 23 gives an overview of the complete test program.

To investigate the interfacial IMCs of reballed BGAs using different reballing methods, all the reballed BGA components were subjected to thermal aging. For purposes of comparison, non-reballed lead-free BGA components were also subjected to isothermal aging. Two isothermal aging conditions, 100°C for 24 hrs and 125°C for 350 hrs, were examined.

Table 6 lists the sample matrix. The samples after solder removal and the samples after solder ball re-attachment, including the non-aged and aged ones, were cut, molded, and cross-sectioned. An environmental scanning electron microscope (FEI Quanta FEG ESEM 200) and an energy-dispersive X-ray spectroscopy (Oxford Instruments INCA 4.09) were used to investigate the composition of IMCs as well as the IMC growth.

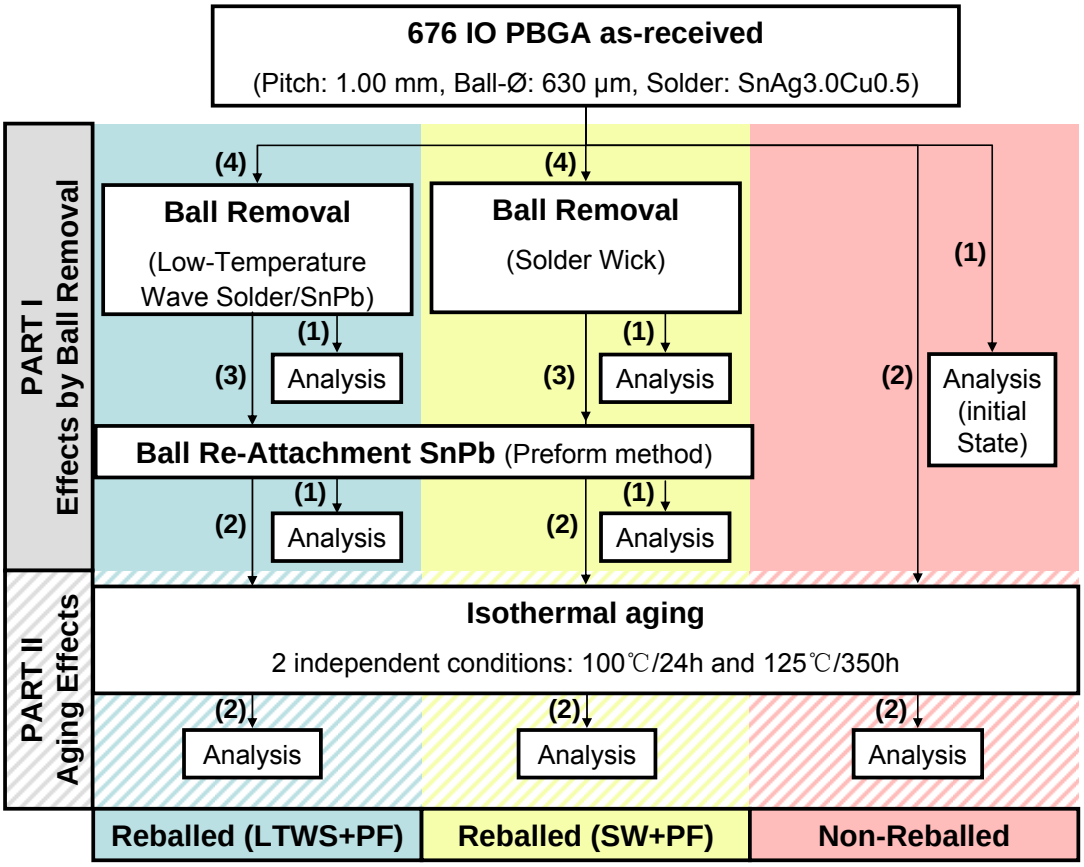

Figure 23: Overview of the test program carried out on interfacial IMC changes with different solder ball removal procedures (low-temperature wave solder "LTWS" and solder wick "SW": PART I) and isothermal aging (PART II). The numbers in parentheses indicate the number of samples for each step. After every step cross-sections were prepared for analysis.

Table 6: Sample matrix of non-reballed and reballed components

676 I/O BGA	Non-Reballed			Reballed (LTWS+PF)			Reballed (SW+PF)		
	Non-aged	100°C 24 hrs	125°C 350 hrs	Non-aged	100°C 24 hrs	125°C 350 hrs	Non-aged	100°C 24 hrs	125°C 350 hrs

3.3.2. Interfacial IMC Analysis of Non-Reballed BGAs (Initial State)

As shown in a previous study [66], Ni_3Sn_4 is the first phase formed and the only phase observed at the interface when Ni reacts with liquid Sn (< 260℃). However, the IMC formation is different when the solder material contains Cu, i.e., SAC305 solder. Studies revealed that if the Cu concentration in the solder exceeded 0.3-0.4 wt.%, the IMC formation at the interface was $(Cu,Ni)_6Sn_5$ [67]. The $(Cu,Ni)_6Sn_5$ IMC is based on the Cu_6Sn_5 lattice, and Ni dissolves into the lattice and replaces Cu atoms.

The non-reballed components were the BGAs with SAC305 solder balls. SAC305 solder reacted with the Ni pad during the soldering process. Since SAC305 solder contained 0.5 wt.% Cu, the expected IMC formed at the interface after soldering was $(Cu,Ni)_6Sn_5$. There was only one layer of interfacial IMC that was found at the interface of non-reballed BGA, as shown in Figure 24. The energy-dispersive X-ray spectroscopy (EDS) results of the IMC formation at the interface is shown in Table 7. Based on the atom percentage of the different elements, the IMC was confirmed to be $(Cu,Ni)_6Sn_5$.

Table 7: EDS detection results of interfacial IMCs in non-reballed BGAs (non-aged)

Element	Ni	Cu	Sn
Atom%	33.00	20.49	46.50

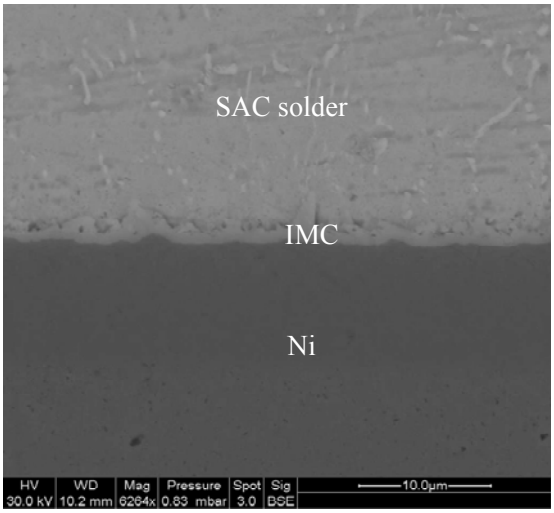

Figure 24: Non-reballed BGA interface (non-aged)

3.3.3. Interfacial Changes Due to Reballing Process

As mentioned in Section 2, the package surface may be damaged during the solder ball removal procedure. The surfaces of the packages were investigated after the solder removal procedure. Figure 25 shows an image of a pad using low-temperature wave solder without any damage. Damage to the solder mask induced by the solder wick method is shown in Figure 26.

Two BGA components were cross-sectioned after the solder ball removal step to investigate the thickness and the composition of the residue solder. Figure 27 shows the cross-section of a component using the low-temperature wave solder

method and Figure 28 shows the cross-section of a component using the solder wick method. The residue solder of a sample using the low-temperature wave solder method was SnPb with a thickness of 15 μm, and the residue solder of another sample using the solder wick method was SAC with a thickness of 9.5 μm. Since the components went through a SnPb solder wave in the low-temperature wave solder removal procedure, the original SAC solder was removed and left a layer of SnPb solder on the package pad.

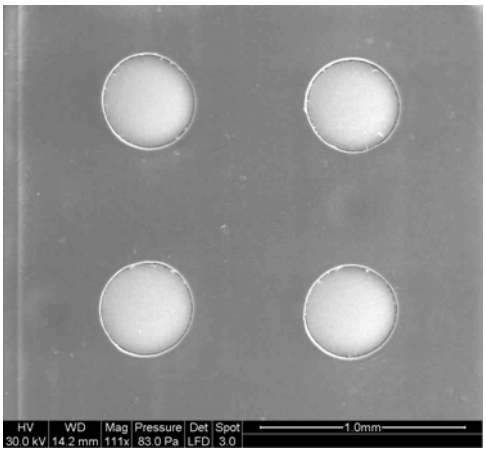

Figure 25: Good solder mask of a BGA after low-temperature wave solder method

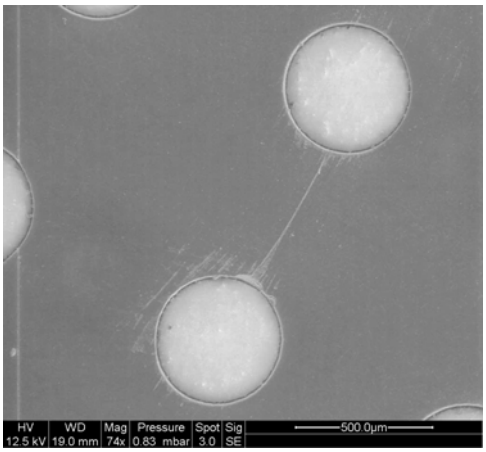

Figure 26: Solder mask damage on a BGA induced by the solder wick method

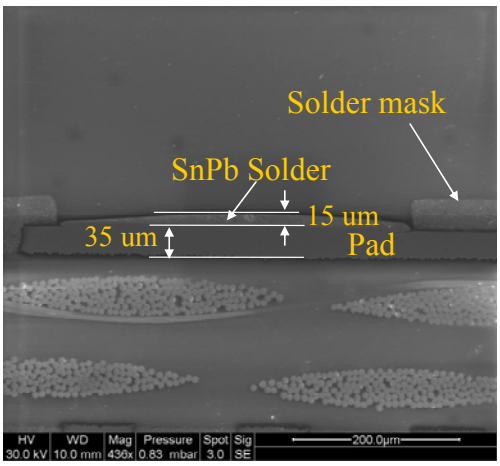

Figure 27: Cross-section of BGA pad area after solder ball removal using low-temperature wave solder method

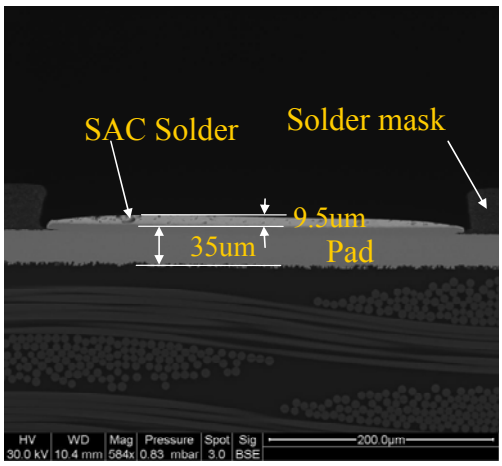

Figure 28: Cross-section of BGA pad area after solder ball removal using solder wick method

The BGA components after solder ball removal had different solder materials. Thus it was important to find out the interfacial IMC composition to get a better understanding of reballed BGAs. Figure 29 and Figure 30 show the components after the solder removal procedure. Based on the EDS results shown in Table 8, the interfacial IMCs were ternary Cu-Ni-Sn IMCs, but the compositions were different.

Table 8: EDS detection results of interfacial IMC in the samples after solder ball removal

Element (atom %)	Ni	Cu	Sn
Sample after low-temperature wave solder	26.84	24.23	48.94
Sample after solder wick	8.98	45.82	45.20

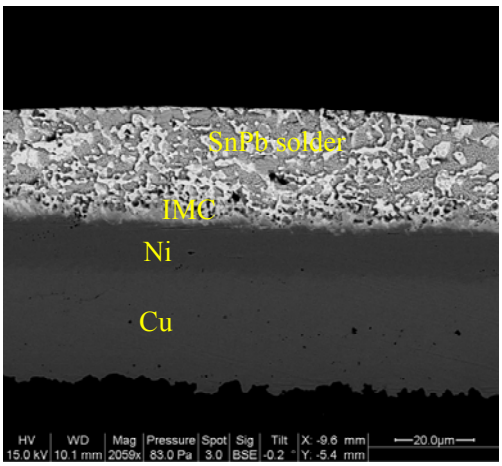

Figure 29: Interface of the BGA after low-temperature solder wave method

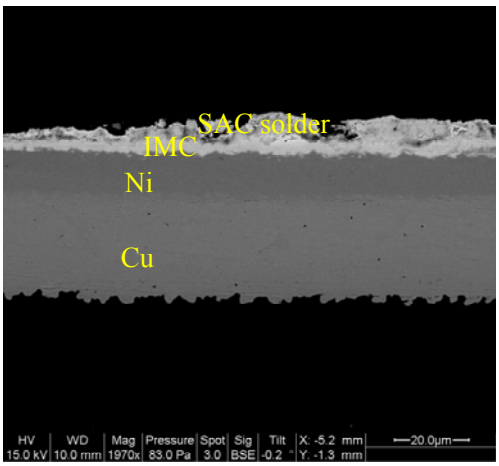

Figure 30: Interface of BGA after solder wick method

For the component using the low-temperature wave solder removal method, there was a layer of Cu-Ni-Sn IMC at the interface. During the re-attachment procedure, it was a four-layer structure reacted with each other at the interface for reballed (LTWS+PF) BGAs, SnPb solder ball/SnPb solder/Cu-Ni-Sn IMC/Ni pad. The composition of the interfacial IMCs in the reballed (LTWS+PF) BGAs (shown in Table 9) was close to $(Ni,Cu)_3Sn_4$. For the component using the solder wick removal method，there was a layer of Cu-Ni-Sn IMC at the interface and a layer of SAC solder. During the re-attachment procedure, it was also a four-layer structure reacted with each other at the interface for reballed (SW+PF) BGAs, SnPb solder ball/SAC solder/Cu-Ni-Sn IMC/Ni pad. The composition of the interfacial IMCs in the reballed (SW+PF) BGAs was also shown in Table 9, which was close to $(Cu,Ni)_6Sn_5$.

Table 9: EDS detection results of interfacial IMCs of reballed BGAs after solder ball re-attachment

Element (atom %)	Ni	Cu	Sn
Reballed (LTWS+PF) BGA	25.55	16.77	57.68
Reballed (SW+PF) BGA	24.35	29.76	45.89

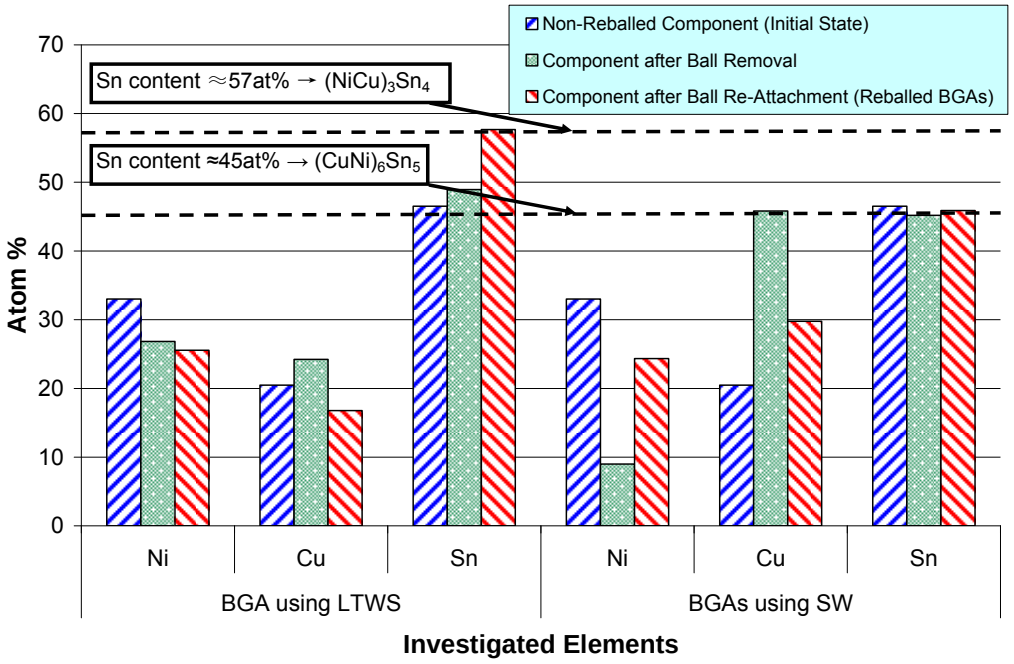

Figure 31: Element percentage of the interfacial IMCs in the BGAs after the solder ball removal and solder ball re-attachment procedures

In order to get a better understanding of the interfacial IMCs changes after the solder ball removal and solder ball re-attachment procedures, the EDS composition results of interfacial IMCs in the non-reballed components, the components after

solder ball removal, and the components after solder ball re-attachment were plotted, as shown in Figure 31.

There was a phase change in the component using the low-temperature wave solder method after the solder ball re-attachment procedure. The non-reballed SAC BGA (initial state) had an interface IMC composition close to $(Cu,Ni)_6Sn_5$. During the solder ball removal procedure, the SAC solder melted, and the interfacial IMC layer dissolved in liquid solder [68]. Liquid Sn reacted with Cu and Ni, which formed a new layer of interfacial IMC at the interface. After attaching the SnPb solder balls on the pads of the component, the Cu amount in the interfacial IMC layer dropped compared with the component after solder ball removal procedure, as shown in Figure 31. Because there was no Cu in the SnPb solder balls, there was a large driving force for Cu dissolved into the bulk solder and formed Cu-Sn IMCs in the reflow process (see Figure 32). In the meantime, the interfacial IMC layer dissolved into the liquid solder, and Ni from the component pad kept diffusing into the interfacial IMC layer, which formed a new layer of interfacial IMC with a composition close to $(Ni,Cu)_3Sn_4$. The main reason for the phase change at the interface is the Cu amount: there was not enough Cu (0.3-0.4 wt%) to maintain $(Cu,Ni)_6Sn_5$. The interfacial IMCs changed to a more stable state, $(Ni,Cu)_3Sn_4$, which was based on the Ni_3Sn_4 lattice with Cu substituting for the Ni atoms.

For the components using the solder wick method, the Cu amount was found to increase dramatically after the solder ball removal procedure. This was because a Cu braid was used to remove the melted solder in the solder wick method. The Cu dissolved into the liquid Sn during the solder ball removal step, and the solder wick

method gave enough contact time (42 seconds) for the Cu dissolution. Thus, the composition of the interfacial IMCs was close to $(Cu,Ni)_6Sn_5$ but with a high Cu concentration. In the solder ball re-attachment procedure, because SnPb solder balls contained no Cu, the Cu in the interfacial IMC layer dissolved into the bulk solder to form Cu-Sn IMCs (see Figure 33). This also explained why the Cu amount in the interfacial IMC decreased after the solder ball re-attachment procedure. However, the interfacial phase did not change in the whole reballing process, even though the Cu and Ni concentration changed in the ball removal and ball re-attachment procedures.

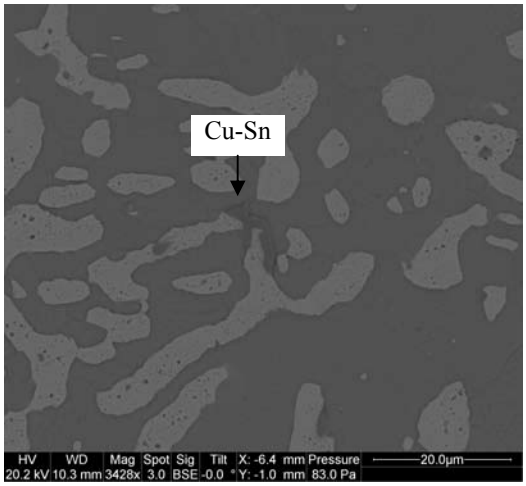

Figure 32: Bulk solder of reballed (LTWS+PF) BGA

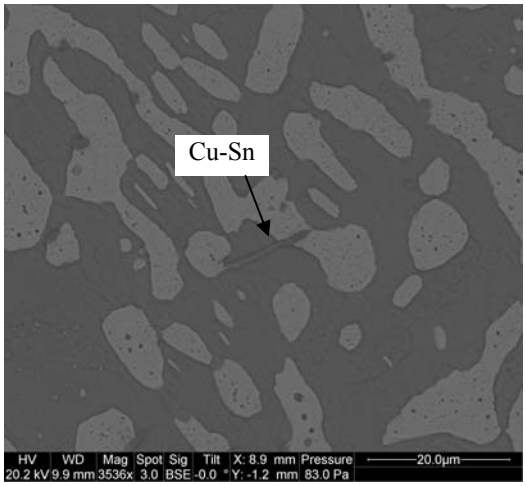

Figure 33: Bulk solder of reballed (SW+PF) BGA

3.3.4. Interfacial IMC Analysis under Isothermal Aging Condition

Both the reballed and non-reballed BGAs were subjected to isothermal aging conditions to evaluate the interfacial IMC growth. There were two isothermal aging conditions used in this study, 100ºC for 24 hours and 125ºC for 350 hours. As discussed in Section 3.3.3, for the reballed BGAs using different solder ball removal methods, the interfacial phase changed. EDS detection was used to document the

interfacial IMC composition of reballed BGAs in order to study the effect of isothermal aging on the interfacial phase change. The interfacial IMC composition of non-reballed BGAs was also studied as a reference. Table 10 lists EDS results of interfacial IMC composition of non-reballed and reballed BGAs. In order to get a better understanding of the interfacial IMC changes.

Table 10: EDS detection results of interfacial IMCs of reballed and non-reballed BGAs

Element (atom %)		Ni	Cu	Sn
Reballed (LTWS+PF)	Non-Aged	25.55	16.77	57.68
	100ºC/24hrs	26.60	16.14	57.26
	125ºC/350hrs	26.83	15.28	57.89
Reballed (SW+PF)	Non-Aged	24.35	29.76	45.89
	100ºC/24hrs	26.14	27.93	45.93
	125ºC/350hrs	32.71	24.76	43.53
Non-Reballed	Non-Aged	33.00	20.49	46.50
	100ºC/24hrs	30.48	24.22	44.54
	125ºC/350hrs	29.73	24.45	45.81

For the non-aged reballed (LTWS+PF) BGAs, the interfacial IMC composition was close to $(Ni,Cu)_3Sn_4$. For the aged reballed (LTWS+PF) BGAs, there was only one layer of interfacial IMC with a composition close to $(Ni,Cu)_3Sn_4$. However, the composition of the interfacial IMC layer remained the same even after aging. A similar situation was found in reballed (SW+PF) BGAs, where the interfacial phase, which was close to $(Cu,Ni)_6Sn_5$, stayed the same even after aging.

Only one layer of interfacial IMC was found in non-aged and aged samples. But the Cu amount of the interfacial IMC decreased slightly as aging time increased. Figure 34 shows the interfacial IMCs in the non-aged reballed (SW+PF) BGA.

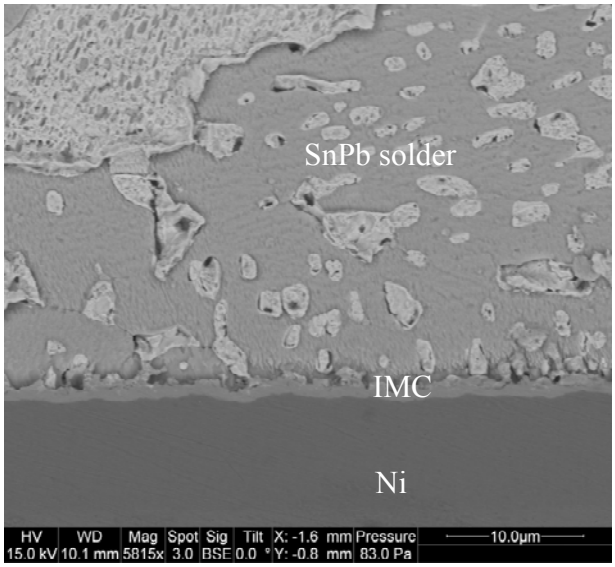

Figure 34: Reballed (SW+PF) BGA interface (non-aged)

For the non-reballed BGAs, the interfacial IMC composition was close to $(Cu,Ni)_6Sn_5$, which was the only phase found even after aging for 350 hours at 125ºC. However, the Cu amount in the interfacial IMC almost remained at the same level as the aging time increased, which was different than what occurred in the reballed BGAs. As aging time increased, the interfacial IMC layer grew and became thicker.

The IMC composition was investigated, and the interfacial IMC thickness was documented. The interfacial thicknesses of IMCs of non-reballed and reballed components are plotted in Figure 35. For each sample, 27 measurements were calculated. The mean and standard deviations are plotted.

The non-reballed components had an interfacial IMC thickness of 2.98±0.44 μm after aging at 125ºC for 350 hours. However, the reballed components had a much thicker interfacial layer due to multiple thermal procedures in the reballing process. In the solder ball removal and solder ball attachment procedures, the solder was in a liquid state, which could react much faster than a solid state. For reballed (LTWS+PF) and reballed (SW+PF) components, although the IMC compositions were different, the interfacial IMC layer thicknesses were equivalent to each other.

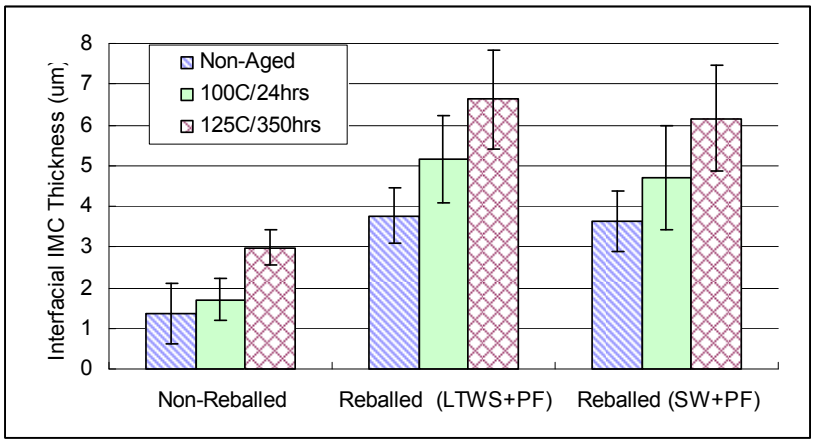

Figure 35: Interfacial IMC thickness of non-reballed and reballed BGAs

3.4. Conclusions

In this section, lead-free (SAC305) 676 I/O and 256 I/O BGAs were reballed with eutectic SnPb solder balls. Two solder ball removal processes and two ball re-attachment processes were examined. For the 676 I/O BGAs, the solder wick and low-temperature solder wave removal process were examined. Ball re-attachment for this component type was conducted with the preform method. For the 256 I/O BGA, the low-temperature solder wave removal process was applied, followed by either the preform method or ball drop re-attachment method.

The ball shear and the cold bump pull test results did not show a correlation with the reballing process. Further, isothermal aging did not appear to greatly influence the interconnect strength of tin-lead solder. Non-reballed lead-free solder balls were found to have greater strength and a wider strength distribution than the reballed tin-lead solder balls. For the cold bump pull test, an increase in pull speed correlated to an increase in solder pull strength. The finding of this study indicated that attachment strength of reballed BGAs was independent of the applied reballing processes

The components using the solder wick solder removal method had a layer of SAC solder on the pad, while the components using the low-temperature wave solder method had a layer of SnPb solder on the pad. The interfacial IMCs of the components were investigated after solder removal procedure, and the ternary Cu-Ni-Sn IMCs were found. However, the Ni concentration in the Cu-Ni-Sn IMC of the component using the solder wick method was lower than that of the component using the low-temperature wave solder method.

The components using the low-temperature wave solder method had phase change after the ball removal and ball re-attachment procedures. There was a layer of $(Ni,Cu)_3Sn_4$ at the interface in the reballed (LTWS+PF) components after reflow. For the components using the solder wick method, there was no phase change at the interface after the ball removal and re-attachment procedures. However, the Cu concentration in the interfacial IMCs changed dramatically after the solder ball removal procedure because of the Cu dissolution from the Cu braid used in the solder wick method. In both reballed (LTWS+PF) and reballed (SW+PF) BGAs, the Cu

concentration decreased after the solder ball re-attachment procedure. The reason was that the Cu dissolved into bulk solder and formed Cu-Sn IMCs during the reflow procedure.

After isothermal aging, there was no phase change at the interface in the non-reballed and the reballed BGAs. The non-reballed BGA has a interfacial IMC layer with the composition as $(Cu,Ni)_6Sn_5$. The interfacial IMC composition in the reballed (LTWS+PF) and the reballed (SW+PF) was $(Ni,Cu)_3Sn_4$ and $(Cu,Ni)_6Sn_5$ respectively. The reballed BGAs had a much thicker layer of IMCs than the non-reballed BGAs. The interfacial IMCs of the non-reballed and reballed BGAs grew after being subjected to isothermal aging. For reballed (LTWS+PF) and reballed (SW+PF) components, although the IMC compositions were different, the interfacial IMC layer thicknesses were equivalent to each other.

Chapter 4: TEMPERATURE CYCLING RELIABILITY TEST AND MICROSTRUCTURAL ANALYSIS OF REBALLED, LEAD-FREE, AND MIXED ASSEMBLIES

4.1. Theory

Reballing technology, which substitutes new solder balls for the original ones, provides a solution for ball grid array (BGA) packages for the shortage of tin-lead array components. Reballing has been used to salvage BGA components, but today it offers a way to replace lead-free solder with tin-lead solder. The reballing process has two major steps: solder ball removal and solder ball re-attachment. Multiple methods are available for the removal and re-attachment steps. Although reballing technology has been around for decades, there is not much literature evaluating the quality and reliability of the reballed BGAs. There are several studies focused on reballed BGAs only target quality evaluation. Beair and Vuono [12] used the temperature cycling test to evaluate the temperature cycling reliability of reballed SnPb BGAs, but there was no test result reported. Chatterji [13] reported fatigue crack propagation at the board side in the reballed SnPb assemblies after they were subjected to the temperature cycling test, but large voids were observed in the reballed BGAs due to an improper reballing process and reflow profile setup. While reballing has been considered as an alternative assembly method, there are several issues yet to be answered for the industry, such as the effect of different reballing methods on the reliability of reballed BGAs and the failure modes of the reballed BGAs.

In cases where conventional tin-lead ball grid array (BGA) components are not available, it may be necessary to use lead-free version of that component with an existing tin-lead assembly process. A solder joint formed due to the mixing of tin-lead and lead-free materials is termed a "mixed solder joint" [25]. The mixing of different solder materials can induce new reliability concerns, because the reliability of solder joint depends on loading conditions, materials properties, and microstructure of the solder joint. The implementation of mixed assemblies has been limited due to concerns about the long term reliability of the mixed solder joints. For leaded components, the reliability of mixed assemblies is not a big concern, because the amount of solder in component finish is too small when compared to solder paste volume. However, for array area packages, the amount of solder in solder ball is comparable to the amount of solder paste, which leads to reliability concerns of mixing metallurgies in array area assemblies. Although there were some studies focused on reliability of mixed assemblies, there was still no clear conclusion [26]-[33]. The reliability of mixed assemblies depends on component type, test condition, reflow parameters, etc.

4.2. Experiment Setup

Two different lead-free (SAC305) plastic overmold ball grid array (PBGA) components (see Table 11) were reballed with SnPb in order to examine the impact of the reballing process on the temperature cycling reliability of those assemblies. The reballing process involves two major steps: solder ball removal and solder ball re-attachment. In this study, two ball removal methods and two ball re-attachment methods were examined. The solder wick and the low-temperature wave solder

processes were used for ball removal. Solder ball preform and ball drop methods were used for ball re-attachment.

Table 12 shows the investigated reballing processes used in this study. The pad finish of the component interposer was Ni/Au, and the pad design was solder mask defined.

Table 11: Parameters of investigated components

Component Type	Ball Population	Component Size	Ball Diameter	Pitch
676 I/O PBGA	full area array	27 mm x 27 mm	630 µm	1.0 mm
256 I/O PBGA	peripheral area array	27 mm x 27 mm	760 µm	1.27 mm

Figure 36: Test vehicle with 6 BGAs on each PCB (Board dimensions: 8 in. (203.2 mm) ×4.5 in. [114.3 mm] × 93 mils [2.36 mm])

Table 12: Reballing process matrix

Component	Reballing Type	Solder Ball Removal Approach	Solder Ball Attachment Approach
676 I/O PBGA	LTWS+PF	Low-temperature wave solder (LTWS)	Preform (PF)
676 I/O PBGA	SW+PF	Solder wick (SW)	Preform (PF)
256 I/O PBGA	LTWS+PF	Low-temperature wave solder (LTWS)	Preform (PF)
256 I/O PBGA	LTWS+BD	Low-temperature wave solder (LTWS)	Ball drop (BD)

Those reballed BGAs, were subjected to the assembly process to form reballed assemblies. For comparison, non-reballed (SAC) BGAs were also subjected to the assembly process to form the lead-free (SAC BGA soldered with SAC305 paste) and the mixed (SAC BGA soldered with Sn37Pb paste) assemblies, by using different reflow profiles according to the metallurgical system. The breakdowns of the BGA assemblies are shown in Table 13. Printed circuit boards (PCBs) were designed for 676 I/O and 256 I/O BGAs. On each PCB, six BGAs were assembled with one daisy chain per part (see Figure 36). The board laminate material was Isola Polyclad 370 HR with a surface metallization of two-ounce Cu (approx. 70 μm), and an organic solderability preservative (OSP) as surface finish. In the application of solder paste, was carried out by stencil printing. The thickness of the printing stencil

was 125 μm (5 mils). The stencil opening matched the pad size on the PCB, which were 530 μm for the 676 I/O and 680 μm for 256 I/O BGA respectively.

Table 13: The breakdowns of 676 I/O and 256 I/O BGA assemblies

BGA I/O	BGA Type / Solder Ball	Assembly Paste	Assembly Profile	Assembly Type
676 I/O	Reballed LTWS+PF / Sn37Pb	Sn37Pb*	(1)	676 I/O Reballed LTWS+PF
	Reballed SW+PF / Sn37Pb	Sn37Pb*	(1)	676 I/O Reballed SW+PF
	Non-Reballed / SAC305	SAC305**	(3)	676 I/O Lead-free (230℃)
	Non-Reballed / SAC305	SAC305**	(4)	676 I/O Lead-free (240℃)
	Non-Reballed / SAC305	Sn37Pb*	(2)	676 I/O Mixed
256 I/O	Reballed LTWS+PF / Sn37Pb	Sn37Pb*	(1)	256 I/O Reballed LTWS+PF
	Reballed LTWS+BD / Sn37Pb	Sn37Pb*	(1)	256 I/O Reballed LTWS+BD
	Non-Reballed / SAC305	SAC305**	(4)	256 I/O Lead-free
	Non-Reballed / SAC305	Sn37Pb*	(2)	256 I/O Mixed

(1) SnPb solder profile: 70-80 s above 183ºC, peak 215ºC

(2) SnPb modified solder profile: 100 sec above 183ºC, peak 215ºC

(3) SAC solder profile: 50-60 sec above 217ºC, peak 230ºC

(4) SAC solder profile: 50-60 sec above 217ºC, peak 240ºC

* no-clean Alpha UP78-OSP, ** no-clean Alpha OM338

All of the assemblies were subjected to preconditioning at 100 °C for 24 h according to IPC 9701. The purpose of preconditioning was bringing all assemblies to approx. the same state prior test. IPC9701 represents that preconditioning simulates a use period and accelerates solder grain growth, intermetallic compound growth, and oxidation [69]. After preconditioning, all the assemblies were subjected to the temperature cycling test with a temperature range of -55 °C to 125 °C. The dwell time and ramp time were 15 minutes each, causing a complete cycle time of 1 hour. The resistance of the daisy chains (one daisy chain per component) was electrically monitored in-situ by event detectors. Failure was defined as the occurrence of a resistance peak of over 300 Ω with 9 additional peaks within 10% of the time to first peak according to IPC-SM-785[70].

4.3. Temperature Cycling Test Results

The temperature cycling test was stopped at 5324 cycles, and the failure data was obtained as cycles-to-failure. The distribution of the failure data was assumed to follow Weibull distribution, and a two-parameter Weibull plot was used to plot the cycles-to-failure data.

All the failure data results of 676 I/O and 256 I/O BGA assemblies were listed in Table 14, where β was the shape factor, η was characteristic life (63.2% failure), and B_{10} was time to 10% failure. Apparently, the characteristic life of reballed assemblies was shorter than that of lead-free and mixed assemblies regardless of component type. Comparing the early failure values, the reballed BGA assemblies failed earlier than the lead-free and mixed assemblies.

Table 14: Cycles-to-failure data of 676 I/O and 256 I/O BGA assemblies

Assembly Type	Sample Size (failure/total)	Slope (β)	Characteristic Life (η)	Cycles to 10% Failure (B_{10})
676 I/O Reballed LTWS+PF	20/20	7.10	2336	1702
676 I/O Reballed SW+PF	24/24	7.98	2123	1601
676 I/O Lead-free (230℃)	23/24	7.33	4273	3143
676 I/O Lead-free (240℃)	23/24	5.72	4276	2885
676 I/O Mixed	20/24	3.92	4498	2533
256 I/O Reballed LTWS+PF	23/23	9.14	2419	1891
256 I/O Reballed LTWS+BD	23/23	8.33	2561	1955
256 I/O Lead-free	21/24	5.20	4624	3000
256 I/O Mixed	11/24	4.18	5929	3461

For the 676 I/O BGA assemblies, two types of reballed assemblies had the same solder ball re-attachment method but different solder ball removal methods. The mean cycles-to-failure of these two types of reballed assemblies was similar with 95% confidence bounds (see Figure 37). Even comparing the early failure values, the two reballed assemblies were close to each other.

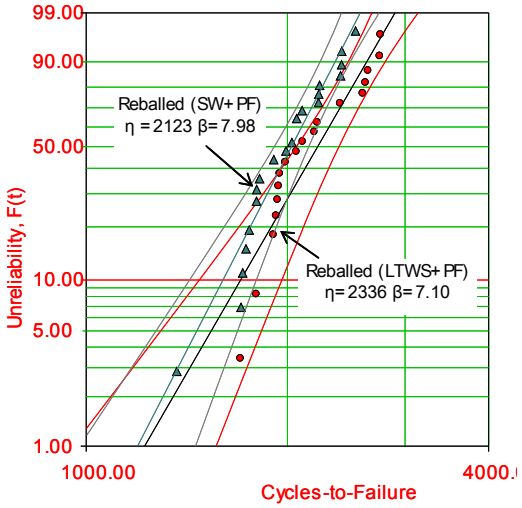

Figure 37: Weibull plot of 676 I/O reballed BGA assemblies with different ball removal procedures (SW=Solder Wick; LTWS=Low-Temperature Wave Solder)

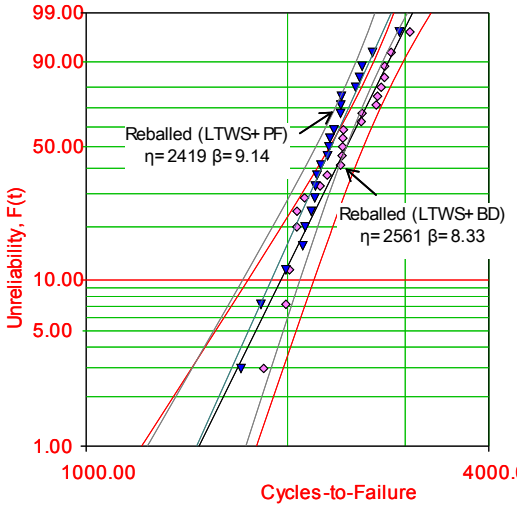

Figure 38: Weibull plot of 256 I/O reballed BGA assemblies with different ball re-attachment methods (PF=Preform, BD= Ball Drop)

For the 256 I/O BGA assemblies, the types of reballed assemblies had the same solder removal method but different solder ball re-attachment methods. These two types of reballed assemblies had similar temperature cycling reliability with 90% confidence bounds (see Figure 38). The two reballed assemblies had similar early failure values, as shown in Table 14. If the one-way analysis of variance (ANOVA) with the alpha selected as 0.05 was applied to these two distributions of reballed assemblies, they were the same distribution.

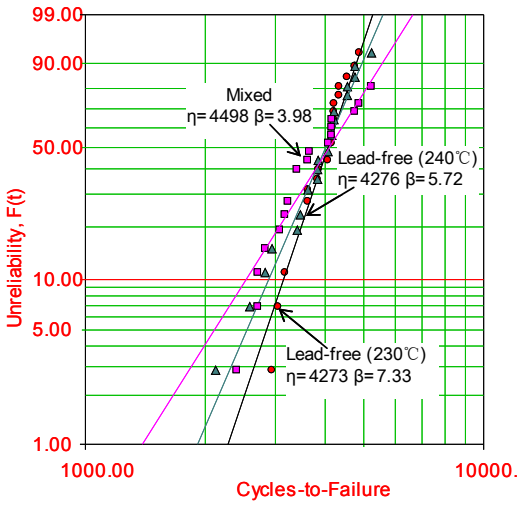

Figure 39: Unreliability of 676 I/O lead-free and mixed BGA assemblies

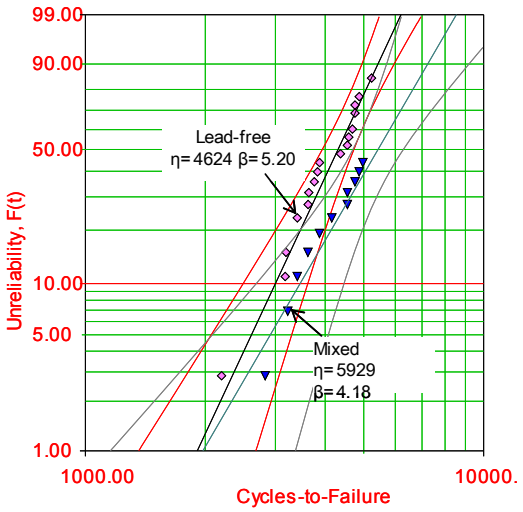

Figure 40: Unreliability of 256 I/O lead-free and mixed BGA assemblies

The temperature cycling reliability of lead-free and mixed BGA assemblies were also tested under temperature cycling test in order to be compared with the reballed SnPb assemblies. For 676 I/O BGA assemblies, there were two types of lead-free assemblies with different reflow peak temperatures. The mean cycles-to-failure of these two lead-free assemblies was very close to each other. The characteristic life of the mixed assemblies was equivalent to that of the lead-free assemblies (see Figure 39). One-way ANOVA analysis ($\alpha = 0.05$) was applied to the distributions of the lead-free and the mixed assemblies, and the results showed that the distributions of the mixed and lead-free assemblies were the same. However, the cycles to 10% failure values showed that the mixed assemblies had more early failures than that of lead-free assemblies. For the 256 I/O BGA assemblies, the lead-free assemblies had a characteristic life of 4624 cycles, and the mixed assemblies had a characteristic life of 5929 cycles. The temperature cycling reliability of mixed assemblies was 28% longer than that of the lead-free assemblies with 90% confidence bounds (see Figure 40).

4.4. Microstructural Failure Analysis Results

After the BGA assemblies failed in the temperature cycling test, the components were cut, molded and cross-sectioned. An environmental scanning electron microscope (FEI Quanta FEG ESEM 200) and an energy-dispersive X-ray spectroscope (Oxford Instruments INCA 4.09) were used to analyze the failure site, crack propagation, and intermetallic compounds. In addition cross-polarized and bright field optical microscopy was carried out to obtain a qualitative overview of the grain structure as well as the phase structure of the samples.

The microstructural failure analysis was carried out on two different components: 256 I/O BGA and 676 I/O BGA. Since the microstructural development and failure modes for both components are the same, the following results are presented for the 256 I/O BGA assemblies only.

4.4.1. Microstructural Development and Crack Propagation in Reballed SnPb BGA Assemblies

Figure 41 shows an intermetallic layer that has been separated from the intermetallic interface. This phenomenon can be found in the majority of the solder balls of the as-received reballed 256 I/O BGA assembly (LTWS+PF). The appearance is known for Ni/Au metallization especially after several reflows. Possible reasons for that are: 1. The presence and cracking of a Ni-P intermetallic or 2. A change in the structure of the intermetallic layer from $(Cu,Ni)_6Sn_5$ to $(Ni,Cu)_3Sn_4$. Because of the fact that the position of the detached layer in the solder joint corresponds with the crack propagation in the temperature-cycled samples it is reasonable to assume that

this phenomenon may reduce temperature cycling reliability. However, the failed samples did not show crack propagation along that layer or the presence of the layer at all.

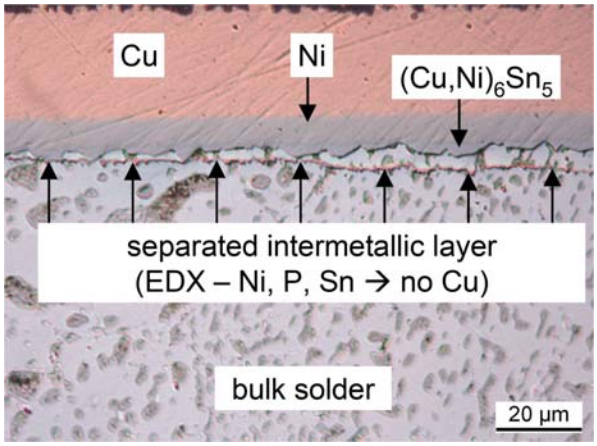

Figure 41: Detached intermetallic layer at the component side of a reballed 256 I/O BGA assembly (LTWS+PF). (bright field optical microscopy)

Figure 42 shows the changes that occur in the microstructure of a reballed SnPb solder joint due to thermo-mechanical loading. The microstructure of the as-received solder joint is in general the same in all shown regions (Figure 42a-c). There are coarse areas with large Pb-rich crystals (bright phase - see Figure 42b), which sometimes solidified dendritic. There are also very fine lamellar structures of alternating Sn-rich and Pb-rich crystals visible. These areas represent the eutectic (e.g. Figure 42c). Also some Cu_6Sn_5 intermetallics can be found in the microstructure due to leached pad material (Cu from board side).

The microstructure of the temperature-cycled solder joint in Figure 42d-f shows significant changes in comparison to the as-received condition (see Figure 42a-c). Phase coarsening, which is represented by the growth of the Pb-rich phase, took place all over the solder joint. This growth causes the fine lamellar structures to

disappear. Figure 42d shows that close to the crack area the Pb-rich phase grew much more intense compared to the growth in the bulk solder (Figure 42e) or at the board side without crack (Figure 42f). The dashed line in Figure 42d separates this area of intense phase growth from the region regular phase growth. The regular phase growth in the bulk solder is expected to be caused by accelerated diffusion at elevated temperatures (Ostwald ripening). The intense phase growth in the crack area, may be caused by higher mechanical stress in that region compared to the bulk solder. Another important change in the temperature-cycled microstructure can be seen at the interface region in Figure 42f. There is a continuous layer of Pb-rich phase covering the intermetallic interface. This phenomenon is related to the growth of the intermetallic layer at elevated temperatures, which is already discussed in Mehrotra's study [40]. For the growth of the Cu/Sn intermetallic, Sn is consumed from the bulk solder causing an enrichment of Pb close to the interface.

Figure 43 shows that the presence of a Pb-rich layer has influence on crack propagation. The shown crack directly propagates along the phase boundary between the Pb-rich and Sn-rich phase. It appears that under a stress loading condition, such as the temperature cycling test, the adhesion between the Pb-rich phase near the interface and the Sn-rich phase in the bulk solder is weak, maybe due to an incoherent phase boundary. A Pb-rich layer is also shown at the interface on the component side in Figure 44, but here the main crack propagation is not along that layer (due to the solder mask defined layout – height approx. 45 μm).

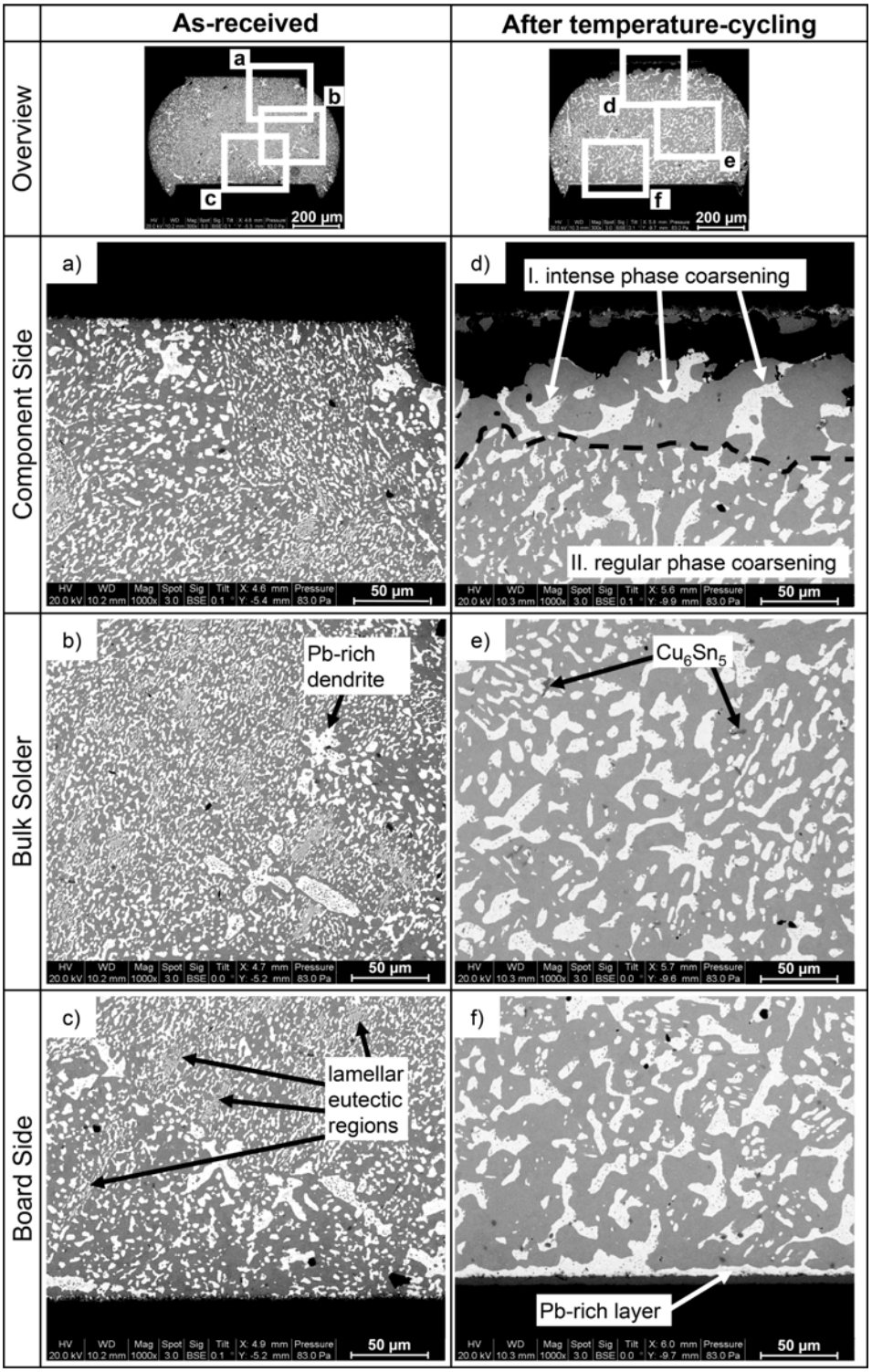

Figure 42: Microstructural comparison of as-received (a-c) and temperature-cycled (d-f) SnPb solder joints of reballed 256 I/O BGA assemblies (LTWS+PF). Phase coarsening is visible all over the solder joint but an intense phase growth can be seen in the crack area. (ESEM - bright = Pb-rich / dark = Sn-rich)

The main failure site in the reballed assemblies was located at the component side near the interface (see Figure 42d and Figure 44) regardless of the component type and reballing method used. Minor cracks have been found near the interface at the board side (see Figure 43). The shown gap between the solder ball and the component pad in Figure 42d occurred due to the continued storage in the temperature-cycling chamber after the component was already failed. The failure site in the reballed assemblies corresponds with those found in various references for SnPb BGA assemblies [13] [28].

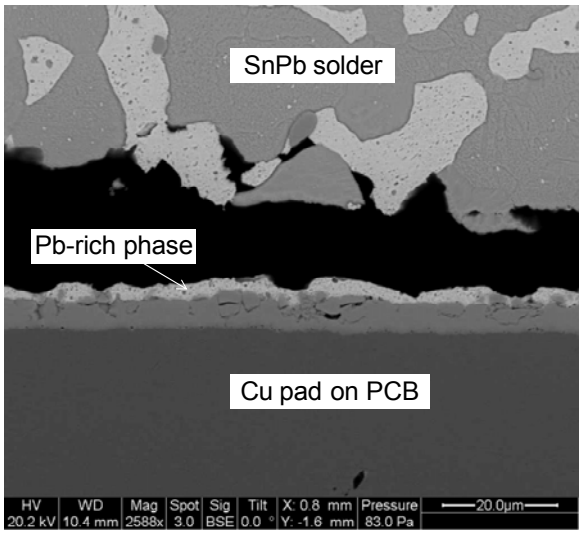

Figure 43: Crack propagation along the phase boundary of a Pb-rich layer at the board side. (Temperature-cycled 256 I/O reballed BGA - LTWS+BD - ESEM)

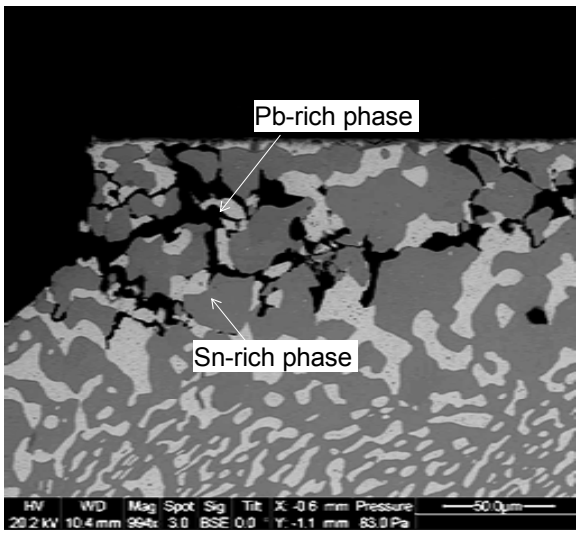

Figure 44: Crack propagation through the bulk solder close to the component side in 256 I/O reballed (LTWS+BD) assemblies. The Pb-rich layer at the interface do not cause the failure (ESEM)

Figure 44 shows a crack propagating through the bulk solder close to the component side. The major part of the crack propagates between the Pb-rich and Sn-rich phase boundary. The cracks often change direction along the Pb phase boundaries and sometimes also change direction perpendicular to the shear force in

order to follow the phase boundary or to reach the next or nearest Pb-rich phase. It is also shown that the crack is located in the intense phase coarsening region as mentioned earlier. The crack propagates along the phase boundaries between the Sn-rich and the Pb-rich phases.

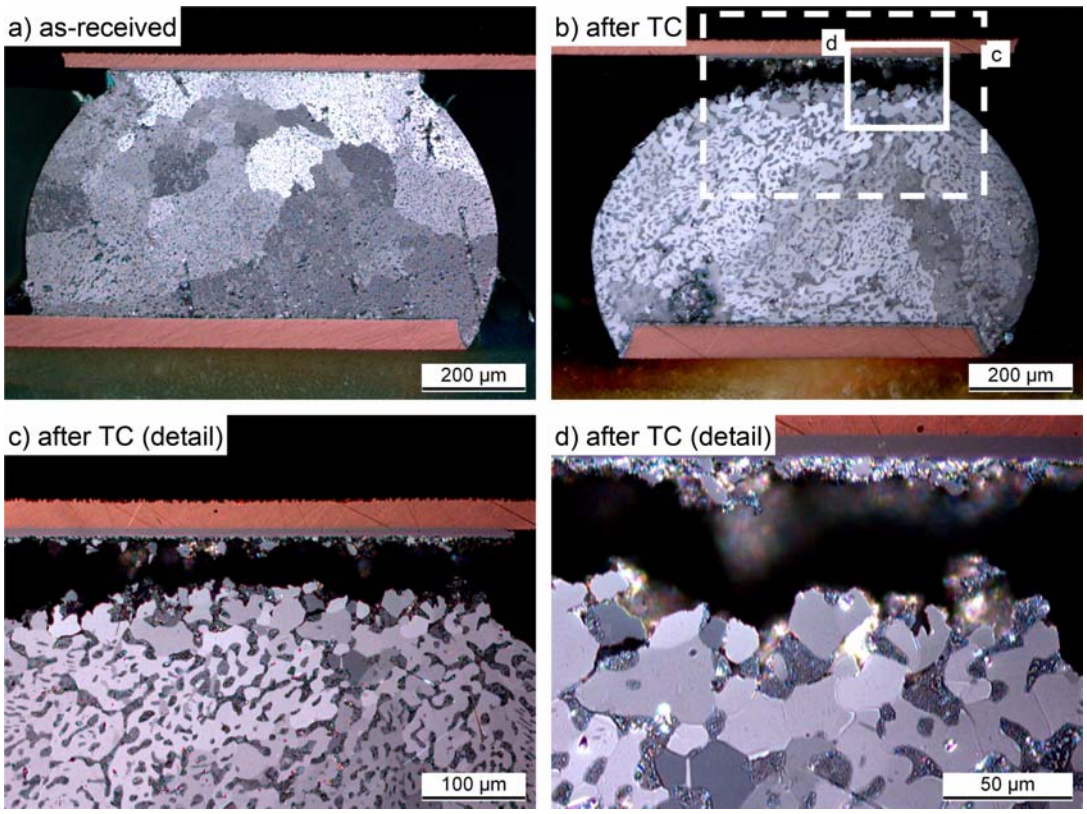

Figure 45: Changes in grain structure in reballed SnPb solder joints (LTWS+PF): a) as-received solder joint b) temperature-cycled solder joint. Detailed pictures of the phase coarsening area close to the crack are shown in c) and d). d) Sn-grains in this area show grain refinement and changes in orientation. (256 I/O BGA - cross-polarized optical microscopy)

To understand the crack propagation in these areas it is necessary to have an idea of the grain structure of the Sn-rich crystal. Figure 45 shows cross-polarized pictures of reballed SnPb solder joints that allow a qualitative overview of the grain structure of the body-centered-tetragonal Sn-rich phase. The differences in contrast

result from differences in orientation. It can be seen that the grain structure in the temperature-cycled state (Figure 45b) refines in the crack area if compared to the as-received state (Figure 45a). This area of grain refinement correlates with the phase coarsening region. The more detailed pictures of the temperature-cycled solder joint (Figure 45c-d) show that the Sn grains become smaller in the crack region and additional grain boundaries are offered for crack propagation. It can also be seen that the Pb-rich phase is located at the grain boundaries of the Sn grains. From these results it can be concluded that the phase boundaries are the weakest part for cracking and grain boundaries between different Sn grains are used for crack propagation in areas with no phase boundaries.

4.4.2. Microstructural Development and Crack Propagation in Lead-Free BGA Assemblies

Figure 46 shows the microstructure of lead-free assemblies before (Figure 46a-c) and after the temperature cycling test (Figure 46d-f). In the as-received assemblies, cellular β-Sn structures can be found all over the solder joint, varying in size (Figure 46a-c). Those cells are surrounded by a large number of small Ag_3Sn intermetallic particles (see Figure 46b). It is assumable that those cells are the result of dendritic solidification and therefore the cell size is depending on solidification, growth direction and the plane of the cross-section. After the temperature cycling test, the number of Ag_3Sn particles decreased while the Ag_3Sn particle size simultaneously increased (see Figure 46e). The microstructure in the bulk solder still shows the cellular β-Sn structures, while in areas near the fatigue crack the cellular structures disappear. Also the phase growth of the intermetallics seems to occur with different

speed, depending on the location in the solder joint. In the crack area the growth is more intense and larger intermetallics can be seen compared to the bulk solder. Also the areas of pure β--Sn increased more significant in the crack region. The dashed line in Figure 46d and Figure 46f marks the abrupt change between the two coarsening speeds. It is assumable that the coarsening in both areas is caused by Oswald ripening, due to the elevated temperature. Furthermore the faster coarsening in the crack region is accelerated by the higher stress level in the crack area. This means that these two different coarsening areas show the difference between thermal aging (in the bulk area) and thermo-mechanical aging (in the crack area).

Figure 47 shows the difference in grain structure between the as-received solder joint and the temperature-cycled solder joint. The as-received solder joint shows only one major grain orientation (Figure 47a), which is the general case for SAC305 solder joints (mainly 1-3 major grain orientations, see Appendix for more images). In the temperature-cycled solder joint, this large area with one major grain orientation is still visible in the centre region of the joint, but there is also a region with grain refinement visible (larger number of small areas with different orientation), surrounding the crack at the component side (Figure 47b). In the detailed pictures (Figure 47c-d) it can be seen, that small grains have formed in the area that corresponds with the intense phase coarsening mentioned in Figure 46d. From Figure 47d it can also be seen that the intermetallics are very often gathered at the grain boundaries between those grains. Similar observations were found in Manock's study [71] and Coyle's study [39].

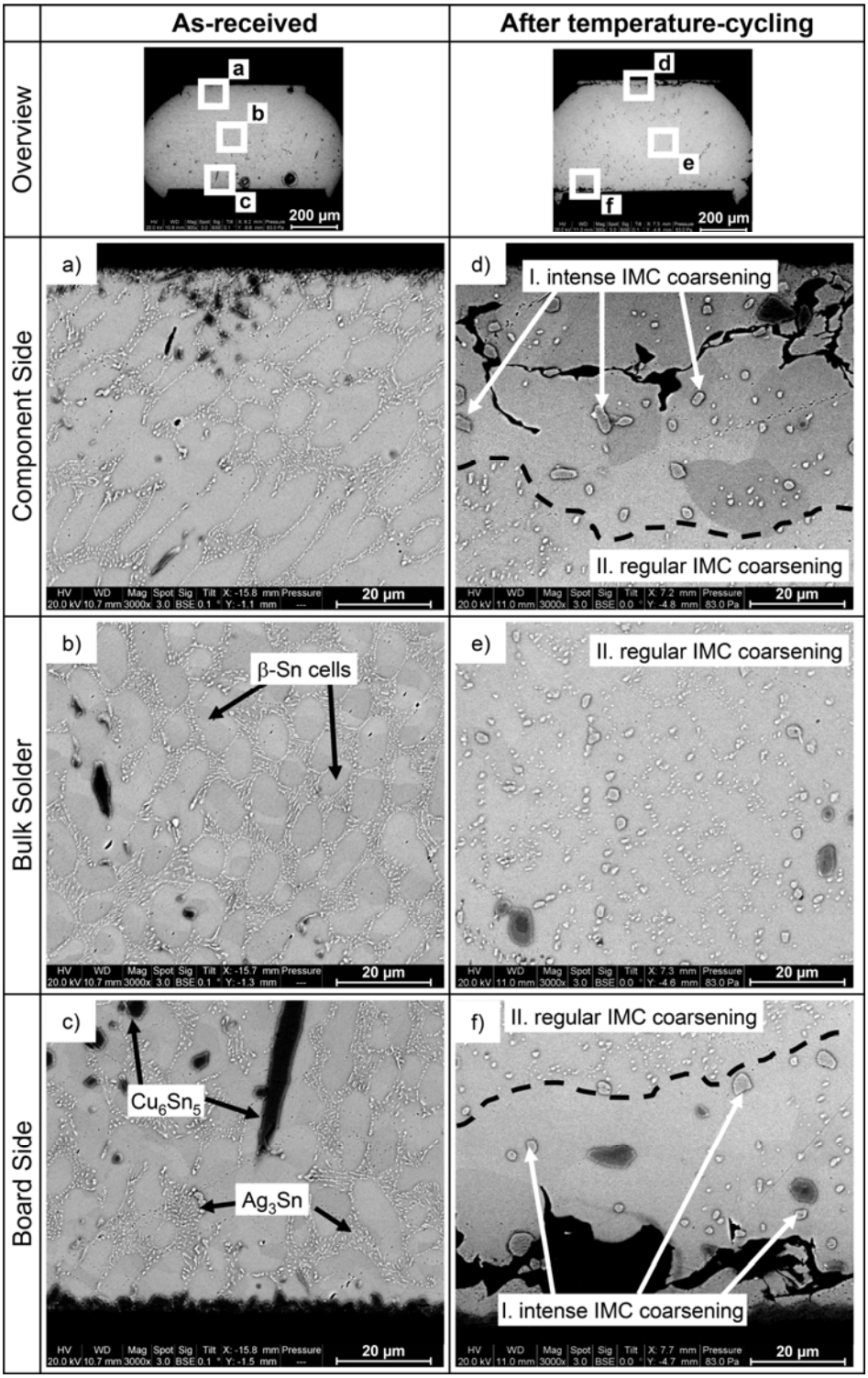

Figure 46: Microstructural comparison of as-received (a-c) and temperature-cycled (d-f) non-reballed SAC305 solder joints. IMC coarsening is visible all over the solder joint but an intense phase growth can be seen in the crack area. (256 I/O BGA - ESEM)

Failure analysis revealed that the main failure site in the lead-free assemblies was near the interface at the component side regardless of the component type (see Figure 46d). In some cases cracks were also found propagating along the interface at the board side (see Figure 46f). These failure sites and crack propagation paths were consistent with Dunford's study [72]. From the crack propagation in Figure 46d and Figure 47d it is assumable that the crack propagates along the boundaries of the refined Sn grains. Sometimes intermetallics can be found along the crack but there are no significant shifts in crack direction in order to follow Sn/IMC phase boundaries.

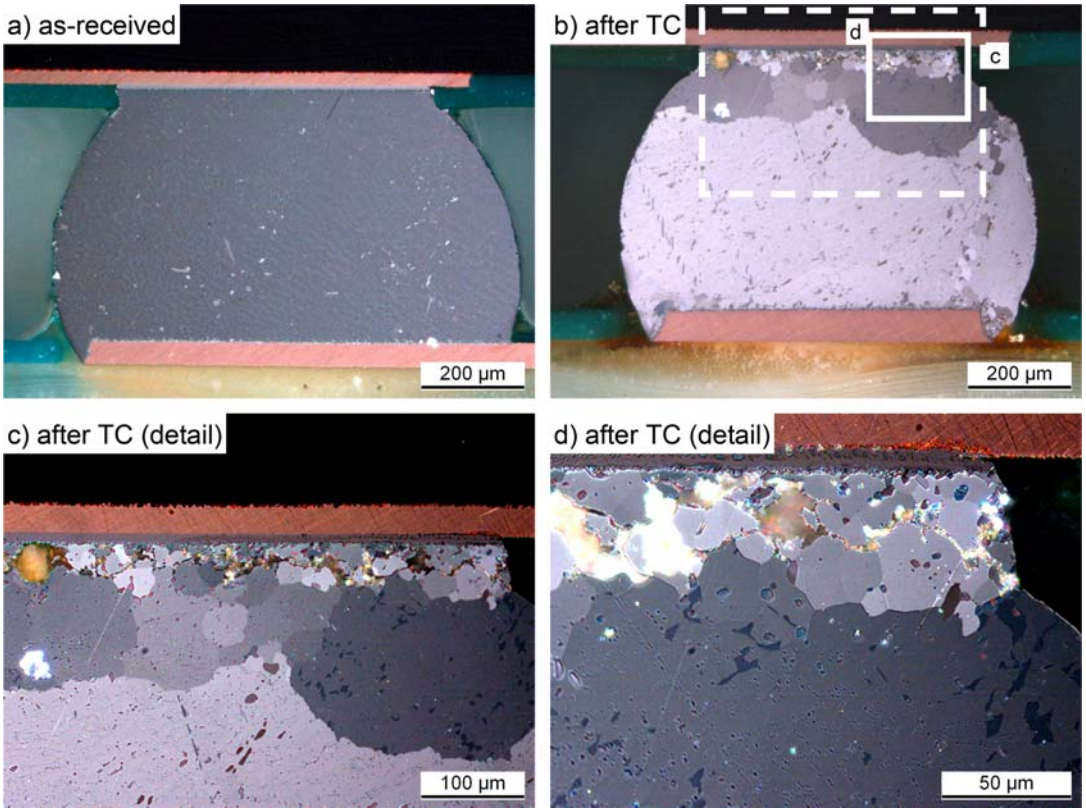

Figure 47: Changes in grain structure in non-reballed SAC305 solder joints: a) as-received b) after temperature-cycling. Detailed pictures of the phase coarsening area close to the crack are shown in c) and d). d) Sn-grains in this area show grain refinement and changes in orientation. (256 I/O BGA - cross polarized optical microscopy)

4.4.3. Microstructural Development and Crack Propagation in Mixed BGA Assemblies

Snugovsky, et al. [26] described the mixing process using a SnPb phase diagram. From this study, they concluded that a full mixture may be achieved at a temperature lower than the melting temperature of the SAC system. Several studies believed that complete mixing in solder joints is directly related to the temperature cycling reliability of mixed assemblies [28] [31] [32].

In this study, a "full mixing" structure was achieved using a modified SnPb profile, with the peak temperature of 215ºC and the time above liquidus (> 183 ºC) of 100 s. The Pb concentration in the mixed assemblies was calculated based on the volume of the solder ball, the volume of the solder paste, and the metal percentage in the paste. The amount of Pb was approximately 3.2 wt% in the 676 I/O mixed assemblies and 3.0 wt% Pb in the 256 I/O mixed assemblies. According to the phase diagram and the calculated amount of Pb in the solder, it is assumable that the Pb-rich phase will solidify as one of the last phases.

The "full mixing" of the solder ball and the solder paste in the BGA assemblies is shown in Figure 48a. It can be seen that the Pb-rich phase is distributed all over the solder joint, but the Pb distribution is not homogeneous inside the solder joint. A possible explanation can be assumed from the presence of pure β-Sn cells which indicate a dendritic solidification of the Sn (see Figure 48b). Since Sn has to solidify as primary phase (according to the phase diagram) and due to the fast dendritic solidification, the IMCs as well as the Pb-rich phase have to solidify

subsequent in the interdendritic/intercellular regions (see Figure 48b). This kind of solidification is well known for SAC solders and causes a very heterogeneous microstructure as well as the heterogeneous distribution of the Pb phase in the investigated mixed assemblies.

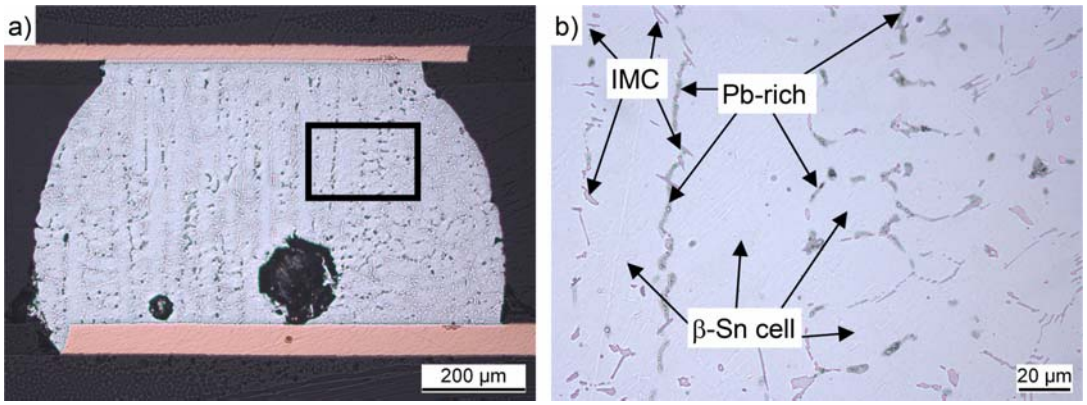

Figure 48: Pb distribution in an as-received mixed solder joint: a) overview of a solder joint showing complete mixing but heterogeneous distribution of the Pb phase (dark phase) over the solder joint. b) detail, showing β-Sn cells surrounded by intermetallics an Pb-rich phases. (bright field - optical microscopy)

Figure 49 allows a comparison of the microstructure of the as-received mixed assemblies versus the temperature-cycled assemblies. Figure 49c shows the presence of β-Sn cells that are surrounded by Ag_3Sn intermetallics and Pb-rich phases. The shape of the IMCs is different and their size is much larger compared with the SAC305 solder. The Pb-rich phase can be found nearby the IMCs and not in the Sn cells. After temperature cycling, it can be seen that the Ag_3Sn intermetallics as well as the Pb-rich phases have grown. There is no Pb-rich phase layer visible at both interfaces as seen for the SnPb assemblies. It appears that the Pb amount in the investigated mixed assemblies is too low for that phenomenon.

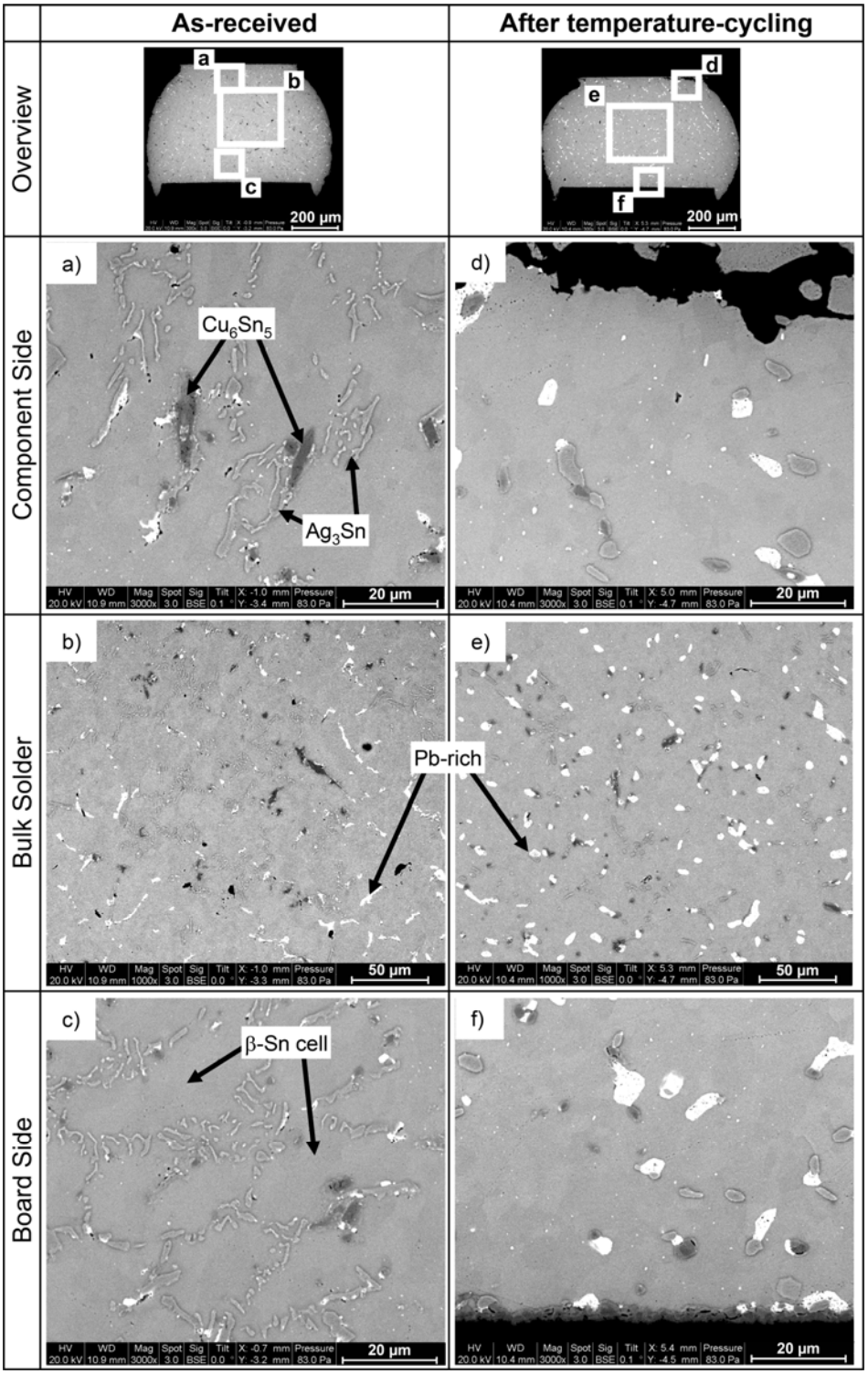

Figure 49: Microstructural comparison of (a-c) as-received and (d-f) temperature-cycled non-reballed mixed solder joints (SAC305+SnPb paste – approx. 3 wt.% Pb). Coarsening of IMCs and Pb-phase is visible. An intense phase growth can be seen clearly in the crack area. (256 I/O BGA - ESEM)

In general, the failure site in mixed assemblies is located at the component side but cracks also propagated at the board side near the interface (see Figure 50b). In some of the survived samples, major cracks were found at the board side that might cause failure with longer temperature cycling. These observations are consistent with previous studies [30] [73].

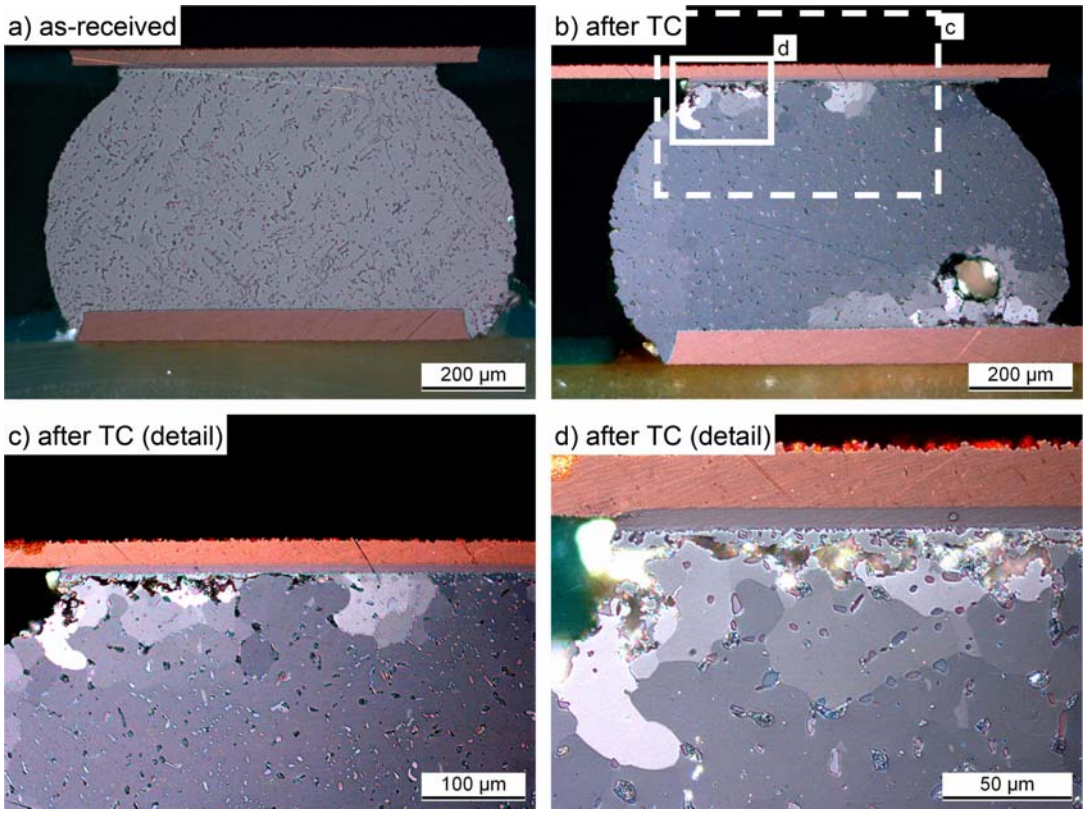

Figure 50: Changes in grain structure in non-reballed mixed solder joints (SAC305 + SnPb – approx. 3 wt.% Pb): a) as-received solder joint b) after temperature cycling Detailed pictures of the crack area are shown in c) and d). d) Sn-grains in the crack area show grain refinement and changes in orientation. (256 I/O BGA - cross polarized optical microscopy)

Figure 50 shows the changes in grain structure due to temperature cycling. The grain structure of the as-received solder joint only shows one major grain orientation (see Figure 50a). Most of the investigated as-received mixed solder joints

have approx. 1-3 major grain orientation (see Appendix for more images). After temperature cycling test, two cracks are visible, which are surrounded by an area with comparably small grains and different orientations (see Figure 50b). The rest of the solder joint (bulk solder or area without crack) still shows one major grain orientation. Figure 50c shows a refined region in front of the crack tip. It is assumable that the crack will propagate through the new grain boundaries in this area. Figure 50c-d also shows that intermetallics and especially the Pb-rich phases are very often gathered at the grain boundaries of the refined grains. The grain structures as well as its changes are comparable with the SAC305 solder.

4.5. Discussion

As discussed in the previous section, the temperature cycling reliability of reballed SnPb assemblies was independent of the reballing method. Failure analysis revealed that the failure site was in the bulk solder at the component side. Although the reballed BGAs on the test assemblies were created with different reballing methods, the microstructure inside the bulk solder and the fatigue life were the same. The temperature cycling reliability of reballed SnPb assemblies was lower than that of the lead-free assemblies. The difference in the temperature cycling reliability of reballed SnPb and lead-free assemblies can be attributed to the differences in microstructures of SnPb and SAC solder. The SnPb solder consists of Sn-rich and Pb-rich phases that form lamellar structures (during the eutectic reaction) as shown in Figure 42b. The cracks in the reballed SnPb assemblies mainly propagated along the Sn and Pb phase boundaries (see Figure 42e). This phase boundary appears to be the weakest point in the bulk solder. If there were no phase boundaries for crack

propagation, the crack propagated through the Sn in order to reach the next Sn-Pb phase boundary. As seen in Figure 42b, the crack also changed direction in order to reach the next phase boundary. The investigation on grain structure revealed that small Sn grains had formed in the crack area (which was also the high stress area) of the solder joint. From that it was assumable that the newly formed Sn-Sn grain boundaries were used for crack propagation since no phase boundary was available.

SAC305 solder contains no Pb and solidifies with cellular β-Sn structures surrounded by Ag_3Sn particles, as shown in Figure 46b. In the lead-free assemblies, there is no Pb phase, the cracks propagated along the Sn-Sn grain boundaries. This could explain why lead-free (SAC305) assemblies outperformed reballed SnPb assemblies. In Liang's study [74] it was found that the Ag_3Sn particles surrounding the dendritic β-Sn structure acted as stress distributors and increased the fatigue resistance of SAC solder. This was also another reason why lead-free solder has better fatigue resistance than SnPb solder.

The microstructure in the mixed assemblies was similar to that in the lead-free assemblies, which was the dendritic Sn structure surrounded by the Ag_3Sn particles, and the darker Cu_6Sn_5 was randomly distributed inside the bulk solder. However, the size and arrangement of Ag_3Sn in the mixed assemblies were different from the lead-free assemblies (see Figure 51). In the mixed assemblies, the Pb-rich phase was distributed randomly inside the bulk solder in the mixed assemblies, but the Pb phase was not found to participate in IMC formation. It was not surprising to find that the temperature cycling reliability of the mixed assemblies was comparable to that of the

lead-free assemblies. The failure site in the mixed assemblies and lead-free assemblies were the same: the bulk solder at the component side.

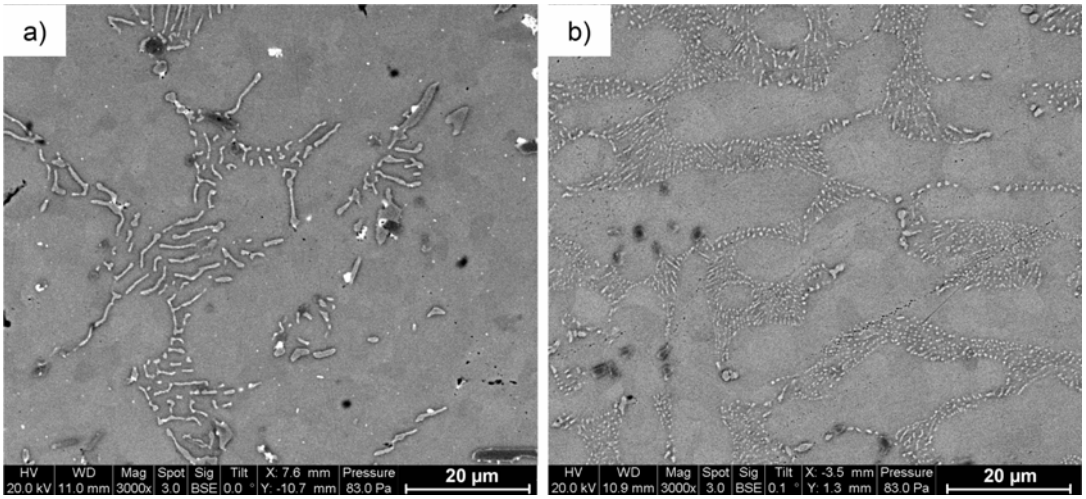

Figure 51: Differences in the phase size and shape of the Ag_3Sn intermetallics between as-received a) mixed and b) lead-free assemblies. These differences may be caused by the change in the solidification sequence and temperatures due to the presence of Pb.

If comparing the as-received state of tin-lead, lead-free, and mixed solder joints, there were more grain orientations in tin-lead solder joints, which offered more phase boundaries and grain boundaries for crack propagation. This observation could explain why tin-lead solder have a lower mean cycles-to-failure under temperature cycling than lead-free and mixed solder joints. In Figure 45, Figure 47, and Figure 50, the failure regions of the temperature-cycled specimens show dramatic changes. Small grains were found in the cracked areas. The grain refinement was found in the tin-lead, lead-free, and mixed assemblies. It is reasonable to assume that this phenomenon was caused by recrystallization due to the high stress in these areas. Recrystallization would cause a complete change of the microstructure. This can be seen for the lead-free and mixed assemblies by the disappearance of the cellular

structures in these areas. Recrystallization would also explain the excessive phase growth (intermetallics in lead-free and mixed assemblies; Pb-rich phases in reballed assemblies) in this area. The growth of new Sn grains led to the displacement of impurities (intermetallics will be pushed out of the new grains) and also formed new grain boundaries that were used as faster diffusion paths than matrix diffusion.

4.6. Conclusions

In this study, 676 I/O and 256 I/O lead-free (SAC 305) BGAs were selected to be reballed with eutectic tin-lead solder balls. The effect of the reballing methods on the temperature cycling reliability of reballed BGA assemblies was examined. The tin-lead reballed BGAs were assembled on PCBs with eutectic Sn37Pb solder paste. As a reference, the lead-free BGAs were assembled with SAC305 solder paste and eutectic tin-lead solder paste to form the pure lead-free SAC assemblies and the mixed (lead-free solder ball/tin-lead paste) assemblies.

All the reballed SnPb, mixed, and lead-free assemblies were subjected to the temperature cycling test with a temperature range of -55 °C to 125 °C and 1 hour per cycle. The test was terminated at 5324 cycles. The mean cycles-to-failure for the reballed tin-lead BGAs were found to be less than 50% of the mean cycles-to-failure for either the lead-free and mixed BGA assemblies. With regards to reballing process, no significant difference was found in the mean cycles-to-failure data. Difference in failure life between tin-lead, lead-free, and mixed was likely due to properties of bulk solder. The mean cycles-to-failure of the mixed assemblies was equal to or better than that of lead-free assemblies.

The failure site of the reballed SnPb BGA assemblies was located in the bulk solder at the component side. Pb-rich phase coarsening occurred near the interface after the temperature cycling test, and the fatigue cracks were located at the phase coarsening regions. The cracks propagated along the phase boundary or along the Sn-Sn grain boundaries if there was no phase boundary. Consistent with test results, no differences were found in failure sites corresponding the reballing process.

The lead-free and mixed assemblies had similar microstructures. For the lead-free assemblies, the typical failure site was located at the component side, in the grain refining area. The fine Ag_3Sn particles coarsened and the amount of particles decreased after the temperature cycling test. In the mixed assemblies, the Pb phase was dispersed throughout the bulk solder, but the Pb phase distribution was not homogenous. Fatigue cracks propagated at both the component side and the board side, but the failure site was still located at the component side in the mixed assemblies.

Chapter 5: TEMPERATURE CYCLING RELIABILITY TEST AND MICROSTRUCTURAL ANALYSIS OF REWORKED LEAD-FREE AND REWORKED MIXED ASSEMBLIES

Rework is defined as the correction of a defect before the printed board assembly leaves the plant, and repair is defined as the correction of a defect found in the field [6]. With the electronics industry predominantly using lead-free solders, it is important to understand the impact of the rework process on the reliability of reworked assemblies. There are not many studies that address the reliability of reworked BGA assemblies, especially the reliability of reworked mixed assemblies [27] [30] [35]. Current literature only focused on the reliability testing on the reworked assemblies. However, whether the reliability of reworked assemblies is comparable to the non-reworked assemblies is still unknown, and the root cause of the reliability difference between reworked and non-reworked assemblies is still not clear. A detailed analysis of microstructure examines differences between reworked and non-reworked BGA assemblies, which are needed in order to achieve a better understanding of rework impact.

5.1. Cu Pad Dissolution and Microstructural Analysis of Reworked Lead-free and Mixed BGA Assemblies

In this section, a pilot study was developed to investigate the impact of multiple rework process on the microstructure of lead-free and mixed assemblies. Since the electronics industry is now using lead-free solder predominately, it is

important to understand the impact of the rework process on the microstructure of reworked assemblies. Some literature addresses Cu dissolution in plated through-hole (PTH) barrels in the rework process [14]-[17]. This creates a concern because it is possible for a hidden defect to be present after reworking PTH assemblies. S. Chada, et al, found out that the amount of Cu dissolution increased as the soldering temperature and time increasing [18]. Thus, the rework process parameters, such as the peak temperature and the time above liquidus, are important to the Cu dissolution in the reworked assemblies. Currently, no literature has focused on the Cu dissolution of reworked ball grid array (BGA) assemblies, which is another possible hidden defect.

5.1.1. Experiment Setup and Rework Process

In this pilot study, a set of test boards was designed and manufactured to test the effect of multiple rework processes on the reworked assemblies. The material that the PCBs were made from was FR4, with Cu pads and organic solder preservative (OSP) finish. Here, 676 I/O plastic ball grid array packages (PBGAs) with Sn3.0Ag0.5Cu (SAC305) solder balls were assembled on PCBs. There were two kinds of assemblies: lead-free assemblies, those using SAC305 solder paste (SAC BGA and SAC solder paste); and mixed assemblies, those using eutectic SnPb solder paste (SAC BGA and tin-lead solder paste). Individual locations on the printed circuit boards (PCBs) were subjected to rework processes one time, three times, and five times. Components on PCBs were cut and cross-sectioned to inspect the dissolution of Cu pads and the morphology of IMCs. An environmental scanning electron

microscope (ESEM) and an energy-dispersive X-ray spectroscopy (EDS) were used to investigate the growth of IMC, as well as the composition of IMC.

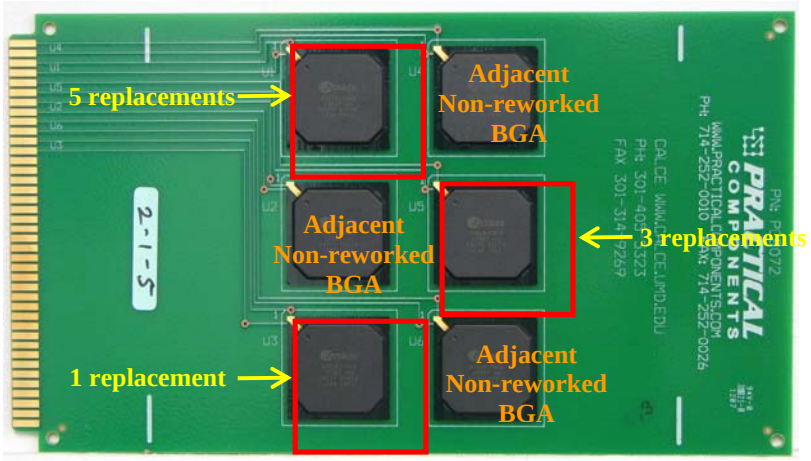

Figure 52: Image of 676 I/O BGA assemblies

Six BGAs were assembled on each board, as shown in Figure 52. Three locations were selected to be reworked (see Figure 52). These three locations were first reworked one time. Then two of the three locations were reworked another two more times, and the last location was reworked two more times. Thus, there were three treatments for these BGA assemblies locations: one replacement, which means the removal of the BGAs on the PCB and their replacement with new BGAs; three replacements, which means the removal of the BGAs three times, and their replacement every time with new BGAs on the PCB; and five replacements, which means the removal of the BGAs five times, and their replacement every time with new BGAs on the PCB. Table 15 lists the test matrix of reworked assemblies. There were two types of assemblies used in this study, lead-free assembly and mixed assembly. The reflow profile of the lead-free assembly had the peak temperature as 240°C and the time above liquidus for 50~60 seconds. While the reflow peak

temperature of the mixed assemblies was 215°C, with the time above liquidus for 100 seconds. The PCB assemblies were subjected to preconditioning at 100°C for 24 hours before being reworked. The assemblies were also subjected to preconditioning after each rework process. The reworked BGAs were cut and molded to investigate the intermetallic compound microstructure and Cu pad. The adjacent non-reworked BGAs as shown in Figure 52 were investigated as well to be compared with the reworked BGAs.

Table 15: Rework test matrix of 676 I/O BGAs

Assemblies Type	Component	Original Assembly Solder Paste	Repair Solder Paste	Reworked Components
Lead-free assemblies	SAC305 676 I/O BGA	Sn37Pb (Indium SMQ-92J)	Sn37Pb (Indium SMQ-92J)	3
Mixed assemblies	SAC305 676 I/O BGA	SAC305 (Alpha OM-338)	SAC305 (Alpha OM-338)	3

The rework process of surface mount technology (SMT) components involves four steps: thermal profile setup, component removal, site redressing, and component placement. To remove the components assembled on the PCB, a thermal profile needs to be set up to melt the solder. A thermal profile is established by various trial runs, as it depends on several factors such as board thickness, type of solder, and component size.

A VJ Electronix SRT1800 rework station with a bottom heater and a hot nitrogen nozzle on top was used to replace the BGA components. The hot nitrogen nozzle was applied to each assembled BGA to heat up the solder, and at the peak

temperature, when the solder melted, the component was removed by suction using a vacuum tool.

After the components are removed from the PCB, there may be residue solder left on the pads. The pads must have a flat surface to ensure the quality of the replacement. In this study, the soldering iron and wick method was used to remove the residue solder from the pads. A fluxed Cu braid was heated by the soldering iron and brushed over the pads. The heated braid melted the residue solder, and the solder was wicked up into the Cu braid. Figure 53 shows the pads after site redressing. The pads had clean surfaces and the solder mask was not damaged during the removal procedure.

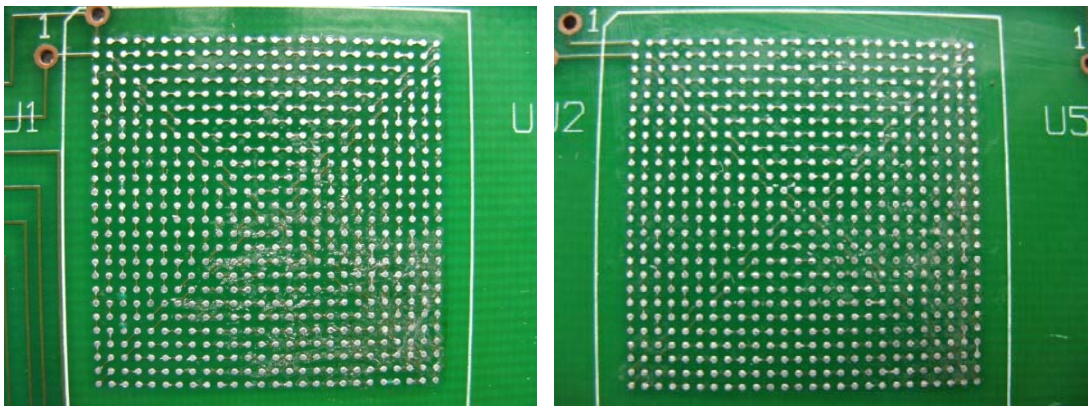

(a) (b)

Figure 53: Pad inspection after site redressing

(a) PCB pad of mixed assemblies; (b) PCB pad of lead-free assemblies

Once the site was redressed, a mini-stencil was aligned and placed on the location, and the solder paste was printed on the pads. This mini-stencil was similar in size to the component and had openings that matched the pads. The lead-free rework used Alpha OM-338 (SAC305), a type of lead-free, no-clean solder paste. The mixed

solder rework used Indium SMQ-92J (6337), a no-clean, tin-lead solder paste. After solder paste was applied to pads, components were aligned and placed by semi-automated techniques on the locations. The hot nitrogen nozzle was placed above the components to melt the solder balls and solder paste. The new BGAs were assembled on the PCBs after cooling to room temperature.

The assemblies were sent to a quick rework house, and the thermal profiles used in component removal and component placement were the same. Both the lead-free assemblies and the mixed assemblies used the lead-free rework thermal profiles. For lead-free reworked assemblies, the peak temperature was 282°C, with 30-second above 217°C, and the cooling rate was 2°C/sec. While the thermal profile of the mixed reworked assemblies had the peak temperature of 282°C and the time above 183°C as 50 seconds. The cooling rate of mixed thermal profile was also 2°C /sec.

5.1.2. Cu Pad Dissolution

When a new component is attached to the pads during the rework process, a reaction occurs between the solder balls and the PCB pads. Cu dissolves into liquid Sn and forms an intermetallic layer at the solder/pad interface. Hamilton and Snugovsky [17] addressed the Cu dissolution that occurs during the lead-free plated-through-hole (PTH) rework process. They found that the Cu pad dissolution rate of the lead-free (SAC) rework process was higher than that of the eutectic tin-lead rework process. Currently, there is no literature that addresses Cu pad dissolution in reworked BGA assemblies. However, the pad dissolution of BGA assemblies during the rework process may lead to hidden concerns. When the solder is in a liquid state,

Cu comes into contact with molten Sn and starts to dissolve rapidly. In the rework process, there are several procedures where solder is in the molten state. Thus, the Cu dissolution of reworked assemblies should be considered. This is especially true for pads with OSP finish, because there is no barrier layer between the Cu and solder after reflow, and the Cu can dissolve into and react with the molten Sn directly.

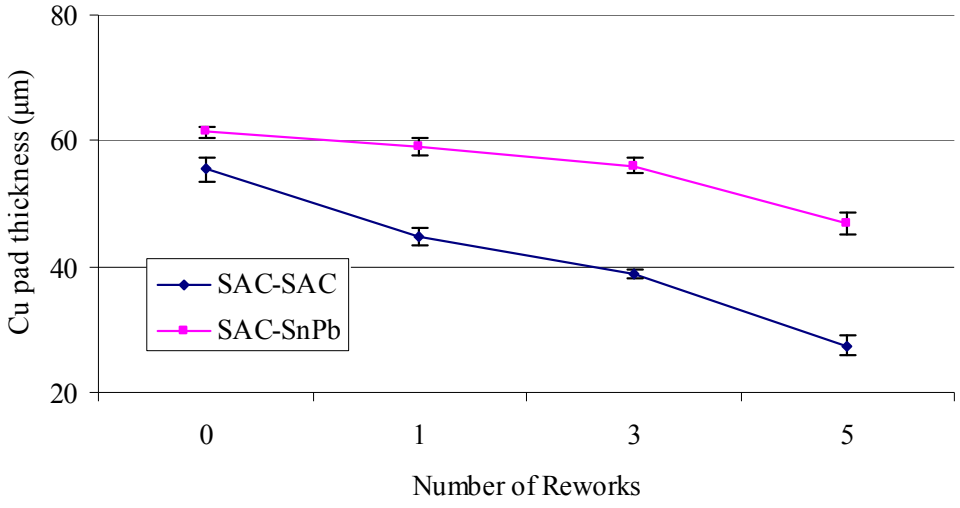

Figure 54: Cu pad thickness of lead-free and mixed assemblies after rework processes (Number of rework "0" stands for adjacent non-reworked BGAs)

In this study, the Cu pad thicknesses of lead-free and mixed assembly joints were measured using ESEM. For each sample, 27 measurements were documented. The results are plotted in Figure 54, and the BGAs with zero rework stands for the adjacent non-reworked BGAs. The Cu pad thickness of unassembled PCB was also documented as reference. The thickness of Cu pad in unassembled board was 65.23±1.42 µm. The Cu pad thicknesses of the adjacent non-reworked lead-free (SAC) BGAs and the non-reworked mixed BGAs were 55.43±1.89 µm and 61.35±1.39 µm,

respectively. However, after five replacements, the Cu pad thickness of the lead-free (SAC) BGAs was only about 50% that of the mixed BGAs (see Figure 55 and Figure 56). In the rework process, lead-free assemblies consumed more Cu than did the mixed assemblies.

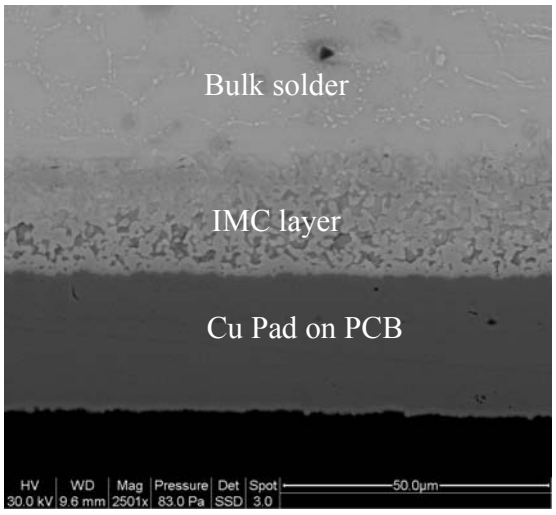

Figure 55: Solder/pad interface in lead-free assemblies after five replacements

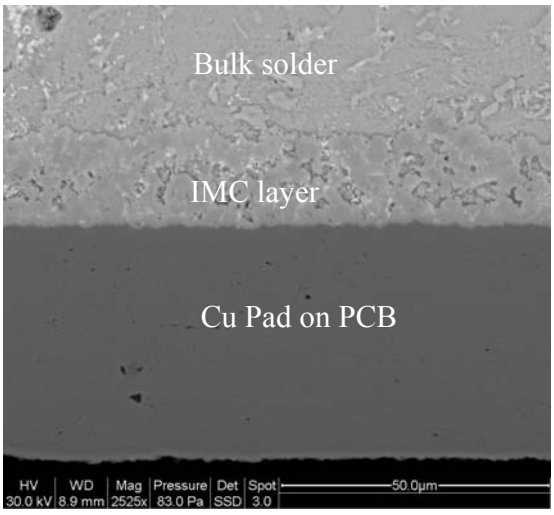

Figure 56: Solder/pad interface in mixed assemblies after five replacements

During the reflow process, liquid Sn and solid Cu react with each other to form intermetallic compounds at the solder/pad interface. Cu dissolves into liquid Sn very fast (in seconds), and there is a large driving force for the chemical reaction between Cu and Sn. The Cu-Sn IMC formation mechanism is controlled by the dissolution of Cu into liquid Sn followed by chemical reactions [66].

In SnAgCu solder, the concentration of Sn is higher than in SnPb solder. A higher concentration of Sn leads to higher Cu dissolution. Thus, the SnAgCu solder can dissolve more Cu than SnPb solder. In eutectic SnPb solder, Pb can be considered a solvent, which decreases the concentration of Sn. In mixed assemblies, when the Cu dissolves into bulk solder, the local Pb concentration will increase at the IMC/bulk

solder interface, which blocks Cu from being dissolved into bulk solder. Thus, Cu pad loss in lead-free assemblies is more than that in mixed assemblies.

5.1.3. Over-Consumption of Cu Pad

In both lead-free and mixed assemblies, Cu pads were over-consumed after five rework processes. The design of the Cu pads allows them to be electrically interconnected with different solder balls (see Figure 57). Figure 58 shows a schematic image of Cu pad connections; the circles indicate sites of over-consumption. During the rework process, the heat tends to be conducted along the Cu, since Cu has very good thermal conductivity. Not as much heat was conducted from the Cu pad to the Cu trace since the connection site between them was narrower compared to the area of Cu pads. Thus, heat concentrated in the connection site led to thicker intermetallic compound formation and over-consumption of the Cu pad after multiple rework processes. The Cu trace was covered by the solder mask as shown in Figure 59. The IMC formation was limited at the location where the Cu pad entered to Cu trace. The board design for the reworked assemblies should be reconsidered, especially the geometry parameter of the Cu pad and the Cu trace, since over-consumption was observed in the samples after subjected to multiple rework processes.

The consumption of the Cu pads was relatively even for the BGAs after one and three replacements. However, the edges of the Cu pads in the BGAs with five replacements were over-consumed. Figure 60 shows backscattered electron images of the edge of the Cu pads or the reworked lead-free and mixed assemblies. Both the

lead-free and the mixed assemblies had similar Cu over-consumption trends. After one replacement, the Cu pads of the samples were relatively even; after three replacements, they had a small amount of over-consumption at the edge; after five replacements, they were almost consumed, and the intermetallic compound replaced the Cu. The heat accumulated in the rework process was not enough to form extra IMC at the connection site between the Cu trace and the Cu pad. After three replacements, the edge of Cu pad was consumed by solder a little. However, the heat accumulation led to Cu over-consumption after five replacements, and the connection site between Cu trace and Cu pad was almost "eaten up" by the solder. The over-consumption of the Cu pads and ultra-thick IMCs may lead to an open circuit of the device under mechanical loading. The reworked assemblies may not have good mechanical reliability if the assemblies have been exposed to multiple rework processes.

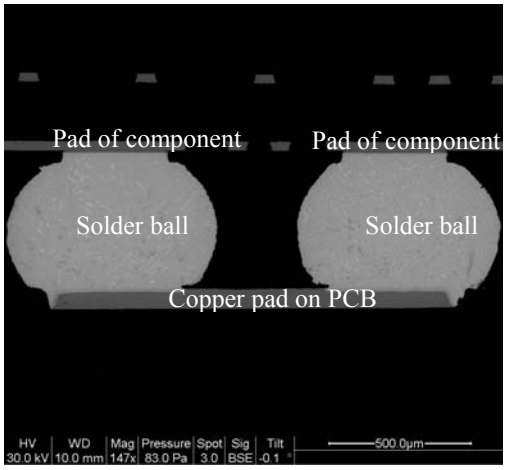

Figure 57: Backscattered electron images of two solder balls connected on Cu pads (mixed assemblies, one replacement)

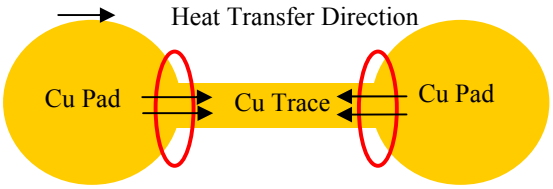

Figure 58: Schematic images of heat transfer between the Cu pads and the Cu trace on a PCB

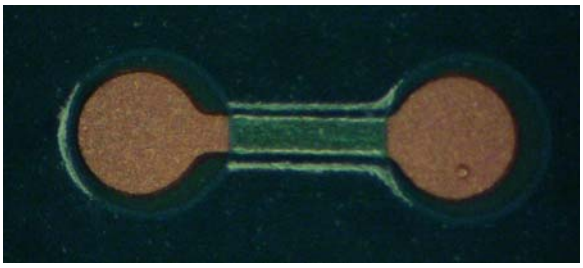

Figure 59: Cu pads and Cu trace on a PCB

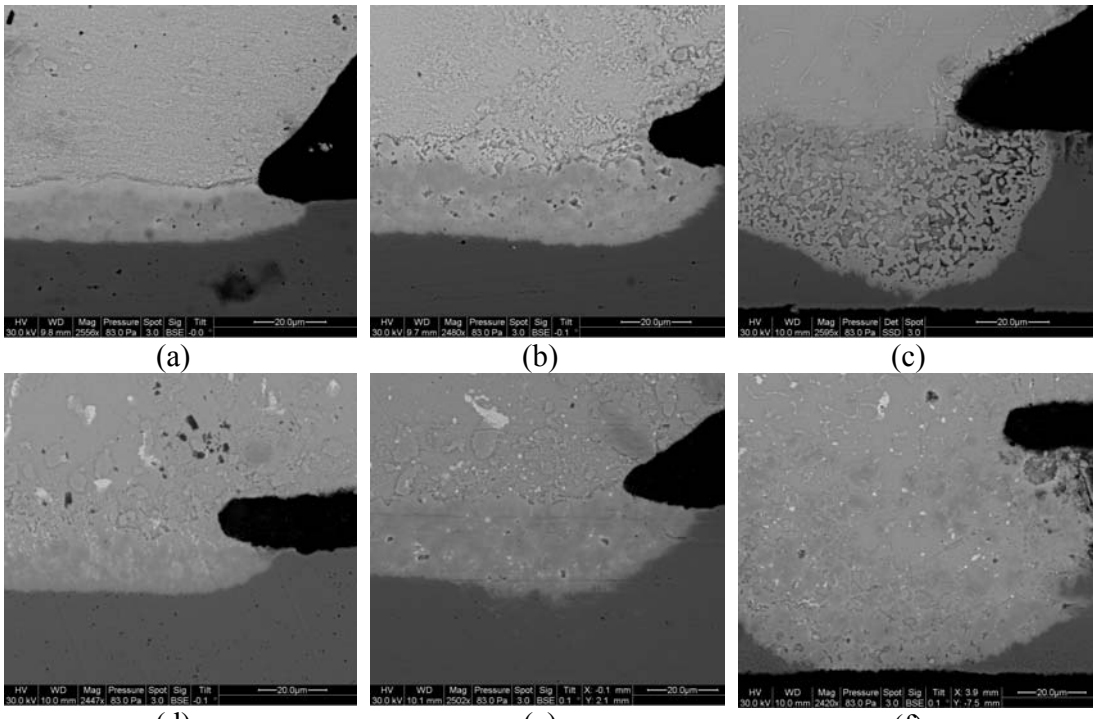

(a) (b) (c)

(d) (e) (f)

Figure 60: Backscattered electron images of the edges of Cu pads

(a) lead-free assembly, one replacement ; (b) lead-free assembly, three replacements ; (c) lead-free assembly, five replacements; (d) mixed assembly, one replacement; (e) mixed assembly, three replacements; (f) mixed assembly, five replacements.

5.1.4. Interfacial Intermetallic Compound Morphology and Thickness

The morphology of the interfacial IMC at the board side in the reworked BGAs and the adjacent non-reworked BGAs was different from that of the as-assembled BGA assembly. The morphology of the interfacial IMC in the as-assembled BGAs was scallop shape as shown in Figure 61. The morphology of the interfacial IMC in the reworked BGAs was fragmentary (see Figure 62). While the morphology of the interfacial IMC in the adjacent non-reworked BGAs already showed some fragmentation at the interface. This fragmentation became more dominant when the assemblies were subjected to multiple rework processes. The strongest fragmentation was found at the interface in the BGAs after five rework processes.

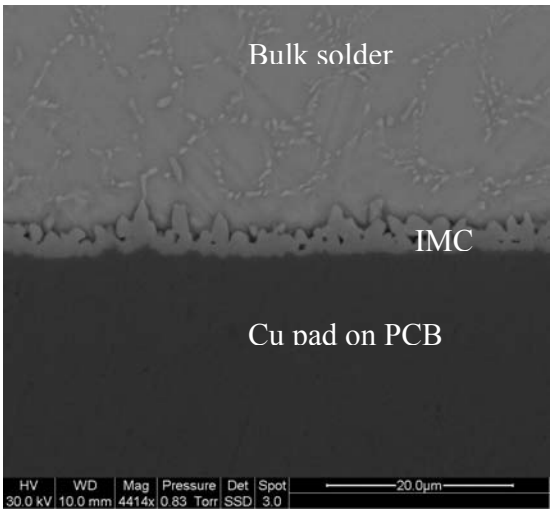

Figure 61: Backscattered electron images of the interfacial IMCs in an as-assembled lead-free assembly

At the point where the solder material becomes liquid, Cu_6Sn_5 is the first phase to form at the liquid Sn/Cu interface [66]. The formation of Cu_6Sn_5 takes place within seconds. Cu dissolves into liquid Sn, and reacts with liquid Sn. An ultra-thin

layer of Cu_3Sn forms between the Cu_6Sn_5 and the Cu pad, but it is too thin to be detected [66]. However, the Cu_3Sn becomes thicker after long periods of isothermal aging [66].

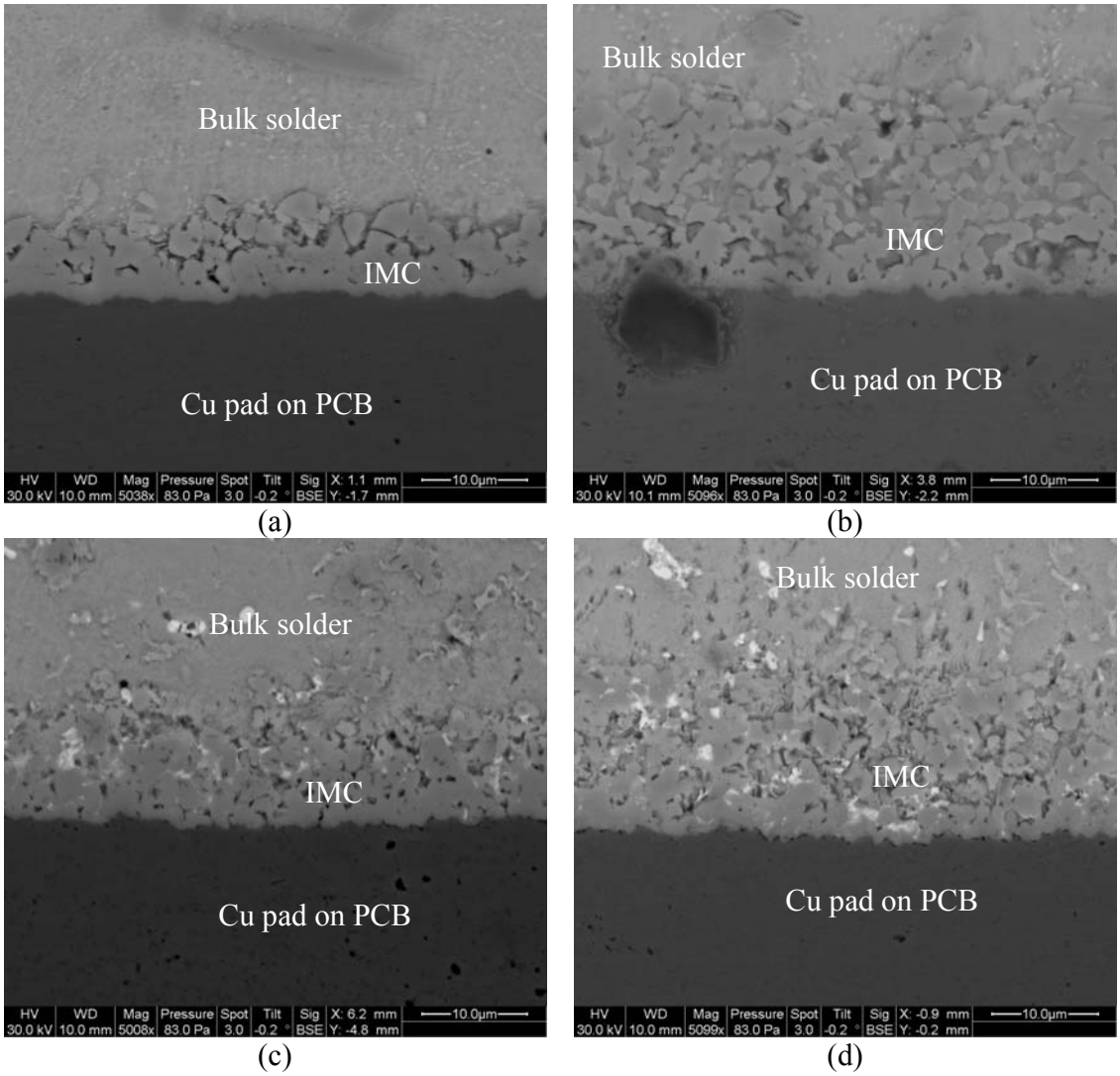

Figure 62: Backscattered electron images of IMCs at solder/pad interface: (a) lead-free assembly, adjacent non-reworked; (b) lead-free assembly, five replacements; (c) mixed assembly, adjacent non-reworked; (d) mixed assembly, five replacements.

The interfacial IMC composition in the reworked and adjacent non-reworked solder joints was Cu_6Sn_5. However, Cu_3Sn was not detected at the interface, perhaps due to the resolution of the ESEM. Unlike the continuous layer of IMC undergoing

isothermal aging, a much thicker layer of IMC with a fragmentary shape was found at the interface of the sample after five replacements. The reason for the IMC morphology was due to the Cu dissolution in liquid Sn and the Cu diffusion at the interface.

During every process where the solder becomes liquid, there are two mechanisms influencing the interfacial IMC layer. The first mechanism is Cu dissolution into the bulk solder. This effect causes decreasing of the interfacial IMC thickness. The second mechanism is IMC layer growth, due to the Cu diffusion from the substrate material. This causes the increasing of the interfacial IMC thickness. Cu dissolution is caused by the low amount of Cu inside of the bulk solder (SAC has 0.5wt% Cu and SnPb has no Cu at all). The major parameters for Cu dissolution are peak temperature and time above liquidus, and for fast dissolution it is necessary to have the solder in liquid state. At the reflow peak temperature of 282 ℃, a Cu amount for the Sn-Ag-Cu system of approximately 2 wt% can dissolve into the liquid bulk solder respectively to the Sn-Ag-Cu phase diagram [75]. Due to the fact, it is reasonable to assume that Cu dissolution will be very fast at the beginning of the rework procedure. That means the thickness of the interfacial IMC will decrease in the beginning. It is also reasonable to assume that the fast Cu dissolution mechanism causes the fragmentary interfacial IMC morphology. The fast Cu dissolution stops if the liquid solder is saturated with Cu or the solder is solidified. The second mechanism, which causes IMC growth, still works even when the solder is solidified and it is just depending on temperature.

The solder becomes liquid in several steps in the rework process, including component removal, site redressing, and component placement. When contacting with liquid solder, the previous IMC formed at the interface starts to dissolve, and Cu atoms dissolve into the liquid Sn very fast. At the same time, IMC layer growth also takes place at the interface. Due to the fast Cu dissolution, the interfacial IMC is not compact any more, and some parts separate from the former compact interfacial IMC. This is why a thick fragmentary IMC morphology is found at the interface of the reworked BGAs.

The adjacent non-reworked BGAs are very close to those reworked ones. From the results and comparison with the as-assembled BGAs, it can be assumed that rework also causes microstructural changes in adjacent components. Rework is not only influencing the reworked BGAs but also the adjacent components. That means the adjacent non-reworked components experienced preconditioning (isothermal aging at 100°C for 24 hours) several times and it is also possible that some of the heat of the rework process has influenced those adjacent components.

The interfacial intermetallic compound layer became thicker after the samples were subjected to reworks. Figure 63 plots the interfacial IMC thickness of lead-free and mixed assembly joints for adjacent non-reworked and reworked samples, and the component with zero rework stands for the adjacent non-reworked components. For each sample, 27 measurements were documented. A. Choubey, et. al showed that the interfacial IMC growth in lead-free assemblies after reworking was much faster than the growth of the interfacial IMCs undergoing thermal aging conditions (normally below 150°C) [25]. In the present study, a similar trend was found among mixed

assembly samples; the interfacial IMC layer of the reworked assemblies was much thicker than the interfacial IMC undergoing isothermal aging conditions (see Figure 63).

The driving force of interfacial IMC growth undergoing isothermal aging is solid/solid interdiffusion, which is much slower than solid/liquid interdiffusion. In each rework process, there are three periods when the solder becomes liquid: component removal, site redressing, and component reflow. Prolonged liquid time enhances the interfacial IMC growth, which leads to much thicker interfacial IMC in comparison to the interfacial IMC undergoing thermal aging.

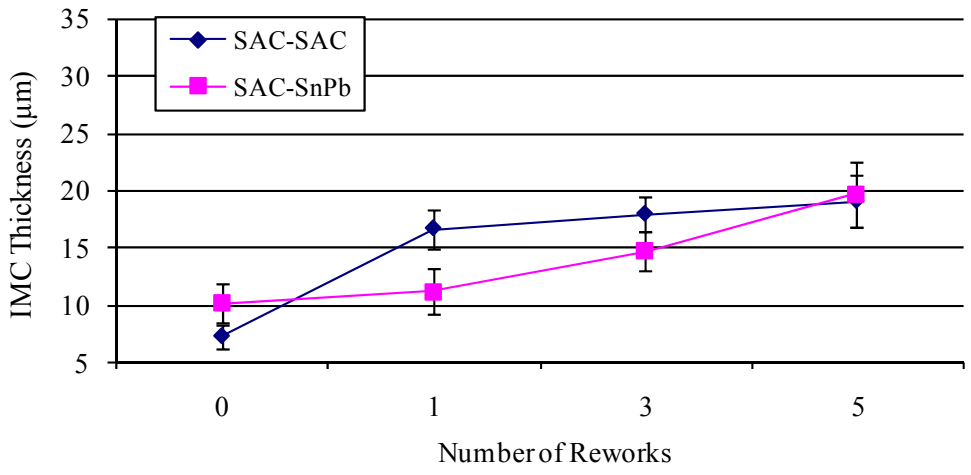

Figure 63: IMC thicknesses of lead-free and mixed assemblies after multiple reworks (Number of rework "0" stands for the adjacent non-reworked BGAs)

In Figure 63, the IMC growth in lead-free assemblies shows a different trend compared to that in mixed assemblies. The IMC growth in the lead-free samples indicates a steep increase of the IMC thickness after one rework process and slowly increases after that. The IMC growth in the mixed assemblies shows a gradual

increase. The IMC growth in the mixed assemblies is attributed to the Pb presence. A. Choubey, et. al, found out that Pb segregation at the interface of the solder and Cu pad retarded the formation of IMCs by influencing the diffusion of Sn and Cu at the interface [25]. From the results, it is assumable that Pb also influence the IMC growth during solid Cu/liquid Sn interdiffusion in the rework process. This explains why IMC growth in mixed assemblies is slower than that of lead-free assemblies after the rework process. The IMC growth rate will decrease with the increasing of the IMC layer thickness, and this can be seen in the lead-free assemblies. The only difference between both assemblies is the presence of Pb, which seems to slow down the growth of the IMCs. However, after multiple rework processes, the reaction time is long enough to form a thick IMC layer at the interface in the mixed assemblies, which is equivalent to that of lead-free assemblies.

5.2. Temperature Cycling Reliability Test and Microstructural Analysis of Reworked Lead-free and Mixed Ball Grid Array Assemblies

With the electronics industry predominantly using lead-free solders, it is important to understand the impact of the rework process on the temperature cycling reliability of reworked assemblies. There are few studies in the literature that address the temperature cycling reliability of reworked BGA assemblies, especially the temperature cycling reliability of reworked mixed assemblies [27] [30] [35]. A detailed analysis of microstructure examines differences between reworked and non-reworked BGA assemblies, which is needed in order to achieve a better understanding of rework impact.

5.2.1. Experimental Setup

For the purpose of this study, 676 I/O lead-free (SAC305) plastic overmold ball grid array (PBGA) components were used to examine the impact of the rework process on lead-free and mixed BGA assemblies. The ball diameter for the 676 I/O BGA was 630µm, and the pitch was 1.0mm. The size of the component was 27mm × 27mm with a full array design. A set of printed circuit boards (PCBs) were designed and fabricated. On each PCB, six BGAs were assembled with one daisy chain per component (see Figure 64). The board laminate material was Isola Polyclad 370 HR, and the surface finish on the boards was an organic solderability preservative (OSP) finish. The board dimensions were 8 in×4.5 in×93 mils, with a surface metallization of two oz/ft^2 Cu (approx. 70µm).

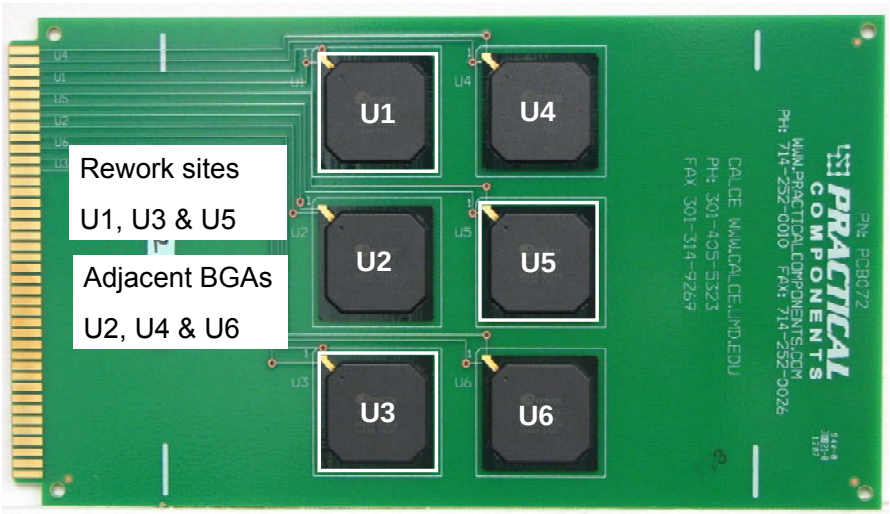

Figure 64: Test vehicle with 6 BGAs on a PCB

Two types of assemblies were used in this study: lead-free and mixed. The lead-free assemblies were SAC305 BGAs soldered with SAC305 solder paste, while the mixed assemblies were SAC305 BGAs soldered with Sn37Pb solder paste. All

assemblies and reflow profiles used for this study were documented prior to testing (see Table 16). For the rework study, three positions of test specimens were selected for rework. These positions, highlighted in Figure 36, include positions U1, U3, and U5.

Table 16: Test setup for lead-free and mixed assemblies

Assembly Type	Component Ball Composition	Assembly Paste	Assembly Profile
Lead-free Assembly	SAC305	SAC305	(1)
Mixed Assembly	SAC305	Sn37Pb	(2)
(1) SAC solder profile: 50-60 sec above 217ºC, peak 240ºC (2) SnPb modified solder profile: 100 sec above 183ºC, peak 215ºC			

5.2.2. Rework Process

All of the assemblies were subjected to preconditioning at 100ºC for 24 hours according to IPC- 9701 [69]. The assemblies were then shipped to a commercial rework facility. Each assembly was baked for 8 hours at 105ºC to avoid moisture-induced stresses before the rework process. Before the rework operation, a thermal profile was established in order to melt the solder. A thermal profile is established by various trial runs, as it depends on several factors such as the board thickness, type of solder, and component size. Normally, the same profile is used to remove and replace the components.

Under the rework operation, BGA packages were removed from pre-selected positions using a hot air rework system. The hot air system uses a directed air nozzle to heat selected packages. The peak package temperature fell between 232^{o}C and 250^{o}C, with a maximum time above 217^{o}C of 35 to 90 seconds. The BGA package was removed using a vacuum attachment, which was a part of the rework system.

Once the package was removed, the next step was site redressing. Excess residual solder left on the Cu pads was removed using a wick braid. The wire braid was heated with a heating-iron, and a de-solder wick drew the solder into the wick braid. The wicking action is similar to a paper napkin soaking up water. The composition of the braid is 98-99% Cu and 1-2% rosin. The de-solder wick is specifically engineered for high temperature, lead-free solders. The use of a de-solder wick also minimized the risk of damage associated with static electricity. The wicks have non-corrosive, ultra-high purity no-clean flux and do not leave ionic contamination on the boards.

After the excess solder was removed from the land area, a cleaning solvent was applied. Next, the area was inspected to ensure that there was no excessive damage to the solder mask. A thin layer of liquid flux was then applied to protect the solderable surfaces from oxidation. Solder paste was applied to the exposed solderable surfaces using a mini-stencil. A mini-stencil is a stencil that is similar to the size of the component and has an opening that matches the pads. For the lead-free assemblies, SAC305 no-clean (Alpha OM338) paste was applied. For the mixed assemblies, Sn37Pb no-clean (Alpha UP78-OSP) was applied. After applying the paste, a new package was positioned on the selected location. The hot air system was

then used to reflow the package. The peak reflow temperature for the SAC305 paste assemblies matched the removal reflow parameters. For the SnPb paste, the peak temperature was between 217°C and 225°C and the time above 183°C was approximately 80 to 100 seconds. After all of the new packages were attached to the board, the interconnects were inspected for defects with an X-ray spectroscopy.

After inspection, the assemblies were subjected to 24 hours at 100ºC for preconditioning purposes. Half of the specimens were subjected to one rework cycle, while the other half were subjected to three rework cycles. After each rework cycle, the assemblies were subjected to another 24 hours at 100ºC. It should be noted that the adjacent components underwent isothermal aging after each rework process and experienced cumulative heat from the exposure to the rework and preconditioning processes.

5.2.3. Temperature Cycling Test Results

A group of the reworked and non-reworked assemblies were subjected to the temperature cycling test with a temperature range of -55ºC to 125ºC. The dwell time and ramp time were 15 minutes each, with 1 hour per cycle. The resistance of daisy chains (one daisy chain per component) for each package was monitored using a data logger. Failure was defined as the occurrence of a resistance peak over 300Ω with 9 additional peaks within 10% of the time to first peak, according to IPC-SM-785 [70]. The test matrix for the temperature cycling test is listed in Table 17.

Table 17: Test matrix for temperature cycling test

Assembly	Temperature Cycling Test (Assemblies/Components)		
	Non-Reworked	1X Reworked	3X Reworked
Lead-free	4/24	6/18	6/18
Mixed	4/24	6/18	6/18

For the temperature cycling test, failure data was obtained as cycles-to-failure. For consistency, the cycles-to-failure data was fit with a two-parameter Weibull distribution function. The failure data results of the non-reworked and reworked BGA assemblies under the temperature cycling test are listed in Table 18. In Table 18, β is the shape factor, η is the characteristic life (63.2% failure), and B_{10} is time to ten-percent failure.

For the lead-free assemblies, the mean cycles-to-failure of the non-reworked BGAs was similar to that of the adjacent BGAs in the reworked assemblies. By applying a one-way analysis of variance (ANOVA), with the alpha selected as 0.05, to the non-reworked and the adjacent BGAs, the BGAs demonstrated the same level of distribution. There was degradation in the mean cycles-to-failure of the lead-free BGAs after the rework process (see Figure 65). After 1X rework, the mean cycles-to-failure of the reworked BGAs decreased 14% compared to that of the non-reworked BGAs, while the mean cycles-to-failure of the reworked BGAs decreased 18% after

3X rework. There was no statistical difference between the 1X reworked BGAs and 3X reworked BGAs using one-way ANOVA.

Table 18: Cycles-to-failure data of non-reworked and reworked assemblies under temperature cycling test

Assembly	Component Type	Slope (β)	Characteristic Life (η)	Time to 10% Failure (B_{10})
Lead-free	Non-reworked	5.39	4263	2809
	1X reworked	5.35	3657	2400
	1X adjacent	4.40	4307	2468
	3X reworked	3.74	3476	1905
	3X adjacent	6.69	4437	3169
Mixed	Non-reworked	5.19	4258	2760
	1X reworked	13.24	6058	5111
	1X adjacent	6.47	5318	3756
	3X reworked	4.45	5272	3454
	3X adjacent	3.60	5058	2708

For the mixed assemblies, the mean cycles-to-failure of 1X adjacent and 3X adjacent BGAs was about 13% higher than that of the non-reworked BGAs. However, there was no statistical difference between 1X adjacent and 3X adjacent BGAs. Unlike the lead-free assemblies, the mean cycles-to-failure of reworked mixed assemblies was greater than that of the non-reworked mixed assemblies (see Figure 66). There was approximate 42% increase in the mean cycles-to-failure after 1X rework, and approximate 24% increase in the mean cycles-to-failure after 3X rework.

But, when compared with 1X reworked mixed assemblies, there was approximate 15% degradation in the mean cycles-to-failure of 3X reworked mixed assemblies.

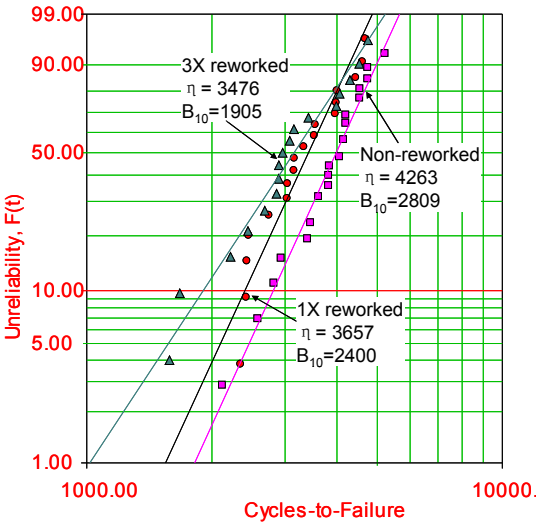

Figure 65: Unreliability of lead-free non-reworked and reworked BGAs

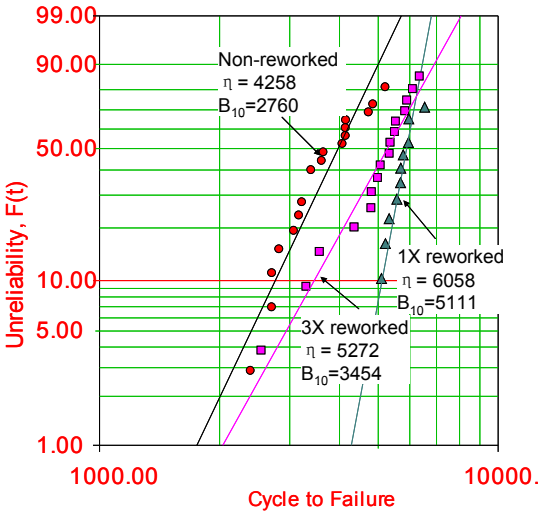

Figure 66: Unreliability of mixed non-reworked and reworked BGAs

The mean cycles-to-failure of non-reworked mixed and lead-free assemblies were similar (see Figure 67). One-way analysis of variance (ANOVA), with the alpha selected as 0.05, was applied to non-reworked lead-free and mixed BGAs, and no statistical difference was found. However, the mean cycles-to-failure of the reworked mixed assemblies was better than that of reworked lead-free assemblies (see Figure 68).

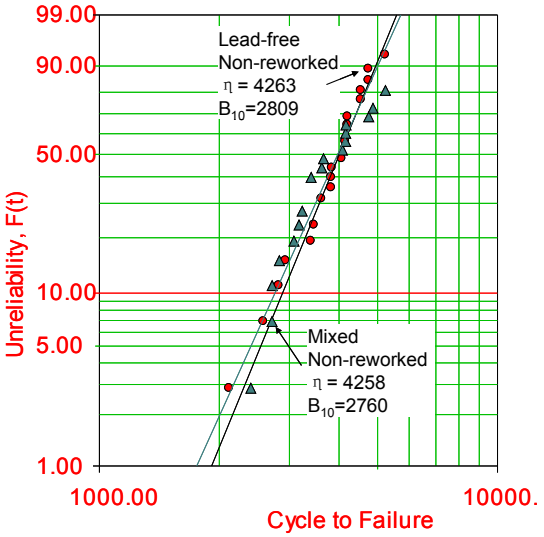

Figure 67: Unreliability of non-reworked lead-free and mixed BGAs

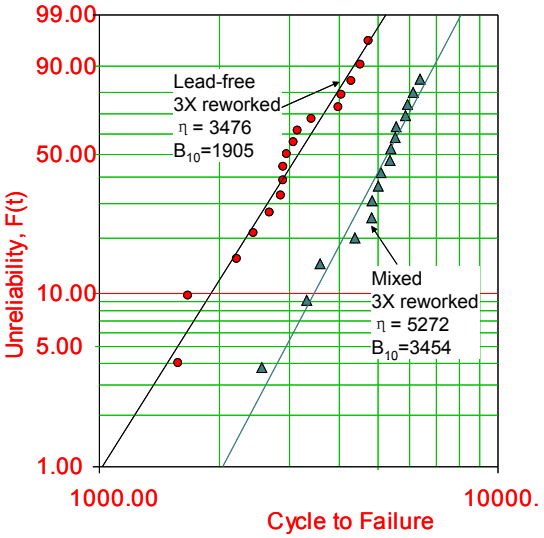

Figure 68: Unreliability of 3X reworked lead-free and mixed BGAs

5.2.3. Pb Distribution in Mixed Assemblies

After the BGA assemblies failed in the temperature cycling test, the components were cut, molded, and cross-sectioned. An environmental scanning electron microscope (FEI Quanta FEG ESEM 200) and an energy-dispersive X-ray spectroscopy (Oxford Instruments INCA 4.09) were used to analyze the failure site, crack propagation, and the intermetallic compounds.

Snugovsky et al. [26] described the mixing process of the SAC BGAs with the SnPb solder paste using a SnPb phase diagram. From this study, they concluded that a complete mixture may be achieved at a temperature lower than the melting temperature. The peak temperature of a reflow profile depends on solder ball composition, ball/solder paste ratio, dwell time, and component size. A majority of studies found that full mixing in solder joints is directly related to the temperature

cycling reliability of mixed assemblies [26] [27] [30] [35] [53]. D. Hillman et al. [53] claimed that partial mixing led to early failure in the ATC test.

In this study, a "full mixing" structure was achieved using a modified SnPb profile, with a peak temperature of 215ºC and a time above liquid (>183ºC) of 100 s. Although the mixed solder joints were considered to be "full mixing" metallurgical structures, the Pb did not distribute homogenously inside the bulk solder, as shown in Figure 69. The white phase in Figure 69 is the Pb-rich phase. The Pb-rich phase distribution was different in the as-received mixed BGAs and the reworked mixed BGAs. As shown in Figure 70, more fine Pb-rich phase particles were distributed homogenously inside the bulk solder in the 3X reworked mixed BGA solder joints than in the as-received mixed BGA solder joints. During the rework procedure, a higher peak temperature profile (peak temperature: 217^{o}C~225^{o}C; time above 183^{o}C: 80–100 s) was used for attaching the BGA components than the reflow profile used in the assembly procedure (peak temperature: 215^{o}C; time above 183^{o}C: 100 s). The peak temperature of the temperature profile in the rework process exceeded the melting temperature of the SAC305 solder (217^{o}C), which allowed for better interdiffusion between the SAC solder ball and the SnPb solder paste. This explained the presence of more fine Pb-rich phase particles in the reworked BGA assemblies than in the as-received BGA assemblies.

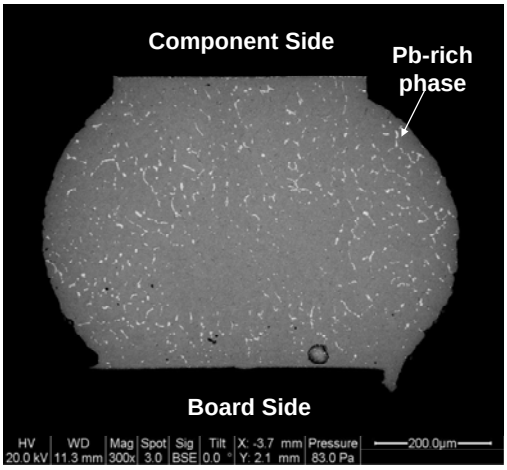

Figure 69: Backscattered images of bulk solder in a mixed assembly

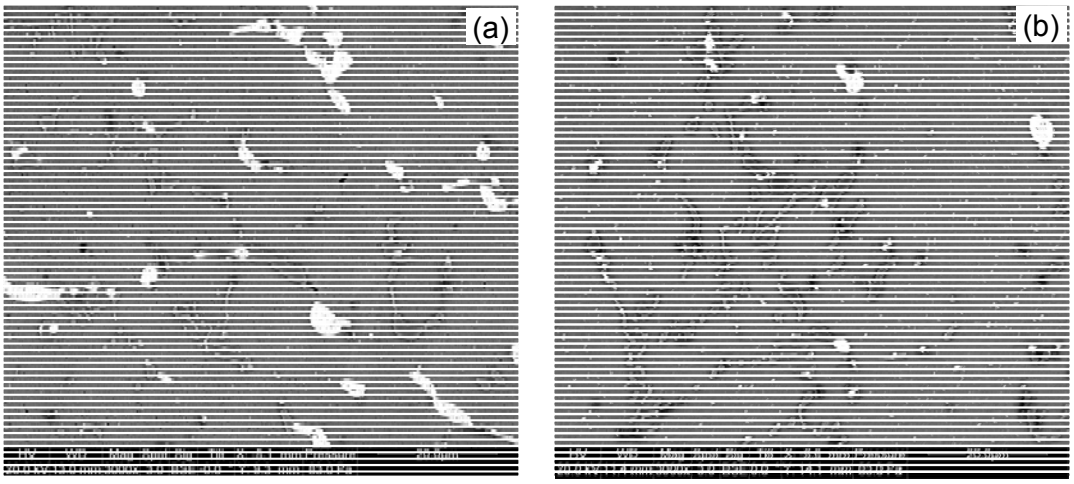

Figure 70: Pb-rich phase distribution inside bulk solder of mixed assemblies. (a) Non-reworked mixed assembly; (b) 3X reworked mixed assembly.

In order to get better understanding of the Pb distribution in the non-reworked and reworked mixed BGA assemblies, the greyscale images in Figure 70 was changed into binary images as shown in Figure 71. The centroid of Pb phases in the binary images was marked with cross. In each binary image, the image was divided into 100 areas, and the particle numbers per area was calculated. For statistical purpose, 9 images for each types of assembly were calculated. The histogram of Pb particle distribution was plotted in Figure 72. The mean value of Pb particle per area

in the 3X reworked assembly was larger than in the non-reworked assemblies, which means there were more Pb particles in the 3X reworked assemblies. The standard deviation of Pb particle per area in the 3X reworked assemblies was smaller than in the non-reworked assemblies, which means the Pb-rich phase distribution in the 3X reworked assemblies was more homogenous.

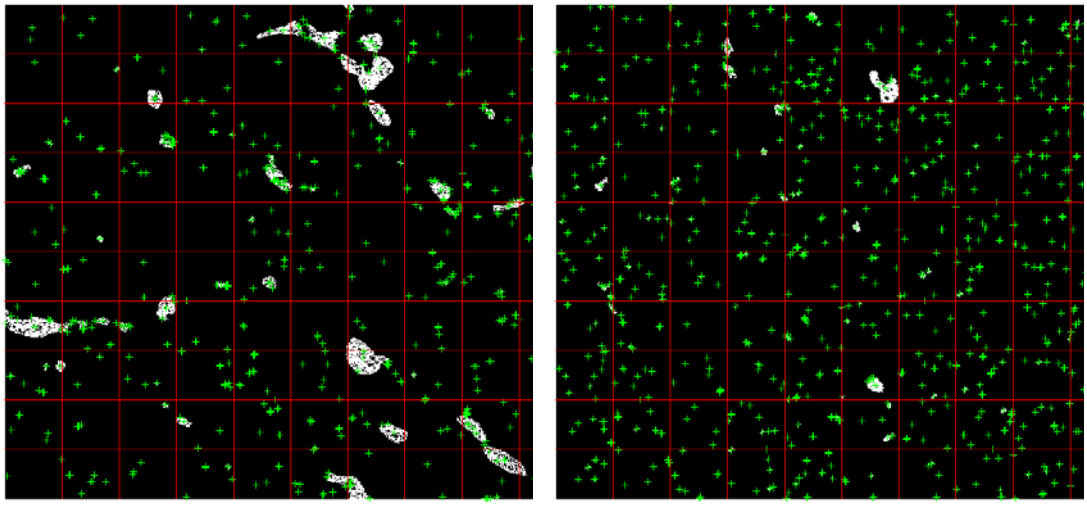

(a) (b)

Figure 71: Binary images of Pb-rich phase distribution inside bulk solder of mixed assemblies. (a) non-reworked mixed assembly; (b) 3X reworked mixed assembly. (White area stands for Pb phase). Red lines are gridline.

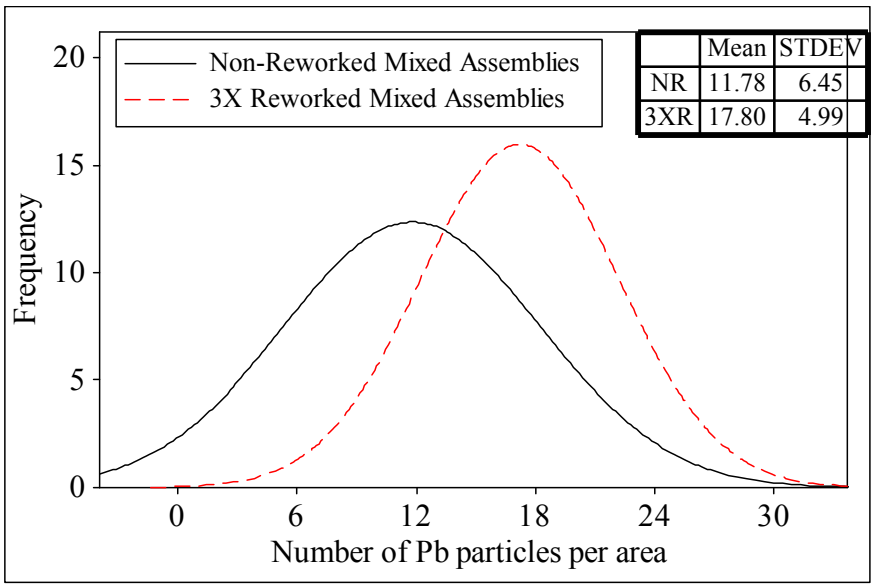

Figure 72: Pb particle distribution in 3X reworked and non-reworked mixed assemblies

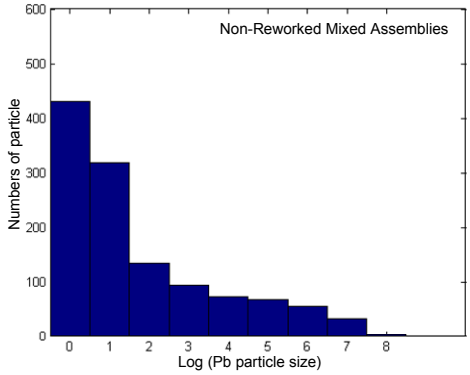

Figure 73: Numbers of particle vs. particle size in non-reworked mixed assemblies

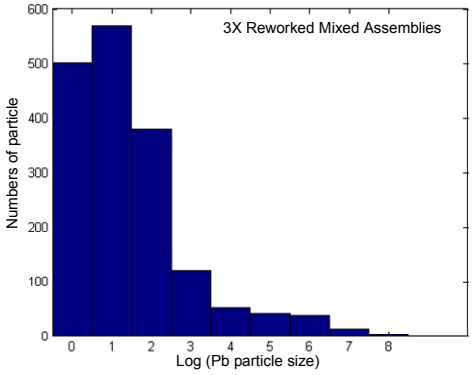

Figure 74: Numbers of particle vs. particle size in 3X reworked mixed assemblies

The Pb particle size was calculated by pixels, and the smallest Pb particle size was 1. Figure 73 and Figure 74 show the relationship between the Pb particle size and the number of the Pb particles. For each type of assembly, 9 images were calculated

and plotted. There were more small particles in the 3X reworked mixed assemblies (see Figure 74), which could explain the Pb phase was finer than that in the non-reworked mixed assemblies.

5.2.4. Cu Over-consumption, Interfacial Intermetallic Compound Thickness and Solder Joint Standoff

Cu over-consumption was found at the location where the Cu pad connected to the Cu trace in the 3X reworked lead-free and mixed BGAs (see Figure 75). The heat that accumulated in the rework process–made Cu was "eaten up" and formed very thick IMCs at the connection location as discussed in Section 5.1.3. Furthermore, the Cu over-consumption was found to have a direct relationship to the pad design on PCB. The pad on the PCB was half solder mask defined. During the manufacturing process, there was misalignment of solder mask which makes opening of the Cu pad was uneven. As shown in Figure 76, the pad with more Cu trace exposure was prone to Cu over-consumption. The open area on the Cu (see circle) can be correlated to the Cu over-consumption area in the solder joint of the reworked assemblies.

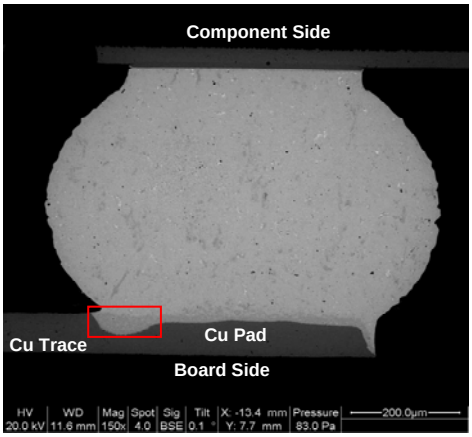

Figure 75: Cu over-consumption in 3X reworked mixed assembly

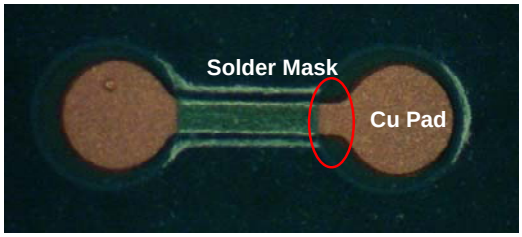

Figure 76: Uneven pad design on a PCB

A thick layer of interfacial IMC was found at the board side in the reworked BGAs. The interfacial IMC thickness at board side in the non-reworked and the reworked BGA assemblies was recorded and plotted (see Figure 77). For each sample, 27 measurements were documented. The interfacial IMC thickness increased according to increases in number of reworks. The solder became liquid over the course of several steps during the rework process, including component removal, site redressing, and component placement. IMC growth in the reworked BGAs was noticeably quick. IMC growth in mixed assemblies was slower than that of lead-free assemblies after the rework process. Pb was believed to slow down interfacial IMC growth in the mixed assemblies. After 3X rework, the thickness of interfacial IMC in the mixed assemblies was about 30% lower than that of the lead-free assemblies.

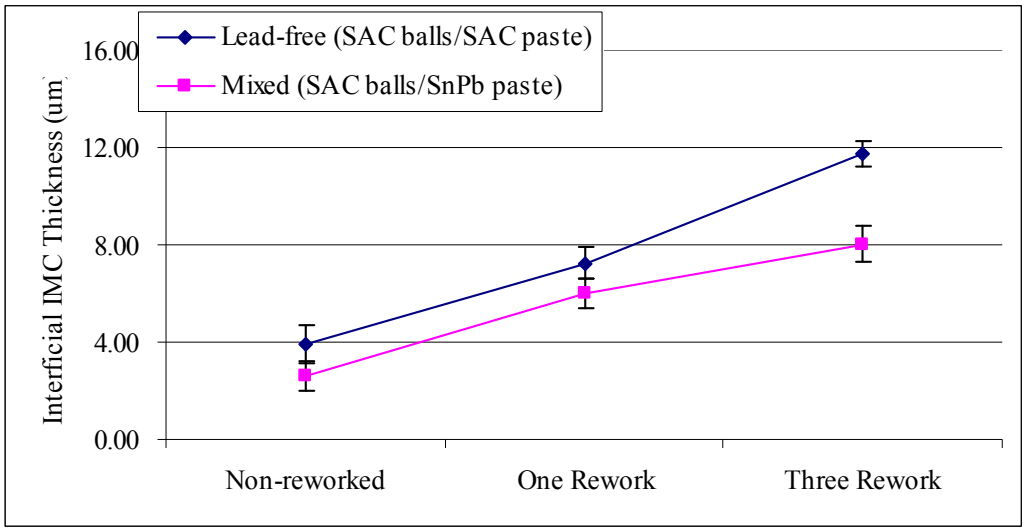

Figure 77: Interfacial IMC thicknesses at the board side in lead-free and mixed assemblies after multiple reworks

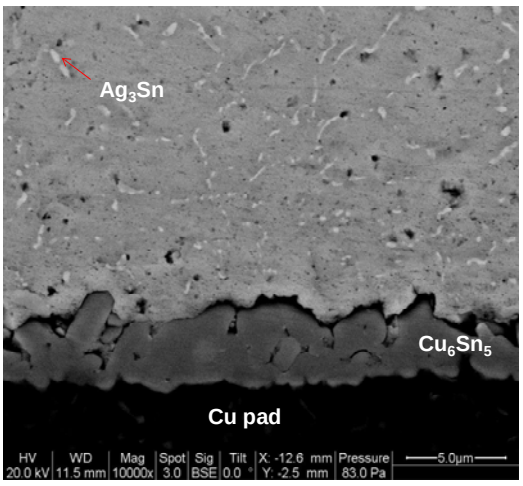

Figure 78: Interfacial IMC layer at the board side in an non-reworked lead-free assembly

The composition of the interfacial IMC layer was investigated by an energy-dispersive X-ray spectroscopy (EDS) system. For both the lead-free and the mixed assemblies, there was only one layer of interfacial IMC at board side, which was Cu_6Sn_5. The Cu_3Sn was not detectable due to the resolution of the EDS. During the

soldering procedure, when the liquid solder contacted the Cu pad, the first phase formed at the interface was Cu_6Sn_5 [66]. The Pb did not react with Sn or Cu, but precipitated in the Sn matrix and the gaps of the IMC layers. Figure 78 shows the interfacial layer at board side in the non-reworked lead-free assemblies.

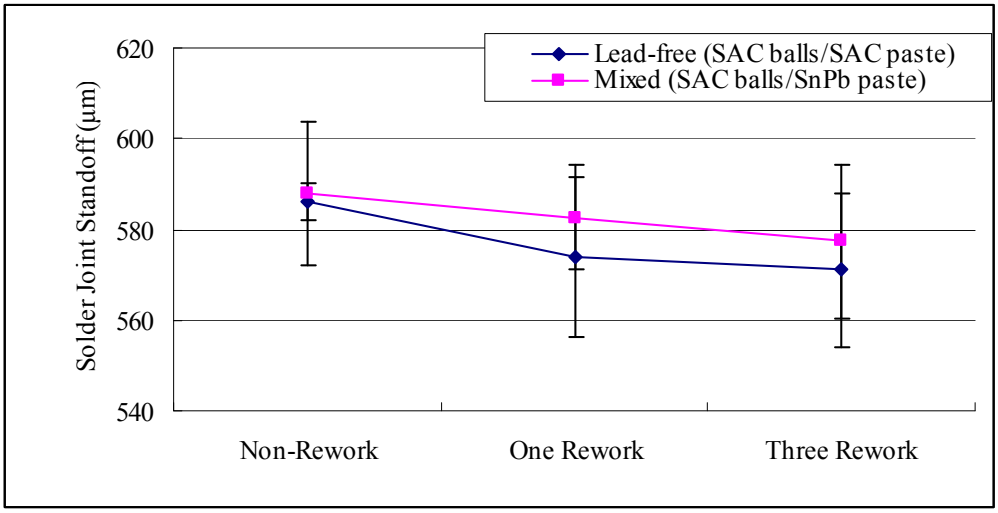

Figure 79: Solder joint standoff in lead-free and mixed assemblies after multiple reworks

Not only was the microstructure important for analyzing the temperature cycling reliability, but also the geometry of the solder joints was important. The solder joint standoff was the distance between the component pad to the board pad excluded the pad thickness. The solder joint standoff of lead-free assemblies and mixed assemblies was plotted in Figure 79. For each sample, 27 measurements were documented. In lead-free assemblies, there was a drop of solder joint standoff in the reworked assemblies. Similarly, the solder joint standoff of mixed assemblies decreased after rework process. In the rework process, higher reflow temperature was used which led to lower solder joint standoff in the reworked assemblies in comparison with non-rework assemblies. The solder joint standoff height result was

consistent with previous study, which revealed that lower reflow peak temperature led to lower standoff height [42].

5.2.5. Microstructural Failure Analysis of the Lead-free and Mixed Assemblies

The microstructure inside the bulk solder of the lead-free and mixed assemblies differed by assembly (see Figure 80 and Figure 81). In the lead-free BGA assemblies, there were larger numbers of Ag_3Sn fine particles around the cell Sn structure. The larger, darker IMC was Cu_6Sn_5, which was distributed randomly inside the bulk solder. In the mixed BGA assemblies, the cell structure was not found. Instead, the Ag_3Sn was needle-shaped and located inside bulk solder, while the darker IMC was Cu_6Sn_5. The white phase was a Pb-rich phase, which was distributed randomly inside bulk solder. Some of the Pb-rich phases were associated with the deposition of IMCs. As discussed in previous section, the Pb distribution in the reworked mixed assemblies was more homogenous in comparison with non-reworked mixed assemblies. However, there was no microstructure difference found in the non-reworked and reworked lead-free assemblies.

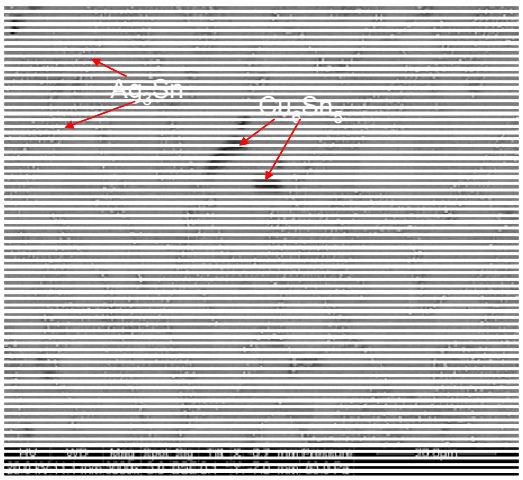

Figure 80: Bulk solder in the lead-free as-received assemblies

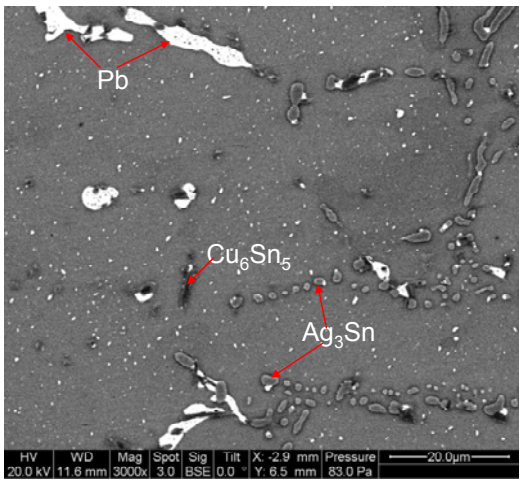

Figure 81: Bulk solder in the mixed as-received assemblies

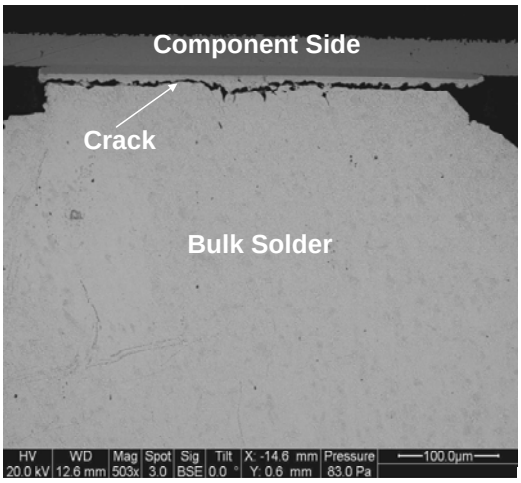

Figure 82: Failure site in 3X reworked lead-free assemblies

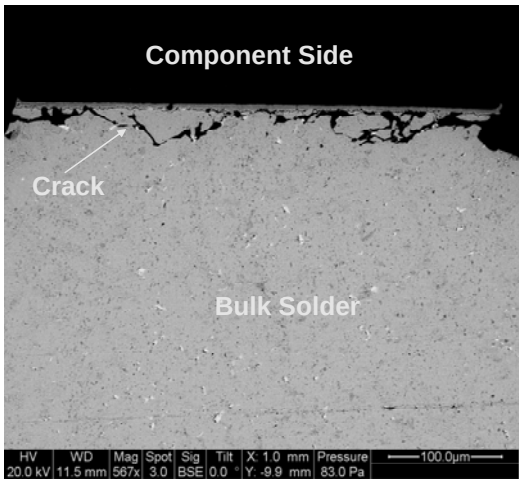

Figure 83: Failure site in 1X reworked mixed assemblies

For both the lead-free and mixed assemblies, the failure sites in the reworked and non-reworked BGAs were at the component side (see Figure 82 and Figure 83). The component pad was solder mask defined and experienced more stress in the temperature cycling test. The failure site was consistent with Snugovsky's study, which was expected to occur at the high-stress region, at the component side [26].

Secondary cracking was found on the board side. Similar to the component side, the stress on the board side was higher than inside the bulk solder. The fatigue crack initiated at the edge of the solder ball and propagated through the phase coarsening region (see Figure 84). The secondary cracking was located near the interface in the non-reworked lead-free and mixed assemblies. However, in the reworked BGAs, the secondary crack propagated along the interface and to the over-consumption area (see Figure 85).

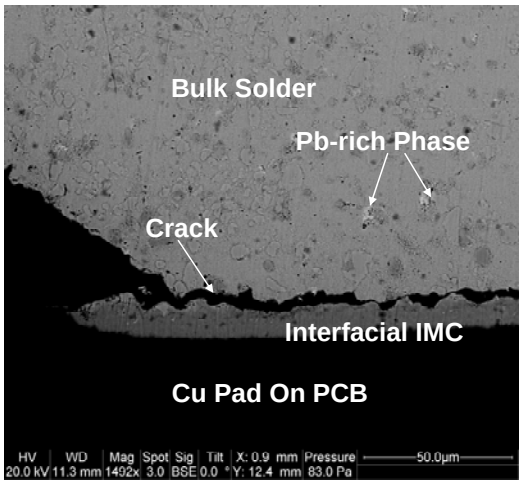

Figure 84: Secondary cracking in non-reworked mixed assemblies

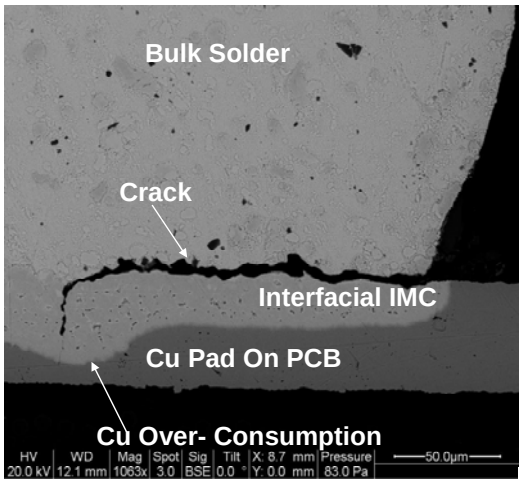

Figure 85: Secondary cracking in 3X reworked lead-free assemblies

5.2.6. Discussion

As discussed in the temperature cycling test results section, the mean cycles-to-failure of reworked lead-free assemblies was lower than that of the non-reworked lead-free assemblies. However, no difference was found between the non-reworked lead-free and the reworked lead-free BGAs in the microstructural analysis. Failure sites for both the non-reworked and reworked lead-free assemblies were found in the bulk solder near the component interface. There were two possible reasons for the

decreased temperature cycling reliability of the reworked BGA assemblies in comparison with non-reworked BGA assemblies. The solder joint standoff in the reworked assemblies decreased because of the increasing reflow temperature in the rework process. The decrease in the solder joint standoff increased the strain rate in the solder joint and reduced the temperature cycling fatigue resistance. CALCE PWA was used to simulate the reliability of lead-free assemblies under temperature cycling test. The simulation results showed that there was approximate 10% decrease in the reliability of 1X reworked lead-free assemblies and approximate 13% decrease in the reliability of 3X reworked lead-free assemblies in comparison with non-reworked lead-free assemblies. The simulation results showed similar trend with the temperature cycling reliability data, which proved that the decreasing of solder joint standoff height led to degradation in the temperature cycling reliability. Another possible reason was the interfacial IMC thickness difference in the reworked and non-reworked assemblies. In the reworked BGA assemblies, the interfacial IMC thickness on the board side was found to be thicker than the interfacial IMC thickness in the non-reworked BGA assemblies. Thicker interfacial IMC, which reduced the ductility of bulk solder and increased stiffness at the board side, led to more fatigue damage at the component side of the reworked BGA assemblies. Similarly, lower solder joint standoff and thicker interfacial IMC was found in the 3X reworked mixed assemblies in comparison with 1X mixed reworked assemblies. This could explain why the 1X reworked mixed BGA assemblies outperformed the 3X reworked BGA assemblies.

While for the mixed assemblies, the geometry parameter could not explain the temperature reliability differences in the non-reworked and reworked assemblies. The

mean cycles-to-failure of the reworked BGA assemblies was superior to that of the non-reworked BGA assemblies in the mixed assemblies. During this study, it was also discerned that there was a more homogenous Pb-rich phase distribution in the reworked mixed BGA assemblies than in the non-reworked mixed BGA assemblies. The root cause was that the peak reflow temperature in the rework process was higher than the peak temperature of the temperature profile used in the assembly process. The higher reflow temperature allowed for more sufficient interdiffusion between the SAC and SnPb solder. It was believed that the Pb distribution in the mixed assemblies was related to the performance of the mixed solder joints under the temperature cycling test. On one hand, the Pb-rich phase hardened the mixed solder joints. Wang et al. [76] discovered that the tensile strength of the mixed solder was greater than that of the lead-free solder. In this study, the Pb-rich phase did not involve IMC formation and segmented at the grain boundary of the Sn-rich matrix. These particles may block the dislocation movement and coalesced, which enhance the mechanical properties of the mixed solder joints. In the meanwhile, the Pb-rich phase particles blocked the dislocation movement and grain boundary sliding, which retarded the large angle grain boundary formation and recrystallization nucleate formation. The retarded process of large angle grain boundary and recrystallization nucleate formation slowed the progress of recrystallization and grain coarsening. Generally, the fatigue cracks initiated and propagated at the recrystallization and grain coarsening region in both the tin-lead and lead-free solder joints [72] [77]. It was assumed that the presence of Pb-rich phase particles slowed down the recrystallization and grain coarsening, which also retarded fatigue crack initiation and

propagation. Based on the previous discussion, and due to the Pb-rich phase distribution in the reworked mixed BGA assemblies being more homogenous than that in the non-reworked mixed BGA assemblies, it was reasonable to find out that reworked mixed BGA assemblies would outperform non-reworked mixed BGA assemblies.

As discussed in the microstructural failure analysis section, secondary cracks were found at the edge of the solder ball and propagated along the interface at the Cu over-consumption area on the board side of the reworked BGA assemblies. The multiple rework processes led to the Cu over-consumption in the reworked assemblies. The thick IMC at the Cu over-consumption area increased the stiffness, which led to higher stress at the board side. The secondary cracking initiated at the phase boundary between the bulk solder and interfacial layer. The intermetallic layer was stiffer and more brittle than the bulk solder material, especially for the Cu over-consumption area, where the thick IMC layer led to a crack propagation path along the secondary cracking. This could cause a reliability risk and lead to cracking. Over 3X rework processes are not recommended due to Cu over-consumption. Otherwise, revising the Cu pad and Cu trace design and conducting good control of solder mask printing are necessary to ensure the temperature cycling reliability of reworked assemblies after multiple rework processes.

5.3. Conclusions

In the pilot study, Cu pad dissolution was observed for joints in both lead-free and mixed assemblies after multiple rework processes. The Cu pad dissolution in

joints of lead-free assemblies was found to be larger than that of mixed assemblies. This was due to the higher concentration of Sn in the lead-free solder, which means there was a faster reaction between liquid lead-free solder and Cu. Cu over-consumption was observed at the edge of pads after five rework processes for both lead-free and mixed assemblies. During the reflow process, heat concentrated at the connection site between the Cu pads and the Cu traces, which led to the formation of ultra thick IMC and over-consumption of Cu pad. A thick IMC and a thin Cu pad may lead to temperature cycling reliability concerns, especially under mechanical loading. Thus, having more than three reworks is not recommended. IMC morphology of the adjacent non-reworked and the reworked samples was different from that of the as-assembled samples. The IMCs presented a fragmentary morphology due to the Cu dissolution in liquid Sn and the Cu diffusion at the interface. The growth of IMCs was much faster than the growth of IMCs undergoing the isothermal aging condition due to the prolonged liquid time in the rework process. Thus, reworked BGAs may have reliability concerns due to the thick IMC layer found at the interface in real applications.

Although there is degradation in the temperature cycling reliability of the lead-free assemblies after the rework process, the rework process is a robust process. It was believed that decreased solder joint standoff and the thick interfacial IMC layer at board side, after multiple rework processes, induced more stress in the reworked BGA assemblies during the temperature cycling test. Microstructural failure analysis revealed that the failure site in the reworked BGA assemblies, located in the bulk

solder near the component interface, was found in the same location on the non-reworked BGA assemblies.

Pb-rich phase distribution was essential to the temperature cycling reliability of mixed BGA assemblies. Although the non-reworked mixed solder joints were defined as “full mixing” solder joints, the Pb-rich phase were not distributed homogenously in the solder joints. As in the rework process, the peak temperature of the thermal profile was higher than that used in the assembly process. This led to a more homogenous Pb-rich phase distributed in the reworked mixed BGA assemblies as compared to the non-reworked mixed BGA assemblies. Pb-rich phases hardened the mixed solder material and retarded the recrystallization and grain coarsening, which contributed to the late failure of the reworked mixed BGA assemblies. The definition of the mixed solder joints was recommended to be revised, since the “full mixing” definition was not precise to describe the Pb-rich phase distribution in the mixed solder joints.

Cu over-consumption was found at the connection site from the Cu pad to the Cu trace on the board in the 3X reworked lead-free and mixed assemblies. The narrow Cu trace design and the misalignment of solder mask printing were believed to be the reasons for the Cu over-consumption phenomenon. During the temperature cycling test, the secondary cracking was found to propagate along the Cu over-consumption area.

Chapter 6: FUTURE WORK

This work has investigated the impact of the reballing methods and the rework processes on the temperature cycling reliability of the BGA assemblies. The temperature cycling reliability testing data has been analyzed with the failure analysis and microstructure change in the solder joints. It was found out that the influence of microstructure changes was larger than the geometry's influence in the temperature cycling reliability of BGA assemblies. However, there are several issues need to be investigated in the future.

Although there was plenty of experimental data in this study, it is better to build a model to simulate the impact of the microstructure changes on the temperature cycling reliability in the mixed BGA assemblies. The modeling can help to quantify the temperature cycling reliability change on the percentage and the degree of Pb-rich phase mixing.

The grain refinement has been observed in the tin-lead, the lead-free and the mixed assemblies. It was found out that the grain refinement was the precursor of cracking initiation and propagation. However, the reason for this grain refinement needs further investigation. Whether this grain refinement is the due to grain recrystallization requires transmission electron microscopy (TEM) to investigate the grain orientation and grain size.

CONTRIBUTIONS

Determined that the solder ball attachment strength and the temperature cycling reliability of the reballed SnPb BGAs were independent of the reballing methods (removal: low-temperature wave solder and solder wick; re-attachment: preform and ball drop).

- The same lamellar microstructure composed of Sn and Pb phases was found in the different reballed SnPb assemblies.

- Failure analysis revealed that the failure sites in the reballed assemblies were in the bulk solder at the component side. The cracking propagated along the phase boundaries.

Determined that a full mixing of Pb-rich phases inside bulk solder of mixed assembly led to equivalent temperature cycling fatigue resistance to the lead-free assembly.

- Pb phase dispersed all over the bulk solder (full mixing metallurgy structure) in the mixed assemblies strengthen the solder materials which led to better temperature cycling fatigue resistant property than the lead-free assemblies.

- The reworked mixed assembly had more homogenous Pb phase distribution which led to the characteristic life of reworked mixed assembly increasing approximately 20% in comparison with that of non-reworked mixed assemblies after 3X rework process.

Determined that there was degradation in temperature cycling reliability of lead-free and mixed assemblies after 3X rework processes.

- The characteristic life of 3X reworked lead-free assemblies was 18% lower than that of non-reworked assemblies. The characteristic life of 1X reworked lead-free assemblies was 14% lower than that of non-reworked assemblies.

- There was 15% degradation in the characteristic life of 3X reworked mixed assemblies in comparison with 1X reworked mixed assemblies.

- Lower solder joint standoff was found in the 3X reworked assemblies because of higher reflow temperature in the rework process. Simulation results proved that the decreasing in the solder joint standoff led to degradation in characteristic life.

APPDENDIX

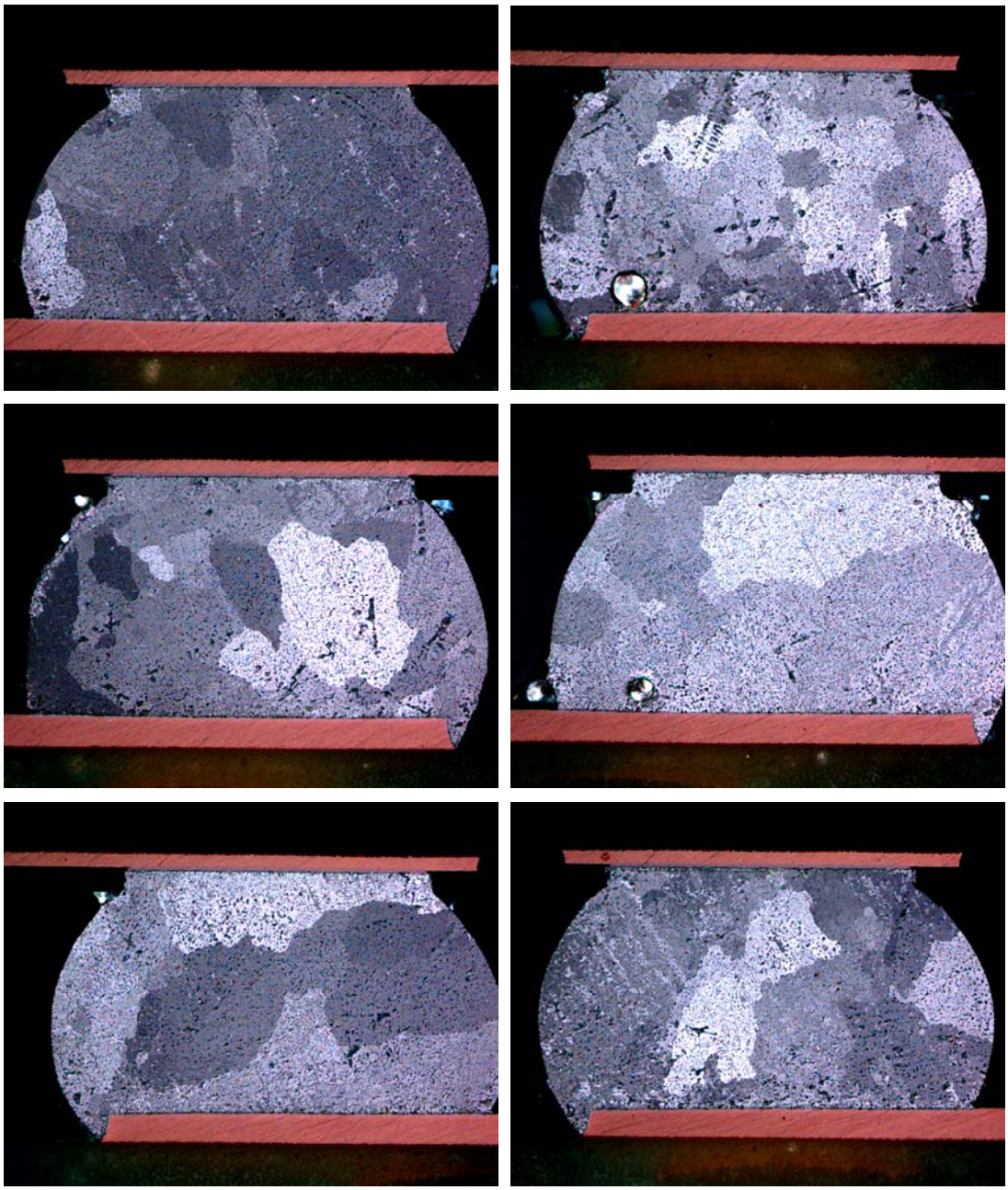

Cross-polarized images of 256 I/O reballed SnPb BGA Assemblies (as-received)

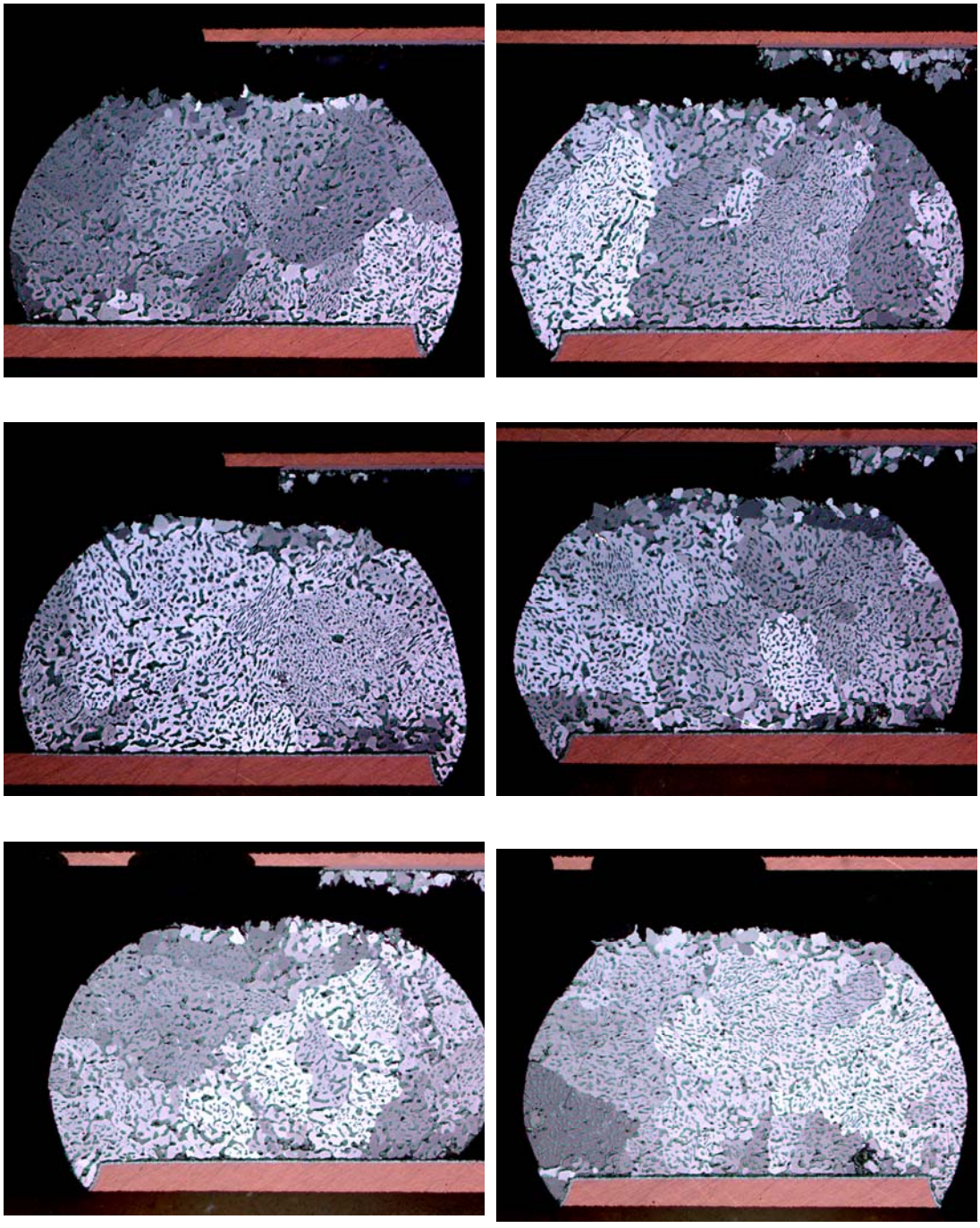

Cross-polarized images of 256 I/O reballed SnPb BGA Assemblies (after TC test)

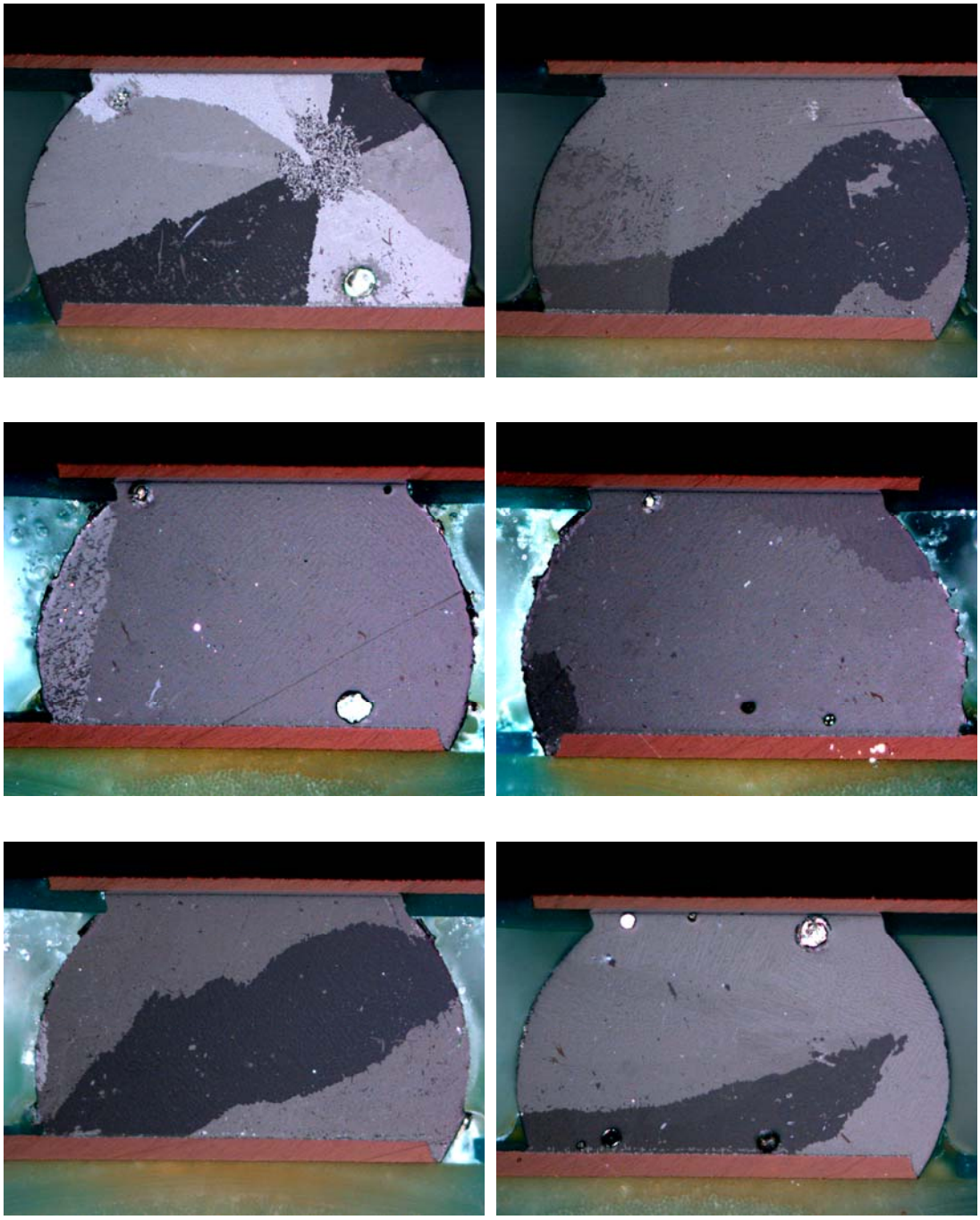

Cross-polarized images of 256 I/O lead-free BGA Assemblies (as-received)

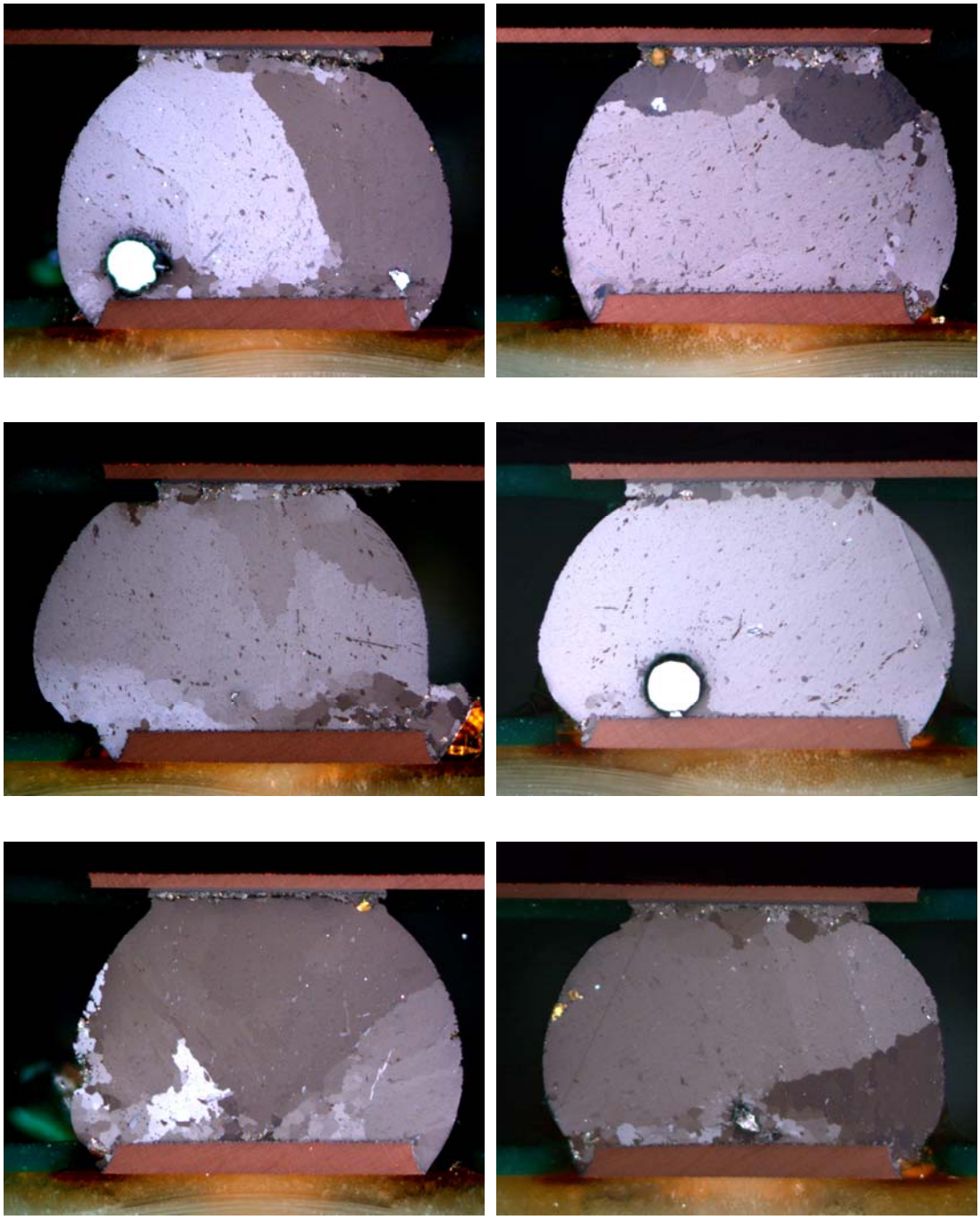

Cross-polarized images of 256 I/O lead-free BGA Assemblies (after TC test)

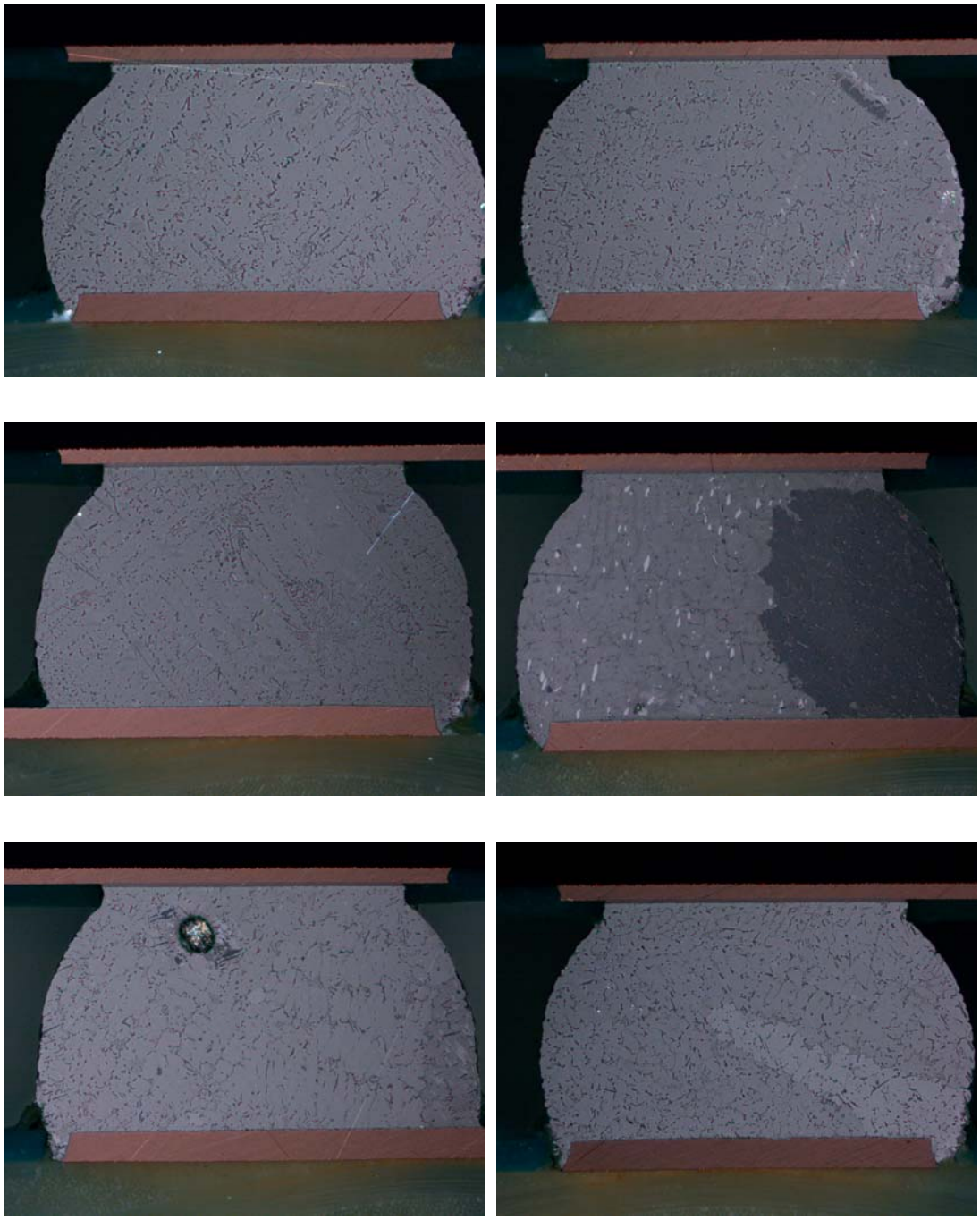

Cross-polarized images of 256 I/O mixed BGA Assemblies (as-received)

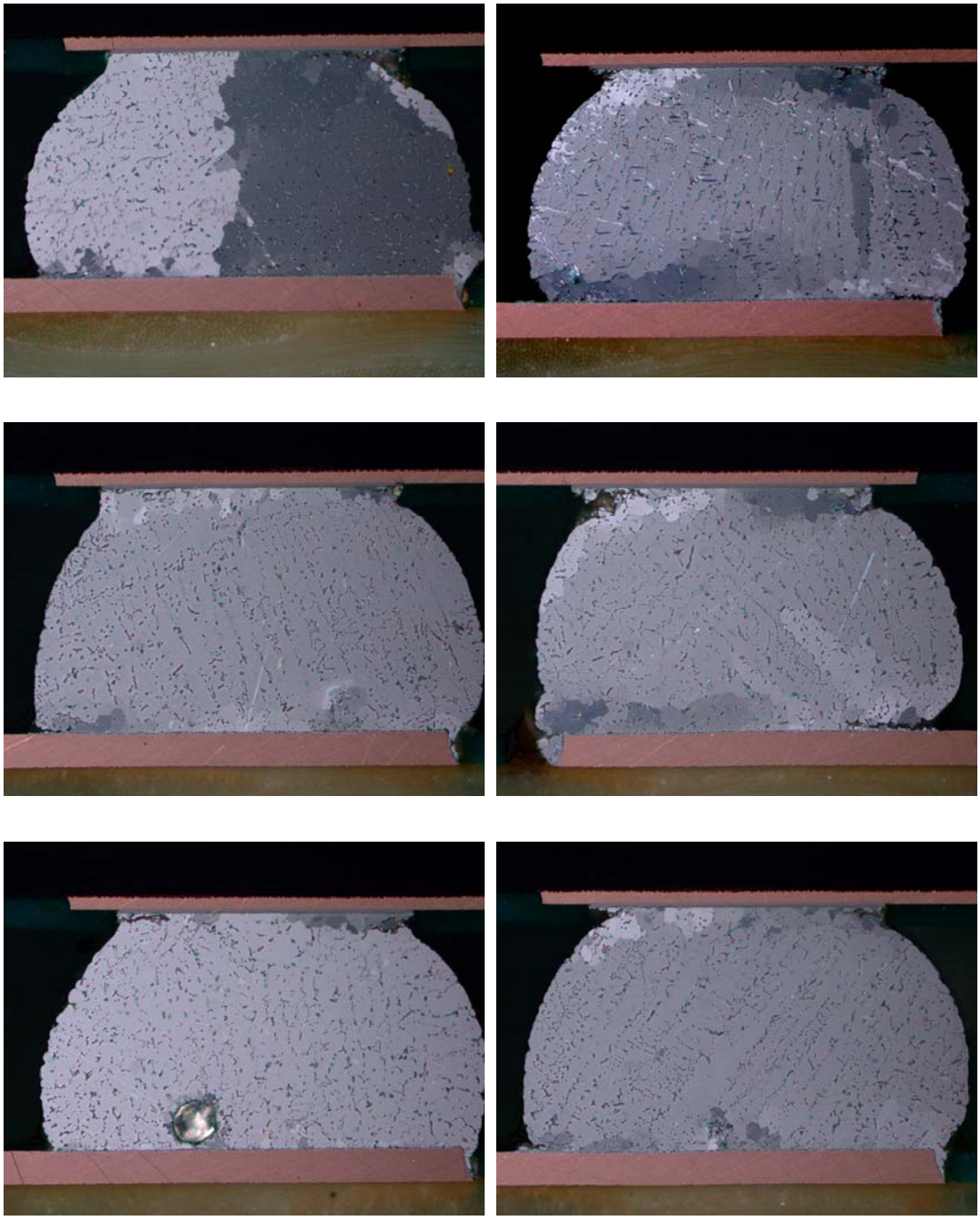

Cross-polarized images of 256 I/O mixed BGA Assemblies (after TC test)

Bibliography

[1] S. Ganesan and M. Pecht, Lead-free Electronics, New York: John Wiley and Sons Inc., 2006.

[2] M. Pecht, Y. Fukuda, and S. Rajagopal, "The Impact of Lead-free Legislation Exemptions on the Electronics Industry", IEEE Transactions on Electronics Packaging Manufacturing, Vol. 27, No. 4, October 2004, pp. 221-232.

[3] R. Ciocci and M. Pecht, "Questions Concerning the Migration to Lead-free Solder", Circuit World, Vol. 30, No. 2, 2004, pp. 34-40.

[4] L. Nie, M. Pecht, and R. Ciocci, "Regulations and Market Trends in Lead-free and Halogen-free Electronics", Circuit World, Vol. 33, No. 2, 2007, pp. 4-9.

[5] C. Handwerker, "Transitioning to Pb-free Assemblies", Printed Circuit Design and Manufacture, March 2005, pp. 17-23.

[6] IPC 7711, "Rework of Electronic Assemblies", North brook, IL, May 2002.

[7] F. Hua, R. Aspandiar, T. Rothman, C. Anderson, G. Clemons, and M. Klier, "Solder Joint Reliability of SnCuAg BGA Components Attached with Eutectic SnPb Solder Paste", Journal of Surface Mount Technology Association, Vol. 16, Issue 1, 2003.

[8] D. Hillman, M. Wells, and K. Cho, "The Impact of Reflowing A Lead-Free Solder Alloy Using A SnPb Solder Alloy Reflow Profile on Solder Joint Integrity", Proceedings of International Conference on Lead-free Soldering, Ontario, Canada, May 24-25, 2005.

[9] G. Grossmann, J. Tharian, P. Jud, and U. Sennhauser, "Microstructural Investigation of Lead-Free BGAs Soldered with Tin-Lead Solder", Soldering and Surface Mount Technology, Vol. 17, No. 2, February 2005, pp. 10-21.

[10] D. Santos, M. DiPietro, F. Andros, R. Alsalih, J. Tripp, and J. Ballus. "Evaluating the Mechanical Reliability of Reballed BGA Modules", Proceedings of the 4th Annual Pan Pacific Microelectronics Symposium, Kauai. HI, February 1999, pp. 385-390.

[11] F. Song and S. W. Ricky Lee. "Reliability Assessment on the Re-balling of PBGA form SnPb to Pb-free Solder Spheres", Proceedings of the 1st Electronics Systemintegration Technology Conference, Dresden, Germany, September 6, 2006, pp. 474-480.

[12] W. Beair and W. Vuono, "Lead Free to SnPb BGA Reballing Process and Reliability", Proceedings of SMTA International 2008, Orlando, FL, August 17-21, 2008, pp. 379-383.

[13] I. Chatterji, "Backward Compatibility, Are We Ready-A Case Study", Proceedings of SMTAI, Chicago, IL, 2006, pp. 416-424.

[14] K. Doss, A. Donaldson, A. Tong, and R. Aspandiar, "Studies on the Removal of Copper during Minipot Rework with Different Lead-Free Alloys", Proceedings of SMTA International, October 11, 2007.

[15] A. Donaldson, "The Effect of Critical to Function Parameters of the Lead-Free Mini-Pot Through-Hole Connector Rework Process on the Final Barrel Copper Thickness", Proceedings of SMTA International, October 11, 2007.

[16] C. Hamilton and P. Snugovsky, “Have High Cu Dissolution Rates of SAC305/405 Alloys Forced a Change in the lead Free Alloy Used During PTH Processes?”, Proceedings of the Pan Pacific Conference, January 2007.

[17] C. Hamilton, P. Snugovsky, and M. Kelly, “A Study of Copper Dissolution During Lead Free PTH Rework Using a Thermally Massive Test Vehicle”, Circuits Assembly, May 1, 2007.

[18] S. Chada, W. Laub, R.A. Fournelle, and D. Shangguan "Copper Substrate Dissolution in Eutectic Sn-Ag Solder and Its Effect on Microstructure," Journal of Electronic Materials, Vol 29, No. 10, October 2000, pp 1214-1221.

[19] B. Russell, D. Fritz, and G. S. Latta, “Methodology for Evaluating Data for ‘Reverse Compatibility’ of Solder Joints”, ITAR Issues and Lead-Free Evaluation Highlight Military Technologies Conference, Boston, MA, March 27-28, 2007.

[20] M. Kelly, M. Cole, J. wilcox, J. Bielick, T. Younger, and D. Braun, “Qualification of A Lead-Free Card Assembly and Test Process for A Server Complexity PCBA”, Proceedings of SMTA International, October 11, 2007.

[21] H.G. Sy, P. Arulvanan, and P.A. Collier, “Rework and Reliability of QFP and BGA Lead-free Assemblies”, the 4th Electronics Packaging Technology Conference, Singapore, December 10-12, 2002, pp. 194-199.

[22] N. Butel, “Comparison of the Level 2 Characteristics of HITCETM Substrate Assembled with SAC and High Lead Balls”, Proceedings of SMTA International, October 11, 2007.

[23] D. Manjunath, S. Iyer, P. Damodaran, and K. Srihari, “Developing a Repeatable and Reliable Rework Process for Lead-Free Fine-Pitch BGAs”, IEEE Transactions on Electronics Packaging Manufacturing, Vol. 30, No. 4, 2007, pp. 270-278.

[24] A. Gowda, K Srihari and A. Primavera, “Lead-Free Rework Process for Chip Scale Package”, Proceedings of SMTAINEPCON East Conference, Boston, MA, June, 2001.

[25] A. Choubey, M. Osterman, and M. Pecht, “Microstructure and Intermetallics Formation in SnAgCu BGA Components Attached with SnPb Solder Under Isothermal Aging”, IEEE Transactions on Device and Materials Reliability, Vol. 8, Issue 1, 2008, pp 160-167.

[26] P. Snugovsky, A. Zbrzezny, M. Kelly, and M. Romansky, "Theory and Practice of Lead-Free BGA Assembly Using Sn-Pb Solder", Proceedings CMAP (Centre for Microelectronics Assembly and Packaging in Canada) International Conference on Lead-Free Soldering, University of Toronto, Toronto, OB, Canada, May 2005.

[27] I. Chatterji, “Backward Compatibility, Are We Ready-A Case Study”, Proceedings of SMTAI, Chicago, IL, 2006, pp. 416-424.

[28] B. Nandagopal , Z. Mei, and S. Teng “Microstructure and Thermal Fatigue Life of BGAs with Eutectic Sn-Ag-Cu Balls Assembled at 210 ^{o}C with Eutectic Sn-Pb Solder Paste”, Proceedings of 2006 IEEE Electronic Components and Technology Conference, San Diego, CA, 2006, pp. 875-883.

[29] J. Bath, S. Sethuraman, X. Zhou, D. Willie, K. Hyland, K. Newman, L. Hu, D. Love, H. Reynolds, K. Kochi, D. Chiang, V. Chin, S. Teng, M. Ahmed, G. Henshall, V. Schroeder, Q. Nguyen, A. Maheswari, M.J. Lee, J-P. Clech, J. Cannis, J. Lau, and C. Gibson. "Reliability Evaluation of Lead-Free SnAgCu PBGA676 Components Using Tin-Lead and Lead-Free SnAgCu Solder Paste", Proceedings of 2005 SMTA International, Chicago, IL, September 25-29, 2005, pp. 891-901.

[30] B. Smith, P. Snugovsky, M. Brizoux, and A. Grivon, "Industrial Backward Solution for Lead Free Exempted AHP Electronic Products, Part 2: Process Technology Fundamentals and Failure Analysis", Proceedings of APEX 2008, S15-01, Las Vegas, NV, 2008.

[31] H. McCormick, P. Snugovsky, Z. Bagheri, S. Bagheri, C. Hamilton, G. Riccitelli, and R. Mohabir, "Mixing Metallurgy: Reliability of SAC Balled Area Array Packages Assembled Using SnPb Solder", Proceedings of SMTAI, Chicago, IL, 2006, pp. 425-432.

[32] J. Nguyen, D. Geiger, D. Rooney, and D. Shangguan, "Solder Joint Characteristics and Reliability of Lead-Free Area Array Packages Assembled Under Various SnPb Soldering Process Condition", IEEE Transactions on Electronics Packaging Manufacturing, Vol. 31, Issue 3, July 2008, pp.227 – 239.

[33] R. Kinyanjui, Q. Chu, P. Snugovsky, and R. Coyle, "Solder Joint Reliability of Pb-free SnAgCu Ball Grid Array (BGA) Components in SnPb Assembly

Process," Proceedings of APEX 2008, S15-02, Las Vegas, NV, March 31-April 3, 2008.

[34] H. McCormick, P. Snugovsky, C. Hamilton, Z. Bagheri, and S. Bagheri, "The Great SAC Debate: The Reliability of SAC305 and SAC405 Solders in A Variety of Applications," Proceedings of PanPac Symposium, January 31, 2007, pp. 333-341.

[35] B. Nandagopal, D. Chiang, S. Teng, P. Thune, L. Anderson, R. Jay, and J. Bath, "Study on Assembly, Rework Process, Microstructures and Mechanical Strength of Backward Compatible Assembly," Proceedings of SMTAI, Chicago, IL, September 25-29, 2005, pp. 861-870.

[36] R. Kinyuanjui and Q. Chu. "The Pb-Free SnAgCu Ball Grid Array (BGA) Components in SnPb Assembly Process Characterization and Solder Joint Reliability", Proceeding of SMTAI, Orlando, FL, October 7-11, 2007.

[37] G. Grossmann, J. Tharian, P. Jud, and U. Sennhauser, "Microstructural Investigation of Lead-free BGAs Soldered with Tin-Lead Solder", Soldering & Surface Mount Technology, Vol. 17, No. 2, 2005, pp. 10-21.

[38] H. McCormick, P. Snugovsky, Z. Bagheri, and S. Bagheri, "Pb-Free Test Vehicle, Microstructure and ATC Behavior of SAC305 and SAC405 BGAs Assembled with SnPb Solder", Proceedings of International Conference on Lead-Free Soldering, Toronto, ON, Canada, May 16-18, 2006, No. 11, pp. 1-9.

[39] R.Coyle, P. Read, R. Popowich, D. Fleming, S. Kummerl, and I. Chatterji, "A Comprehensive Solder Joint Reliability Study of SnPb and Pb Free Plastic Ball Grid Arrays (PBGA) Using Backward and Forward Compatible

Assembly Processes", Proceedings of IPC APEX 2008, Las Vegas, NV, March 31-April3, 2008.

[40] M. Mehrotra, L.A. Brack, E.J. Siméus, S.R. Stegura, T.Q. Do, K.R. Ladera, R.W. Jayne, and W.M. Lyons, "BGA Backward Compatibility Temperature Cycle Test Data for Harsh Environments", Proceeding of SMTAI, Orlando, FL, October 7-11, 2007.

[41] A. Kannabiran, E.T. Pannerselvam, and S.M. Ramkumar, "Forward and Backward Compatibility of Solder Alloys With Component and Board Finishes", IEEE Transactions on Electronics Packaging Manufacturing, Volume: 30, Issue: 2, April 2007, pp. 138-146.

[42] M. Ahmad, K. Liu, G. Ramakrishna, and J. Xue, "Impact of Backwards Compatible Assembly on BGA Thermomechanical Reliability and Mechanical Shock, Pre- and Post-Aging", Proceedings of SMTA International Conference, Orlando, FL, August 17-21, 2008, pp. 306-321.

[43] M. Brizoux, A. Grivon, B. Smith , and P. Snugovsky, "Industrial Backward Solution for Lead-Free Exempted AHP Electronic Products, Part 1: Use Context and Reliability Characterization", Proceedings of IPC APEX 2008, S15-01, Las Vegas, NV, March 31-April 3, 2008.

[44] C. Hunt and M. Wickham, "Impact of Lead Contamination Effects on Reliability of Lead Free Alloys", Proceedings IPC Printed Circuits Expo 2006, S39-01, 2006.

[45] M. Wickham, L. Zou, M. Dusek, and C. Hunt, "Measuring the Reliability of Electronics Assemblies During the Transition Period to Lead-Free Soldering",

NPL Report DEPC MPR 030, National Physical Laboratory, UK, August 2005.

[46] A. Zbrzezny, P. Snugovsky, T. Lindsay, and R. Lau, “Reliability Investigation of Mixed BGA Assemblies”, IEEE Transactions on Electronic Package Manufacturing, Vol. 29, No.3, July, 2006, pp. 211-216.

[47] A. Zbrzezny, P. Snugovsky, T. Lindsay, and R. Lau, “Reliability Investigation of Mixed BGA Assemblies - Case Studies”, Proceedings of 2005 SMTA International, Chicago, IL, September 25-29, 2005.

[48] J. L. Evans, C. Mitchell, M. Bozak, L. N. Payton, M.R. McQuenney, and J. R. Thompson, “Reliability of SAC BGA Using SnPb Paste for Harsh Environment Electronics”, Proceedings of SMTAI, Chicago, IL, September 25-29, 2005, pp. 365-370.

[49] M. Cole, M. Kelly, M. Interrante, G. Martin, C. Bergeron, M. Farooq, and M. Hoffmeyer, “Reliability Study and Solder Joint Microstructure of Various SnAgCu Ceramic Ball Grid Array (CBGA) Geometries and Alloys”, Proceedings of SMTAI, Chicago, IL, 2006.

[50] J. Nguyen, D. Geiger, D, Rooney, and D. Shangguan, "Reliability Study of Lead-Free Area Array Packages with Tin-Lead Soldering Processes", Proceedings of SMTAI, Chicago, IL, 2006, pp. 433-438.

[51] J. Nguyen, D. Geiger, D, Rooney, and D. Shangguan, "Backward Compatibility Study of Lead-Free Area Array Packages with Tin-Lead Soldering Processes", Proceedings of APEX, S09-03, Anaheim, CA, 2006.

[52] F. Sun, “Solder Joint Reliability of Sn-Ag-Cu BGA and SnPb Solder Paste”, Proceedings of the 6th International Conference on Electronic Packaging Technology, Shenzhen, China, Aug. 30- Sept. 2 2005, pp. 714- 719.

[53] D. Hillman, M. Wells, and K. Cho, “The Impact of Reflowing a Pb-free Solder Alloy Using a Tin/Lead Solder Alloy Reflow Profile on Solder joint Integrity”, Proceedings CMAP (Centre for Microelectronics Assembly and Packaging in Canada) International Conference on Lead-free Soldering, University of Toronto, Toronto, ON, Canada, May 2005.

[54] L. Chen, Y. Ye, S. Liu, S. Chen, Y. Tu, Z. Song, and Z. Xiang “The Influence of Process Parameters to Double-Sided Assembly BGA Reliability in Backward Compatible Soldering”, Proceeding of SMTAI, Orlando, FL, October 7-11, 2007.

[55] A.R. Zbrzezny, P. Snugovsky, T. Lindsay, and R. Lau, “Reliability Investigation of Sn-Ag-Cu BGA Memory Modules Assembled with Sn-Pb Eutectic Paste Using Different Reflow Profiles”, International Conference on Lead-free Soldering, CMAP, Toronto, ON, Canada, May 24-26, 2005.

[56] S. Bagheri, and P. Snugovsky, “Solder Joint Microstructure and Reliability Study of Ceramic Ball Grid Array (CBGA) Components”, Proceedings of the CMAP International Conference of Lead Free Soldering, 2006.

[57] JEDEC JESD22-B117A, “Solder Ball Shear”, October 2006.

[58] Y. Zheng, C. Hillman, and P. McCluskey, “Intermetallic Growth on PWBs Soldered with Sn3.8Ag0.7Cu”, Proceedings of the 52nd Electronic Components and Technology Conference, 2002, pp. 1226-1231.

[59] R.J. Coyle and P.P. Solan, “The Influence of Test Parameters and Package Design Features on Ball Shear Test Requirements”, the 26th IEEE/CPMT International Electronics Manufacturing Technology Symposium, 2000, pp. 168-177.

[60] F. Song and S.W.R. Lee, “Effects of Testing Conditions and Multiple Reflows on Cold Bump Pull Test of Pb-free Solder Balls”, Proceedings of the 6th International Conference on Electronic Packaging Technology, August 30-Sepember 2, 2005, pp.474 – 480.

[61] F. Song and S.W.R. Lee, “Investigation of IMC Thickness Effect on the Lead-Free Solder Ball Attachment Strength: Comparison between Ball shear Test and Cold Bump Pull Test Results,” Proceedings of the 56th Electronic Components and Technology Conference, May30-June2, 2006, pp. 1196 – 1203.

[62] G.J.S. Chou, “Microstructure Evolution of SnPb and SnAg/Cu BGA Solder Joints During Thermal Aging”, Proceedings of 2002 8th International Symposium on Advanced Packaging Materials, Stone Mountain, GA, 2002, pp. 39-46.

[63] F. Zhang, C.C. Chum and M. Li, “Effect of Au on Interfacial Reactions of Eutectic SnPb and SnAgCu Solders with Al/Ni(V)/Cu Thin Film Metallization”, Proceedings of the 52nd Electronic Components and Technology Conference, 2002, pp. 726-731.

[64] C. L. Hernandez, P. T. Vianco, and J. A. Rejent, “Effect of Interface Microstructure on the Mechanical Properties of Pb-free Hybrid Microcircuit

Solder Joints", Proceedings of the IPC/SMTA Electronics Assembly Expo, S19-1, October 27-29, 1998.

[65] I. Ahmad, A. Jalar, B.Y. Majlis, and R. Wagiran, "Reliability of SAC405 and SAC387 as Lead-Free Solder Ball Material for Ball Grid Array Packages", International Journal of Engineering and Technology, Vol. 4, No. 1, 2007, pp. 123-133.

[66] T. Laurila, V. Vuorinen, and J. K. Kivilahti, "Interfacial Reaction between Lead-Free Solders and Common Base Materials", Materials Science and Engineering, R 49, 2005, pp. 1-60.

[67] C. E. Ho , R. Y. Tsai , Y. L. Lin , and C. R. Kao, "Effect of Cu concentration on the reactions between Sn-Ag-Cu solders and Ni", Journal of Electronic Materials, Vol. 31 No. 6, pp. 584-590, June 2002.

[68] D.Q. Yu, C.M.L. Wu, C.M.T. Law, L. Wang and J.K.L. Lai, "Intermetallic Compounds Growth Between Sn–3.5Ag Lead-Free Solder and Cu substrate by Dipping Method", Journal of Alloys and Compounds, Vol. 392, 2005, pp. 192-199.

[69] IPC-9701, "Performance Test methods and Qualification Requirements for Surface Mount Solder Attachments", Northbrook, IL, January 2002.

[70] IPC-SM-785, "Guidelines for Accelerated Reliability Testing of Surface Mount Solder Attachments", Northbrook, IL, November 1992.

[71] J. Manock, R. Coyle, B. Vaccaro, H. McCormic, R. Popowich, D. Fleming, P. Read, J. Osenbach, and D. Gerlach, "Effect of Temperature Cycling Parameters on The Solder Joint Reliability of a Pb-free PBGA Package",

Journal of Surface Mount Technology, Vol. 21, No. 3, July-September, 2008, pp. 36-46.

[72] S. Dunford, S. Canumalla, and P. Viswanadham, "Intermetallic Morphology and Damage Evolution under Thermomechanical Fatigue of Lead (Pb)-Free Solder Interconnections", Proceedings of Electronic Components Technology Conference 2004, June 2004, pp. 726-736.

[73] J. Bath, S. Sethuraman, X. Zhou, D. Willie, K. Hyland, K. Newman, L. Hu, D. Love, H. Reynolds, K. Kochi, D. Chiang, V. Chin, S. Teng, M. Ahmed, G. Henshall, V. Schroeder, Q. Nguyen, A. Maheswari, M.J. Lee, J-P. Clech, J. Cannis, J. Lau, and C. Gibson. "Reliability Evaluation of Lead-free SnAgCu PBGA676 Components Using Tin-Lead and Lead-free SnAgCu Solder Paste", Proceedings of 2005 SMTA International, Chicago, IL, September 25-29, 2005, pp. 891-901.

[74] J. Liang, S. Downes, N. Darriavach, D. Shangguan, and S.M. Heinrich, "Effects of Load and Thermal Conditions on Pb-Free Solder Joint Reliability", Journal of Electronic Materials, Vol. 33, No. 12, 2004, pp. 1507-1514.

[75] K.-W. Moon and W.J. Boettinger, "Accurately Determining Eutectic Compositions: The Sn-Ag-Cu Ternary Eutectic", Journal of the Minerals, Metals and Materials Society, Vol. 56, No.4, April 2004, pp. 22-27.

[76] F. Wang, M. O'Keefe, and B. Binkmeyer, "Microstructural Evolution and Tensile Properties of Sn-Ag-Cu Mixed with Sn-Pb Solder Alloys", Journal of Alloys and Compounds, 477 (2009), pp. 267-273.

[77] D. Frear, D. Grivas, and J. W. Morris, “A Microstructural Study of the Thermal Fatigue Failures of 60Sn-40Pb Solder Joints”, Journal of Electronic Materials, Vol. 17, No.2, pp. 171-180, 1988.